

**DESIGN, CONSTRUCTION AND PERFORMANCE
ANALYSIS OF A ROTARY TYPE REGENERATIVE
HEAT EXCHANGER**

A MASTER'S THESIS

In

Mechanical Engineering

Middle East Technical University

12826

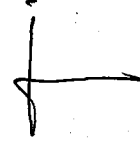
MS-

By

Mehmet TARAKÇI

February 1991

Approval of the Graduate School of Natural And Applied Sciences.



Prof. Dr. Alpay ANKARA
Director

I certify that this thesis satisfies all the requirements as a thesis for the degree of Master of Science in Mechanical Engineering.



Prof. Dr. Rüknettin OSKAY
Chairman of the Department

We certify that we have read this thesis and that in our opinion it is fully adequate, in scope and quality, as a thesis for the degree of Master of Science in Mechanical Engineering.



Assoc. Prof. Dr. Cemil YAMALI
Supervisor

Examining Committee in Charge :

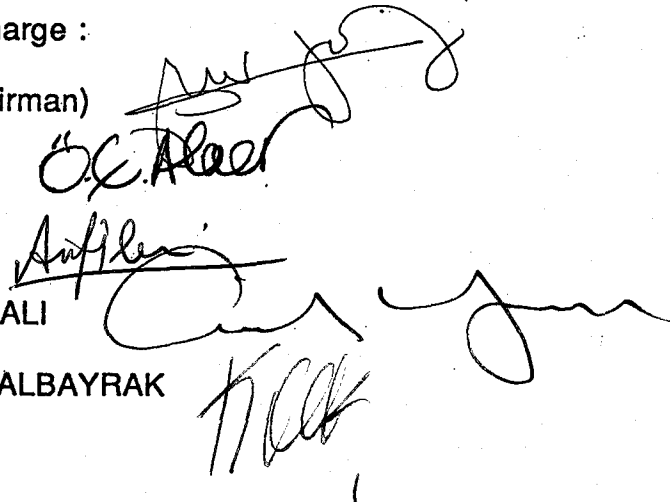
Prof.Dr. Hafit YÜNCÜ (Chairman)

Prof. Dr. Ercan ATAER

Assoc.Prof.Dr. Arif İLERİ

Assoc. Prof. Dr. Cemil YAMALI

Assoc. Prof. Dr. Kahraman ALBAYRAK



ABSTRACT

DESIGN, CONSTRUCTION AND PERFORMANCE ANALYSIS OF A ROTARY TYPE REGENERATIVE HEAT EXCHANGER

TARAKÇI, Mehmet

M.S. in Mechanical Eng.

Supervisor : Assoc. Prof. Dr. Cemil YAMALI

February 1991, 128 pages

In this study, rotary type regenerative heat exchanger is designed, constructed and tested in order to evaluate its performance and to find its effectiveness.

As a matrix material of rotary type regenerative heat exchanger, two different materials (0.35 mm galvanized sheet iron and 0.40 mm aluminum sheet) with considerably different thermal properties are used.

The effects of various design parameters on the effectiveness of the rotary regenerator are investigated. These parameters are; mass flow rate

of hot and cold air, thermal conductivity of matrix material, rotational speed, heat capacity rate ratio of the fluids, matrix heat capacity rate ratio, heat transfer surface area.

Experimental results show that effectiveness of the rotary type regenerative heat exchanger increases with an increase in the number of transfer units. Matrix heat surface area as well as the matrix heat capacity rate ratio and rotational speed increases the effectiveness of the rotary type regenerative heat exchanger.

Key words : Counter flow rotary type regenerative heat exchanger, rotary regenerator, thermal storage type heat exchanger, air preheater, thermal wheels, effectiveness.

Science code : 625.04.05

ÖZET

DÖNER TİP BİR REJENERATİF ISI DEĞİŞTİRGEÇİNİN TASARIMI, YAPIMI VE ÇALIŞMA ANALİZİ

TARAKÇI, Mehmet

Yüksek Lisans Tezi, Makina Müh. Bölümü

Tez Yöneticisi : Doç. Dr. Cemil YAMALI

Şubat 1991, 128 sayfa

Bu çalışmada, döner tip regeneratif ısı değiştirgecinin çalışmasını tayin etmek ve etkenliğini bulmak için, bir döner tip regeneratif ısı değiştirgecinin tasarımı, yapımı ve deneysel çalışmaları gerçekleştirilmiştir.

Döner tip regeneratif ısı değiştirgecinin matris malzemesi olarak, (0.35 mm'lik galvanizli sac ve 0.40 mm'lik alüminyum sacı) ısı özellikleri birbirinden tamamen farklı olan iki malzeme kullanılmıştır.

Döner regeneratifin etkenliğine etki eden çeşitli tasarım parametreleri araştırılmıştır. Bu parametreler şunlardır; sıcak ve soğuk

havanın debisi, matris malzemesinin ısıl geirgenliđi, dnüş hızı, akışkanların ısı kapasitesi oranı, matris ısı kapasitesi oranı, ısı geiş yüzey alanı.

Deneyssel alıřmalar sonucunda, ısı geiş birim sayısının artmasıyla dner tip rejeneratif ısı deđiřtirge etkenliđinin arttıđı grlmřtr. Matris ısı kapasitesi oranı ve dnme hızı gibi, matris ısı geiş alanı dner tip rejeneratif ısı deđiřtirgecinin etkenliđini arttırmıřtır.

Anahtar Kelimeler : Ters akımlı dner rejeneratif ısı deđiřtirgeci, dner rejeneratr, ısıl depolama tip ısı deđiřtirgeci, hava ilk ısıtıcıları, ısıl tekerlekler, etkenlik.

Bilim Kodu : 625.04.05

ACKNOWLEDGEMENTS

The author wishes to express his gratitude to Assoc. Prof. Dr. Cemil YAMALI for his friendly assistance, valuable guidance and supervision throughout this thesis.

I am also grateful to Dr. Murat SÖNMEZ for his kind helps during this study.

Sincere thanks are due to Salih Zeki CEYLAN (from ALARKO-ALSAC Inc. in İstanbul) for the supplement documents that he provided.

I wish to express my thanks to chief of the machine shop Mr. Mehmet ÇAKMAK for his close cooperation in manufacturing, and thanks to machine shop technicians for carefull machining parts.

Particular thanks are due to Mr. Veysel GÜN and his staff for their help in the construction of the experimental set-up.

The author's thanks are also due to Mr. Ali GEZER for his help in the printing of the thesis.

TABLE OF CONTENTS

	Page
ABSTRACT.....	iii
ÖZET.....	v
ACKNOWLEDGEMENTS.....	vii
TABLE OF CONTENTS.....	viii
LIST OF TABLES.....	x
LIST OF FIGURES.....	xi
NOMENCLATURE.....	xiv
1. INTRODUCTION.....	1
1.1. Classification of Heat Exchangers.....	2
1.2. Description of Rotary Type Regenerative Heat Exchanger.....	9
2. LITERATURE SURVEY.....	16
3. EXPERIMENTAL APPARATUS.....	25
4. EXPERIMENTAL PROCEDURE AND RESULTS.....	38
4.1. Procedure.....	42
4.2. Evaluation of the experimental Data.....	43
4.3. Results.....	48
5. DISCUSSION AND CONCLUSION.....	65
5.1. Conclusions.....	68
5.2. Recommendations.....	69

LIST OF REFERENCES.....	70
APPENDICES	
A. SPECIFICATIONS OF INSTRUMENTS.....	75
B. CALCULATION OF FLOW RATE.....	79
C. CALCULATION OF THE CONVECTION HEAT TRANSFER COEFFICIENT.....	82
D. A SAMPLE EVALUATION OF EXPERIMENTAL DATA.....	87
E. ENGINEERING DRAWINGS OF THE ROTARY TYPE REGENERATIVE HEAT EXCHANGER.....	91

LIST OF TABLES

Table	Page
3.1 Matrix material made of composite material.....	28
3.2 Matrix material that contains aluminum.....	28
C.1. Pressure Drop Across the Rotary Regenerator for the Matrix Geometry of the Galvanized Sheet Iron Rotor.....	83
C.2. Pressure Drop Across the Rotary Regenerator for the Matrix Geometry of the Galvanized Sheet Iron + Aluminum Sheet Rotor.....	83

LIST OF FIGURES

Figure	Page
11. Classification of Heat Exchangers.....	5
1.2. Rotary Regenerator Types.....	7
1.3. Fixed-Matrix Regenerator.....	7
1.4. Heat Transfer Surface Area Density Spectrum of Exchanger Surfaces.....	8
1.5. A Disk Type Rotary Regenerator.....	10
1.6. Rotary Regenerator Equipped with Purge Section to Clear Contaminants from the Heat Transfer Surface.....	14
3.1. Schematic Diagram of the Rotary Regenerative Type Heat Exchanger Test Set-up.....	26
3.2. Thermal Conductivity of Some Metals.....	27
3.3. General Views of the Rotary Regenerator and the Test Set-up.....	35
3.4. General View of the Reductor and the Test Set-up.....	36
3.5. General View of the Copper-Constantan Thermocouples System.....	37
3.6. General View of the Digital Tachograp System.....	37
4.1. Schematic Diagram of Thermocouple System.....	44
4.2. Rotary Regenerator Effectiveness (ϵ) as a Function of C_r^* and NTU for $C^* = 1$ and Galvanized Sheet Iron.....	51

4.3. Rotary Regenerator Effectiveness (ϵ) as a Function of C_r^* and NTU for $C^* = 1$ and Galvanized Sheet Iron + Aluminum Sheet.....	52
4.4. Rotary Regenerator Effectiveness (ϵ) as a Function of C^* and NTU for $C_r^* = 13$ and Galvanized Sheet Iron	53
4.5. Rotary Regenerator Effectiveness (ϵ) as a Function of C^* and NTU for $C_r^* = 13$ and Galvanized Sheet Iron +Aluminum Sheet	54
4.6. Rotary Regenerator Effectiveness (ϵ) as a Function of C^* , C_r^* and NTU for rpm = 2.7 and Galvanized Sheet Iron	55
4.7. Rotary Regenerator Effectiveness (ϵ) as a Function of C^* and NTU for $C_r^* = 13$ and Galvanized Sheet Iron	56
4.8. Rotary Regenerator Effectiveness (ϵ) as a Function of C^* and NTU for $C_r^* = 13$ and Galvanized Sheet Iron + Aluminum Sheet.....	57
4.9. Rotary Regenerator Effectiveness (ϵ) as a Function of C_r^* for $C^* = 1, NTU = 1.62$ and Galvanized Sheet Iron	58
4.10. Rotary Regenerator Effectiveness (ϵ) as a Function of C_r^* for $C^* = 1, NTU = 1.62$ and Galvanized Sheet Iron + Aluminum Sheet.....	59
4.11. Rotary Regenerator Effectiveness (ϵ) as a Function of N, C_r^* for $C^* = 1, NTU = 1.62$ and Galvanized Sheet Iron.....	60

Figure	Page
4.12. Temperature Distributions in the Rotary Regenerator for $C^* = 1, C_r^* = 13, NTU = 8.2$ and Galvanized Sheet Iron.....	61
4.13. Temperature Distributions in the Rotary Regenerator for $C^* = 1, C_r^* = 0.9, NTU = 1.15$ and Galvanized Sheet Iron.....	62
4.14. Temperature Distributions of the Hot Fluid at the Exit of the Rotary Regenerator for $C^* = 1, C_r^* = 0.9,$ $NTU = 1.62$ and Galvanized Sheet Iron.....	63
4.15. Temperature Distributions of the Cold Fluid at the Exit of the Rotary Regenerator for $C^* = 1, C_r^* = 0.9,$ $NTU = 1.62$ and Galvanized Sheet Iron.....	64
A.1. Power Distribution of the Variac.....	77
B.1. Distribution of the Velocity in the Inlet Tube.....	80
C.1 Fanning friction factor as a Function of Reynolds Number for the Matrix Geometry of the Galvanized Sheet Iron Rotor	84
C.2 Fanning friction factor as a Function of Reynolds Number for the Matrix Geometry of the Galvanized Sheet Iron + Aluminum Sheet Rotor.....	85

NOMENCLATURE

Symbol

A	Heat transfer surface area (m^2)
A_{cr}	Cross-sectional area of the matrix material (m^2)
A_{fr}	Frontal area (m^2)
A_0	Free flow area (m^2)
b	Thickness of the matrix material (m)
C	Fluid heat capacity rate, $\dot{m}c_p(W/^\circ C)$
C^*	Heat capacity rate, ratio of the fluids, C_{min}/C_{max} (dimensionless)
c_p	Specific heat of fluid at constant pressure ($J/kg^\circ C$)
C_r	Heat capacity rate of a rotating matrix ($W/^\circ C$), $C_r = M_w \cdot c_w \cdot N$
C_r^*	Matrix heat capacity rate ratio, C_r/C_{min} (dimensionless)
c_w	Specific heat of the matrix material ($J/kg^\circ C$)

Symbol

D_{hyd}	Hydraulic diameter (m)
D_R	Diameter of the rotary regenerator (m)
d_r	Diameter of rotor axle (m)
f_f	Fanning friction factor
G	Mass velocity ($\text{kg}/\text{m}^2 \text{ sec}$)
g	Gravitational acceleration (m/sec^2)
h	Convection heat transfer coefficients ($\text{W}/\text{m}^2\text{°C}$)
j	Colburn factor
k	Thermal conductivity ($\text{W}/\text{m}^{\circ}\text{C}$)
L	Length of the rotary regenerator (m)
M_w	Total mass of the matrix (kg)
\dot{m}	Mass flow rate (kg/sec)
N	Rotational speed of the rotor (rev/sec)
NTU	Number of heat transfer units, $\text{NTU} = \frac{1}{\frac{C_{\min}}{(hA)_H} + \frac{C_{\min}}{(hA)_c}}$
Pr	Prandtl number
Re	Reynolds number

r	Radius of flanged tube (m)
r_{hyd}	Hydraulic radius (m)
St	Stanton number
T	Temperature (C)
T^*	Nondimensional temperature

$$T^* = \frac{T - T_{c,i}}{T_{h,i} - T_{c,i}}$$

t^*	Nondimensional angular position
V	Total volume of regenerator matrix (m ³)
v	Velocity (m/sec)
z^*	Nondimensional axial distance
Q	Volume flow rate (m ³ /sec)
β	Heat transfer surface area density, A/V , (m ² /m ³)
ϵ	Regenerator effectiveness
ρ	Density (kg/m ³)
μ	Dynamic viscosity (kg/m sec)
σ	Porosity, A_o/A_{fr} , (dimensionless)

Subscripts

c	Cold side, cold fluid
c,i	Cold fluid at the inlet of the regenerator

c,o	Cold fluid at the exit of the regenerator
H	Hot side, hot fluid
H,i	Hot fluid at the inlet of the regenerator
H,o	Hot fluid at the exit of the regenerator
max	Maximum
min	Minimum
w	Wall



CHAPTER 1

INTRODUCTION

Because of the increase in the cost of energy, research in that field gained momentum. Producing energy (in all form) is costly, difficult and in addition to that it is also necessary to transfer it to the location where it is consumed.

The recovery of the waste energy especially for the situation in which it can be reused at the place of recovery is quite important and results in very important saving in terms of money and also in terms of environmental effects. For that reason, systems designed to recover energy is spreading more and more. Rotary type regenerative heat exchanger which is one of the devices used to recover waste energy is widely used not only because it is easy to install in the existing systems but also it has a small volume and very practical as far as the operating is concerned. Because of its wide range of application, researches concentrated their efforts on rotary type regenerative heat exchanger.

Some of the known application areas of the rotary type regenerative heat exchanger are the followings : large and small air conditioning and ventilation systems, large factories, energy systems and combustion and burning equipment.

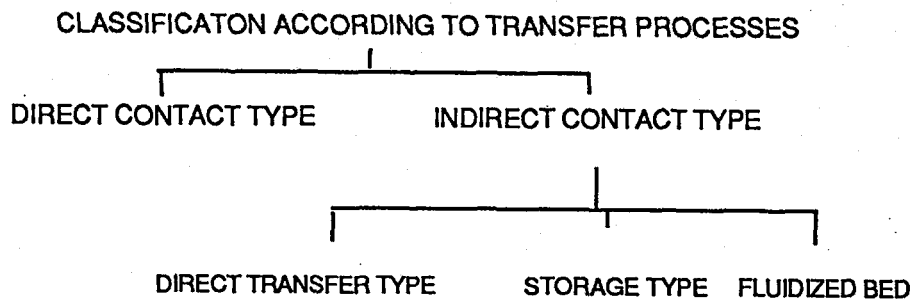
1.1. CLASSIFICATION OF HEAT EXCHANGERS

A heat exchanger is a device which provides heat exchange between two or more fluids at different temperatures. Heat transfer between the fluids takes place through a separating wall. Since the fluids are separated by a heat transfer surface, they do not mix. Common examples of such heat exchangers are the shell-and-tube exchangers, automobile radiators, condensers, evaporators, air preheaters, and "dry" cooling towers. If no phase change occurs in any of the fluids in the exchanger, it is sometimes referred to as a sensible heat exchanger. Usually there are no internal thermal energy sources in a heat exchanger, except fired heaters, electric heaters, and nuclear fuel elements. If the fluids are immiscible, the separating wall may be eliminated, and the interface between the fluids serves as a heat transfer surface as in a direct contact heat exchanger.

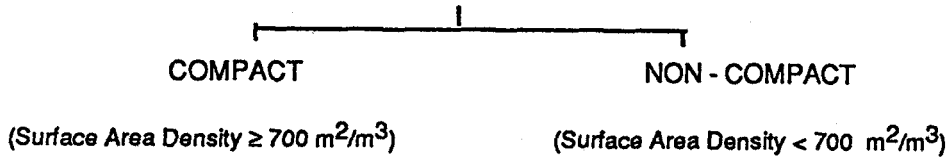
A heat exchanger consists of the active heat exchanging elements such as a core or a matrix containing the heat transfer surface, and passive fluid distribution elements such as headers, manifolds, tanks, inlet and outlet nozzles or pipes, or seals. Usually there are no moving parts in a heat exchanger; however, there are exceptions such as a rotary regenerative exchanger, in which the matrix is mechanically driven to rotate at some design speed.

The heat transfer surface is the surface of the exchanger core which is in direct contact with fluids and through which heat is transferred by conduction. That portion of the surface which also separates the fluids is referred to as primary or direct surface. To increase heat transfer area, appendages known as fins may be connected to the primary surface to provide extended, secondary, or indirect surface. Fins may form flow passages for the individual fluids but do not separate the fluids.

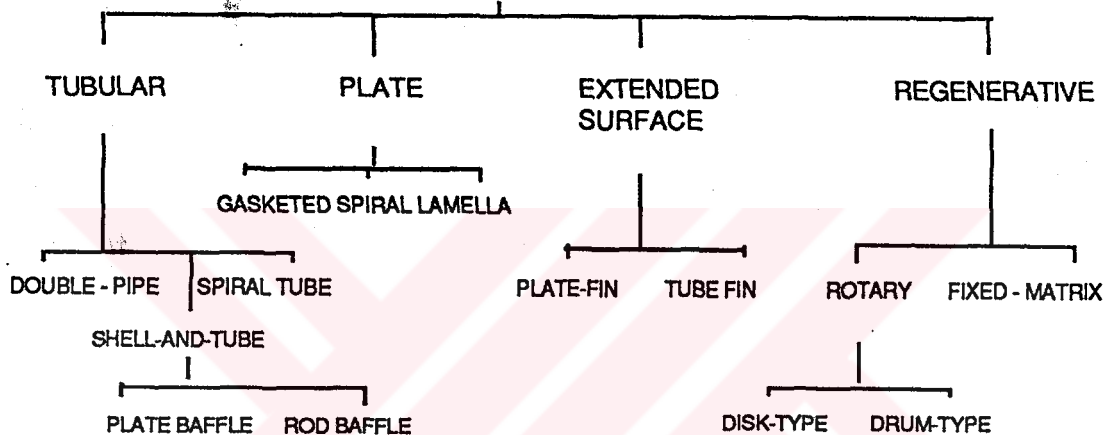
Heat exchangers are used in the process, power, automotive, air conditioning, refrigeration, cryogenics, heat recovery, alternate fuels, and manufacturing industries, as well as key components of many products available in the marketplace. These heat exchangers may be classified according to the transfer processes, degree of surface compactness, construction features, flow arrangements, number of fluids, and fluid phase changes or process function. These classifications are summarized in Figure 1.1 [1].



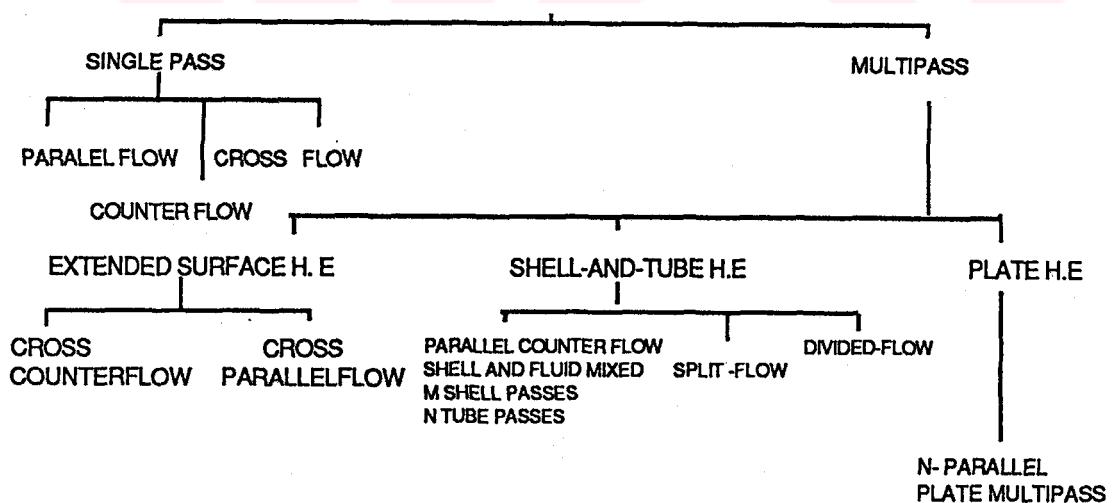
CLASSIFICATION ACCORDING TO SURFACE COMPACTNESS



HEAT EXCHANGER CLASSIFICATION ACCORDING TO CONSTRUCTION



HEAT EXCHANGER CLASSIFICATION ACCORDING TO FLOW ARRANGEMENTS



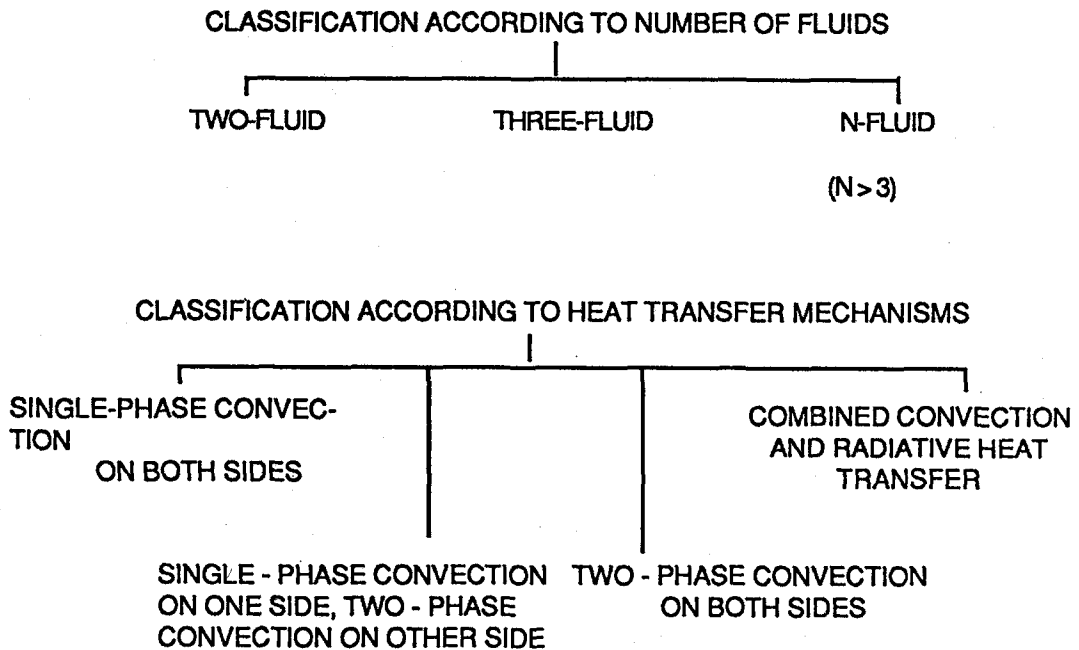


Figure 1.1 Classification of Heat Exchangers.

According to transfer processes used in the heat exchanger a rotary type regenerative heat exchanger is a storage type heat exchanger. In storage type heat exchangers, hot and cold fluids flow through the same passages alternately. While the hot fluid flows through a passage, thermal energy is transferred from the hot fluid to the wall of the channels that the fluid flows through, and the energy is stored in the wall. Later, as the cold fluid starts flowing through the same passage, energy stored in the wall is given to the cold fluid. This heat exchange continues periodically. i.e. heat is not transferred through the wall but is alternately stored and rejected by it.

Regenerative type heat exchangers can be divided into two groups according to construction; rotary regenerators and fixed-matrix regenerators. Furthermore rotary regenerators are subdivided into disk

type and drum type. In a rotary regenerator, matrix rotates continuously with a constant fraction of it being in the hot-fluid stream and the remaining fraction being in the cold-fluid stream. The axis of rotation is parallel to the fluid flow. The duration of the time during which one rotation is completed is called "total period". The matrix of a regenerator is made of a large number of flow passages covered by matrix walls, like a honeycomb. In a period of rotation every matrix passage (or channel) passes through the hot fluid stream and then the cold fluid stream. As the rotation of regenerator continues and as the hot fluid flows through the matrix channels, certain fraction of its internal energy is transferred to the matrix walls and is stored there. Then, due to the rotation the same matrix channels, this time, exposed to the flow of the cold fluid and the energy which is stored in the wall is transmitted to the cold fluid. This exchange is repeated periodically.

In a disk type rotary regenerator the matrix is in the form of a disc and the hot and cold fluids flow axially as in Figure 1.2 a. On the other hand in a drum type rotary regenerator, the matrix is in the shape of an annular drum and the fluids flow radially (Figure 1.2b) [2].

A fixed - matrix regenerator consists of a storage matrix through which hot and cold fluids alternatively travel. When hot fluids travel through the matrix, heat which is stored in the matrix is released. After a certain period of time the hot fluid flow is shut off and cold fluids are circulated, picking up heat from the matrix.

Another classification of heat exchangers is made according to the "compactness" criterion as, compact and non - compact heat exchangers.

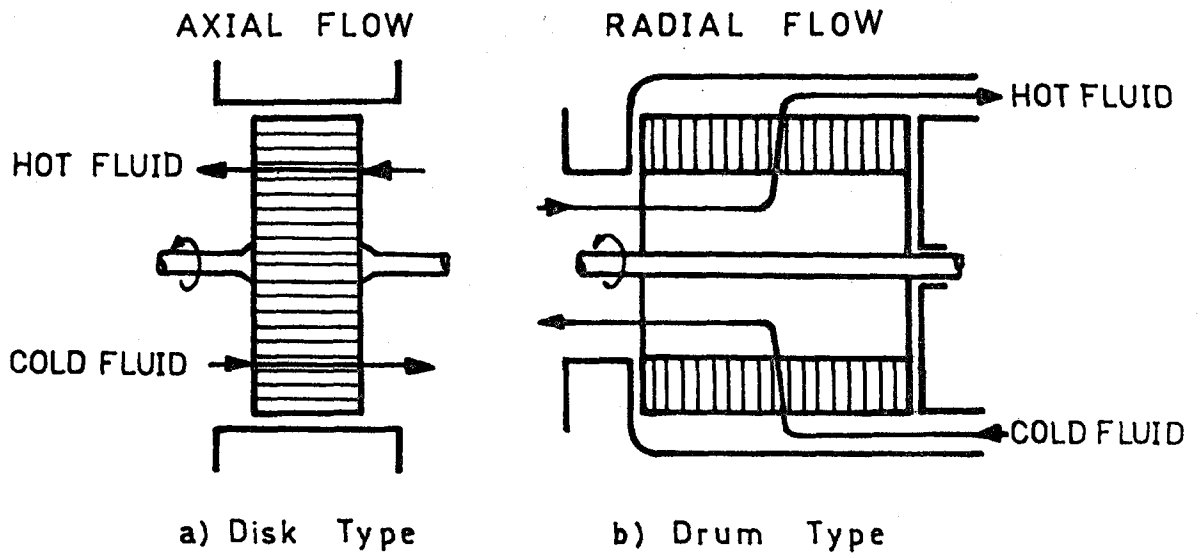


Figure 1.2. Rotary Regenerator Types

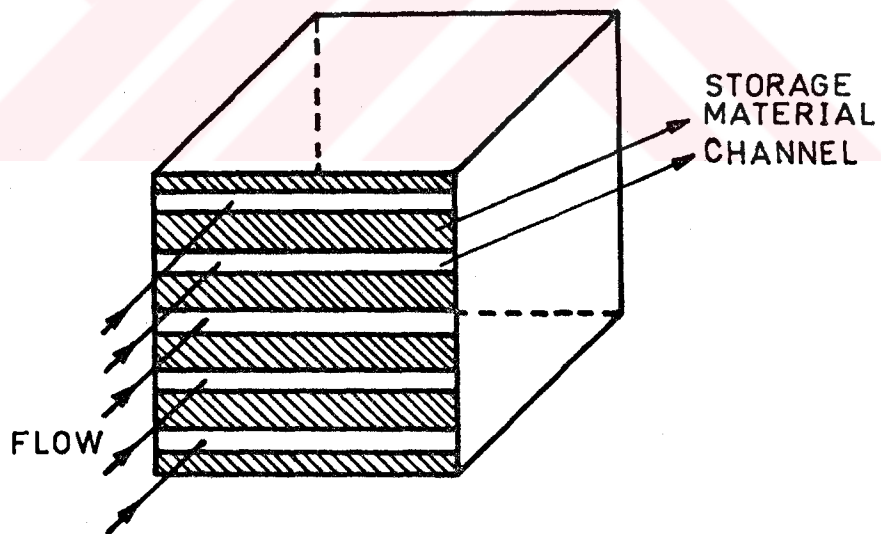


FIGURE 1.3. Fixed - Matrix Regenerator

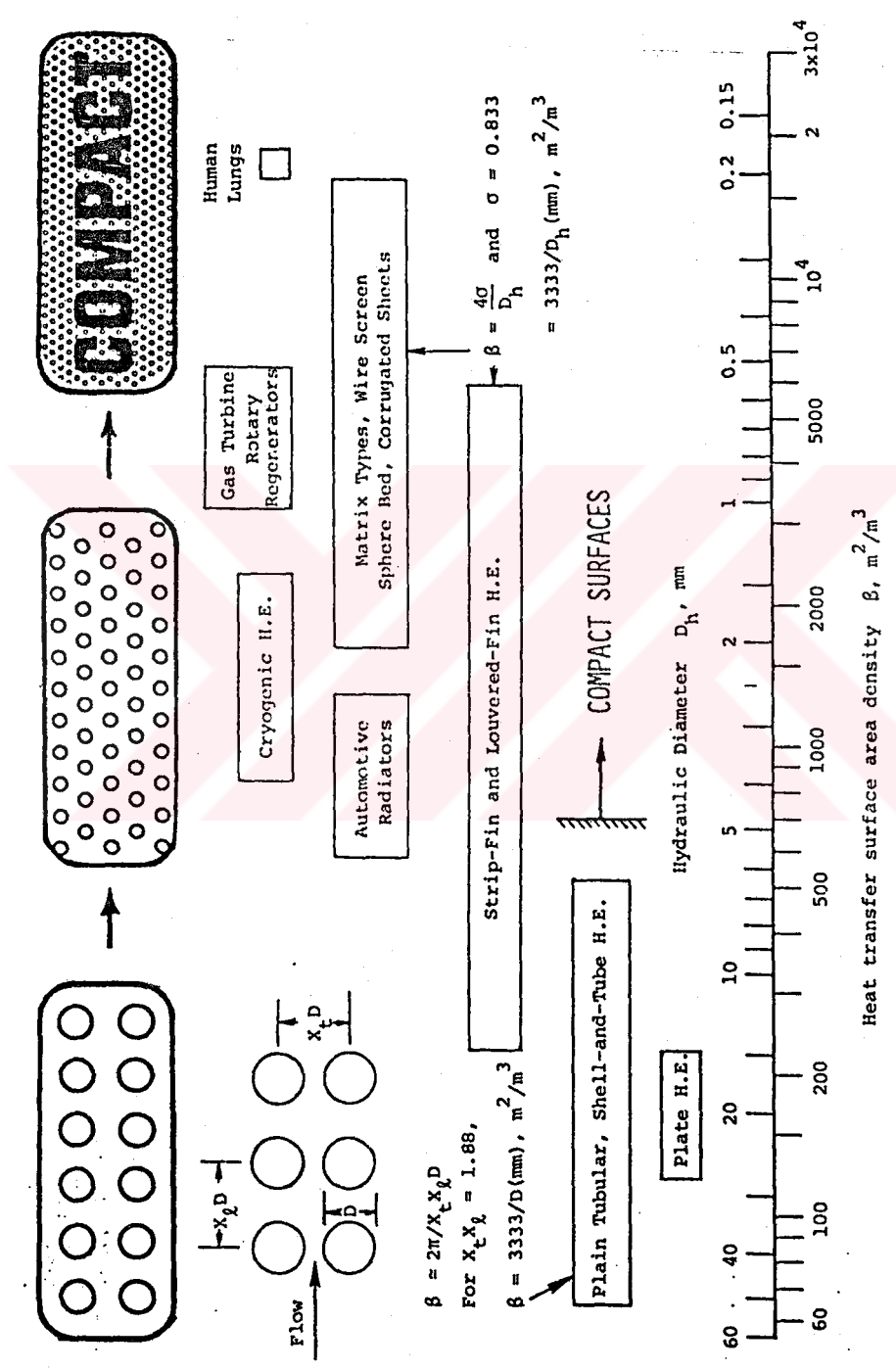


Figure 1.4. Heat Transfer Surface Area Density Spectrum of Exchanger Surfaces [1].

The ratio of the heat transfer surface area to the total volume of the heat exchanger is defined as "surface area density, β ". If β is greater than $700 \text{ m}^2/\text{m}^3$ then that exchanger is called "compact heat exchanger".

In practice the surface area density for rotary regenerators is taken between 700 and $6600 \text{ m}^2/\text{m}^3$. In that respect the rotary regenerators are highly compact heat exchangers. The convective heat transfer coefficient for gaseous fluids is much smaller than the liquids. Therefore, in order to reduce the total volume of a gas-to-gas heat exchanger it is necessary to use compact type heat exchanger.

1.2. DESCRIPTION OF ROTARY TYPE REGENERATIVE HEAT EXCHANGERS

In this study disk type rotary regenerators are considered. As it is explained in the preceding part, rotary regenerators are highly compact heat transfer devices. A disk type rotary regenerator simply consists of the disk which contains ondulated sheets with many small channels between them (Figure 1.5). These channels are called "matrix" and constitute heat transfer surfaces and flow passages. The rotor in which the matrix is packed is placed in a duct. The inlet and exit to the matrix is so arranged that hot and cold fluids flow paralel to the axis of rotation of the rotor and due to many paralel channels in the matrix fluid streams do not mix with each other and a certain number of channels are exposed to hot stream while the

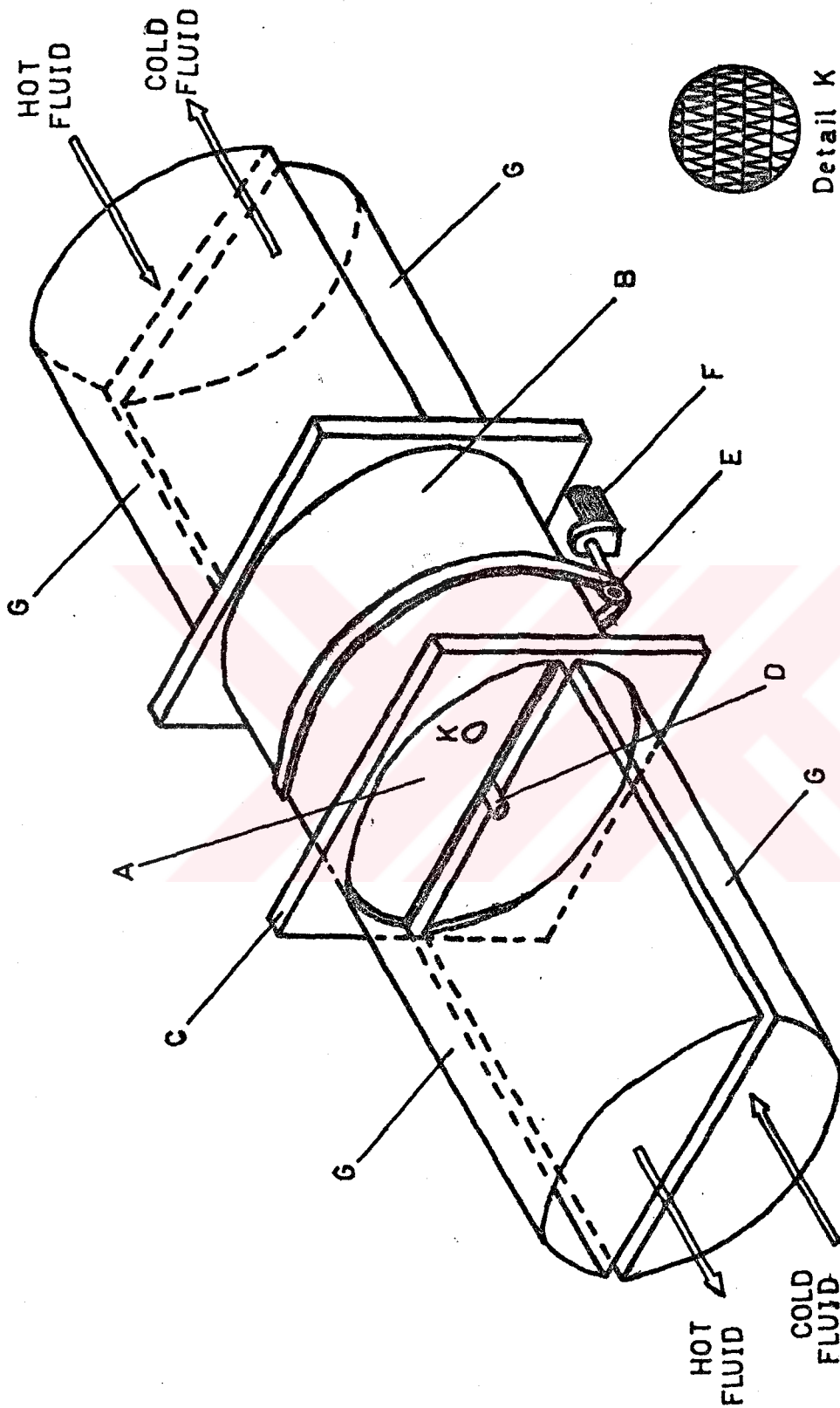


Figure 1.5. A Disk Type rotary Regenerator : A, Heating Surface Elements. B, Rotor in which the Elements are Packed. C, Housing in which the rotor rotates. D, Support and Bearing Assemblies. E, Belt-pulley system. F, Drive Mechanism. G, Hot and Cold Fluid Ducts.

remaining channels are exposed to the cold stream. As the disk is slowly rotated the many channels of the matrix is exposed to hot and cold gases alternately.

In the literature, a disk type rotary regenerator is sometime called "Heat Wheels, Thermal Wheels, Regenerative Type Air Preheater, Ljungstrom HeatExchanger, Air-to-Air Heat Recovery Wheels".

The rotary regenerators are used in a variety of applications, such as in base-load electric power stations, in heating plants, in the recovery of waste thermal energy, in gas turbines, in heating, refrigeration, ventilating and air-conditioning systems where the moisture in the exhausted air condenses in the matrix during the hot period and re-evaporates as it comes into contact with the supplied air. The regenerator which is designed for that purpose is called "wet regenerator" [3].

There are four matrix types which are used in rotary regenerators. The first type consists of a metal frame packed with a core of knitted mesh stainless steel or aluminum wire, resembling to a pot-scraper. The second, called a laminar matrix, is fabricated from corrugated metal sheets with parallel flow passages between them by using some special production techniques as explained in reference [17]. The third variety is also a laminar matrix but is constructed from a ceramic matrix of honeycomb configuration. This type is used for higher temperature applications. In the fourth variety of the rotary matrix types, again laminar flow regimes are obtained but the flow passages are coated with a hygroscopic material so that latent heat may be recovered. In a hygroscopic heat wheel, the hot fluid

stream gives part of its water vapor (moisture) to the coating; the cold gases which enter the wheel to be heated are drier than the matrix coat and a part of the absorbed water is given to the cold fluid.

As reported by Iliffe [4], in 1816 a heat regenerator was proposed and constructed by Dr. Stirling in connection with a regenerative hot-air engine. Such heat regenerators were mainly used as furnace air preheaters until the development of gas turbine applications required compact heat exchangers of high thermal efficiency ratio and low pressure drop. Since the late 1960 s the costs of generating thermal energy has been high compared to other sources of heat energy and more attention has been given to those methods which have stressed the recovers of waste energy. There is, for example, solar energy which must be temporarily stored during the day for use at later peak demand periods. Other efforts have been directed at recovering the waste energy in the heating and cooling systems of buildings, a source which did not appear to be economically significant during prior years.

There are three main advantages of the rotary regenerative type heat exchanger compared to the direct-transfer type (recuperator) : [2,5]

1. A much more compact heat transfer surface can be obtained.
2. The heat exchanger is less expensive per unit heat transfer area.
3. Because of the periodic flow reversals the surface has the self-cleaning ability. In recuperative heat exchangers, the fluids flow

in separate channels and always in the same direction and same deposits therefore accumulate and lead to decreased heat transfer and increased pressure drop. In regenerative exchangers, the hot and cold fluids flow in opposite direction (to obtain counter flow operation) but alternately through the same channels. Therefore, any sooty deposits tend to be blown out by the succeeding cold fluid flow.

The major disadvantages of the rotary regenerators are the followings:

1. There is some mixing of the hot and cold fluids due to leakage and carry-over. If any purge sector (Figure 1.6) is not used then there must be some mixing of the fluids because, during the rotation of the matrix, the trapped hot fluid in the channels is carried to the cold side and at the same time by the same mechanism the cold fluid in the channels passes to the hot side. This type of leakage is called "carry-over leakage". This leakage decreases the effectiveness of the heat exchanger and also the toxic components in the hot fluid might pass to the supply air. (If this contamination is undesirable, the carry-over of the exhaust gas can be eliminated by adding a purge section, where a small amount of clean air is blown through the wheel and then exhausted to the outside) [3,6].

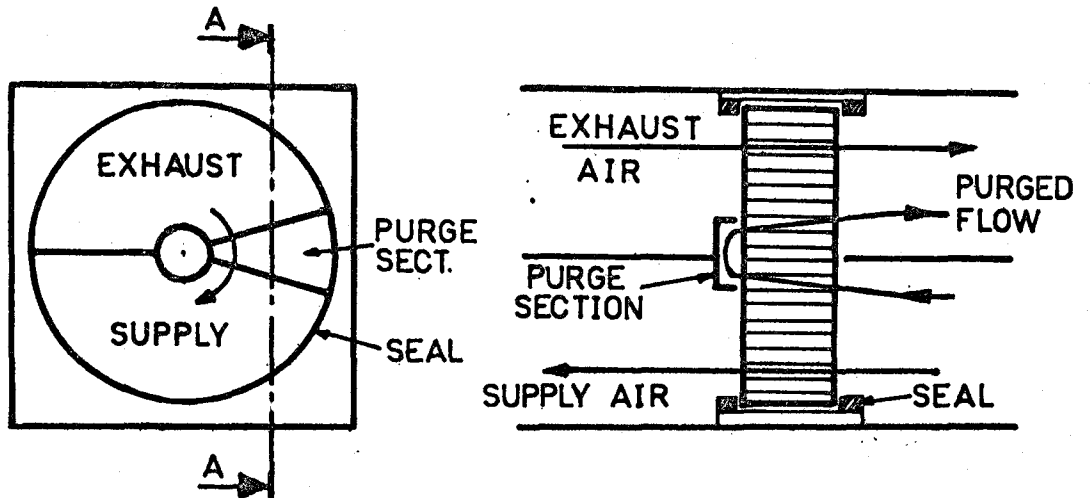


Figure 1.6. Rotary Regenerator Equipped with Purge Section to clear Contaminants from the Heat Transfer Surface.

2. If the fluids are at different pressures, as in the gas-turbine regenerators, the sealing problem becomes important. Due to sealing design limitations the maximum pressure difference between the hot and cold fluids should be less than four bars. However, for the regenerators which are used as air preheater in boilers and furnaces, the sealing problem is not so important because the pressures of the hot and cold fluids (combustion air and flue gases) are approximate equal to each other.
3. Due to high compactness, pressure losses are greater than those of the recuperators.

The objective of this thesis is to evaluate the performance of a counter-flow rotary regenerator. To achieve this goal a rotary type

regenerative heat exchanger is designed, constructed and tested in the laboratory. Effects of various parameters on the performance of the regenerator is studied in a systematic way.



CHAPTER 2

LITERATURE SURVEY

As previously mentioned fixed-matrix regenerators were used in the iron industry to preheat furnace intake air. Demands related to the use of gas turbines in power plant applications encouraged research on rotary regenerators and most of the theories related to these regenerators were extensions of those for fixed-matrix types. Thus, the analysis and review of rotary regenerators which follows is preceded by a survey of analysis of fixed-matrix regenerators.

The idea of a rotary regenerative air preheater was born sixty eight years ago. Frederick Ljungstrom invented and patented the design in 1922.

The earliest theoretical analysis related to the thermal energy storage in a fixed matrix regenerator was made by Anzelius in 1926, then again by Nusselt in 1927, by Hausen in 1927-1929 and finally by Schumann in 1929. They studied the storage type heat exchange by considering the following cases : [7]

1. The length of the heating or cooling period is infinitely small, i.e. the regenerator is switched to hot or cold fluid flow infinitely often. (This assumption corresponds to infinitely large rotational speed for rotary regenerators.

2. The thermal conductivity of the solid is infinitely large.

3. The thermal conductivity of the solid is infinitely large in the direction parallel to the gas flow and finite in the direction normal to the gas flow.

4. The thermal conductivity of the solid is zero in the direction parallel to the gas flow and infinitely large in the direction normal to the gas flow (longitudinal conduction is neglected).

5. The thermal conductivity of the solid is zero in the direction parallel to the gas flow and finite in the direction normal to the gas flow.

The first of these cases is investigated by Nusselt and Hausen. Hausen showed that for this case effectiveness of the regenerator is the same as the counterflow direct transfer type heat exchanger. The second case is studied by Nusselt. His calculations show that the performance of this type of regenerator would be rather poor. Obtaining solutions for the regenerator equations for the first, second and third cases are not so difficult. However, industrial applications of these cases are limited. The fourth case represents the regenerators which is made of corrugated long and thin metal sheets. Since the thickness of the metal walls is very small and thermal conductivity is quite large, the Biot number in the direction normal to the gas flow is very small. Therefore it can be assumed that, the thermal conductivity of the metal is infinitely large in that direction. However, since the length of the regenerator is very large and the crosssectional area is sufficiently small for the longitudinal conduction, the thermal conductivity of the wall can be considered as zero in the direction parallel to the gas

flow. The fifth case covers the fixed matrix regenerators which are made of refractory bricks and the rotary regenerators made of glass-ceramic materials. Unfortunately, the analytical solutions of the regenerator equations for the fourth and fifth cases are quite difficult even with the help of the large number of assumptions made to simplify the differential equations.

In 1953, Coppage and London proposed the ϵ -NTU method similar to that employed for direct transfer type heat exchangers to analyse the regenerators [8]. The advantages, in principle, of the periodic-flow type regenerators were explained briefly, and the mathematical difficulties of analysis of its performance in terms of a more exact theory were expressed. They re-evaluated the Hausen's and Nusselt's solutions in terms of non-dimensional parameters of the ϵ -NTU method.

Harper and Rohsenow studied the effect of rotary regenerator performance on gas-turbine-plant performance [9]. They showed the effect of leakages on regenerator effectiveness.

In 1958, Lambertson investigated performance factors of periodic flow heat exchangers [10]. Lambertson calculated the effectiveness of a rotary regenerator numerically by writing the energy balance equations for the elements. However he did not consider the governing differential equations of regenerators.

In 1964, Bahnke and Howard [11] studied the effect of longitudinal heat conduction on the performance of a rotary regenerator, numerically. They used the same method and finite difference scheme which was studied by Lambertson.

Kays and London [2] presented the following empirical correlation for the influence of C_r/C_{\min} on the effectiveness of a rotary regenerator for $\varepsilon < 90$ percent :

$$\varepsilon \approx \varepsilon_r [1 - 1 / (9 (C_r / C_{\min})^{1.93})]$$

where;

ε_r : Effectiveness of the counterflow recuperator

C_r/C_{\min} : Capacity rate ratio of the matrix material and the fluid that has lower heat capacity rate.

London [2,10] investigated the effect of longitudinal (axial) conduction on the effectiveness. He proposed a correction factor for effectiveness for approximately equal fluid capacity rates case as;

$$\frac{\Delta\varepsilon}{\varepsilon} \cong \frac{k.A_{cr}}{L.C_{\min}}$$

where; $\Delta\varepsilon$: Decrease of the effectiveness

k : Thermal conductivity of the matrix material

A_{cr} : Wall cross-section area for longitudinal conduction

L : Flow length (i.e. length of the regenerator in the axial direction).

London, Sampsell and Gowan [12] investigated the transient response of gas turbine plant heat exchangers in 1964. Solutions were provided in nondimensional graphical form for the transient response of the outlet fluid temperatures of a counterflow gas turbine regenerator, arising from a step input change of one of the inlet fluid temperatures. They used

an electrochemical analog to be able to solve the equations.

In 1977, Holmberg [13] investigated heat and mass transfer in rotary heat exchangers with nonhygroscopic matrix materials. In this study, a numerical method of the finite-difference type is applied to the steady-state performance under conditions of finite rotational speed and finite longitudinal heat conduction. Temperature and absolute humidity distributions are calculated for a set of rotary heat exchanger parameters typical in air conditioning, and temperature and humidity efficiencies are evaluated for different inlet air conditions.

In 1979, again Holmberg [14] analyzed heat and mass transfer in rotary heat exchangers with hygroscopic matrix materials.

In 1981, Leersum and Ambrose [15] derived a mathematical model of condensation, evaporation and heat transfer in a regenerator having a nonsorbing matrix.

London [16] investigated the influence of manufacturing tolerances on the heat transfer friction coefficients. He showed that manufacturing tolerances in passage dimensions have a significant influence on the overall heat transfer and flow friction behavior.

If the compactness (i.e. surface area density) is very high (which is usually the case in regenerators), the hydraulic diameters of the flow passages become very small (e.g. 0,5 mm). Therefore some special manufacturing techniques are necessary to produce very thin metal sheets or glass-ceramic surfaces. Vigor and Leibring [17] introduced the

manufacturing technique originated at the General Motors Research Laboratories in 1962 to manufacture the very thin metal sheets which are used in regenerator matrices. This process, which is called "metal peeling", peels a foil from a rotating metal billet. It is possible to obtain metal foils that have a thickness equal to 0,051 mm. with this technique.

Mondt [18] studied the effects of nonuniformity of the passages of the regenerator matrices. He predicted the convective transfer penalties and flow pressure drop gains by statistically combining nonuniform fin spacing and bulginess into a unique total channel deviation parameter.

Rapley and Webb [19] reported the experimental data related to the heat transfer performance of sine-duct type passages in laminar flow ceramic regenerator matrices (in recent years, uses thin strips of reaction-sintered silicon nitride (Si_3N_4)).

Parameters of design theory and surface geometry and applications of regenerative heat exchanger were investigated by London [20,21,22].

The economics of rotary regenerative type heat exchangers was investigated by Szabo [23] in 1967. In this study a complete cost study was showed how annual owning and operating costs justify the initial extra expense for rotary regenerator and run-around systems.

Dunkle and Maclaine-Cross [24] discussed the heat transfer, mass transfer and pressure drop characteristics of rotary regenerative sensible heat exchangers or regenerators. and in this study, the dimensionless parameters describing regenerator performance are expressed in terms of

the important design variables to simplify the comparison of alternative designs. Effectivity charts are presented for balanced and unbalanced flow. The advantages of the paralel plate regenerator developed by the authors are discussed and a simple design procedure is given. Heat recovery from exhaust air in air conditioning systems using rotary regenerators is common in the United States of America and Canada and it is shown that installations in Australia are well justified economically.

Basic heat transfer and flow friction design data are presented for straight, triangular passage, glass-ceramic heat exchanger surfaces by London, Young and Stang [25].

A model for calculating heat transfer in certain types of rotary heat exchangers is investigated which allows for a simple way of specifying the main design parameters under given thermal conditions by Kern [26].

The performance of a counter flow, rotary heat exchanger operating with either transient or nonuniform inlet temperatures is investigated by Brandemuehl and Banks [27]. In this study, A finite difference model of the governing differential equations, using finite transfer coefficients, is employed to obtain a detail numerical analysis of heat exchanger performance. Results for the complete range of matrix to fluid capacity rate ratio are presented for a balanced and symmetric regenerator. At moderate capacity rate ratios, the numerical analysis predicts unusual temporal periodicity in transient response. An experimental analysis has also been conducted using a counterflow, parallel passage, rotary heat exchanger made from polyester film. The results are used to substantiate predictions of

the numerical model.

A model of rotary heat and mass exchangers with infinite transfer coefficients was theoretically studied by Bulck, Mithchell and Klein [28]. In this study, the continuity and energy conservation equations for one-dimensional transient flow are established and analyzed. Solutions to the equations are obtained by the method of characteristics and the shock wave method.

In 1985, again Bulck, Mitchell and Klein [29] investigated a finite-difference model for performance prediction of rotary dehumidifier with finite transfer coefficients in combination with the ideal dehumidifier model to establish effectiveness correlations.

Exit gas temperature responses of the counterflow rotary regenerator are found for a unit step increase of the inlet temperature of either gas by Romie [30]. In this study, an analytic solution applicable during the first part of the transient shows that the responses cannot be smooth. The overall response is found by dividing the regenerator disk into pie-shaped segments and approximating the area-mean gas temperature leaving a segment as the temperature of the gas leaving a small regenerator located at the center of the segment. The method is shown to give good accuracy and is in agreement with predictions of the analytic solution.

Skrepko [31] investigated transport phenomena in rotary heat

exchangers. In this study, two models describing transport phenomena in rotary heat exchangers are considered; one disregarding and the other including heat conduction in the matrix. Both models are described by the system of energy conservation equations which is solved by analytical methods. On the basis of these solutions the effect of the matrix longitudinal heat conduction on the temperature fields of gases and matrix is studied.

Atthey [32] investigated an approximate thermal analysis for a regenerative heat exchanger. The results are compared with a finite difference solution of the regenerator problem for sets of plant data.



CHAPTER 3

EXPERIMENTAL APPARATUS

Rotary regenerative heat exchanger transfers heat and fluid moisture by rotating continuously from hot fluid stream to cold stream. The cold fluid passes through the other half of the rotor of the rotary regenerator. In the counter-flow-type regenerator hot and cold fluid flow alternately through the small channels in the wheel in opposite directions.

The Rotary type Regenerative Heat Exchanger is designed and constructed in the heat transfer laboratory of Middle East Technical University and has the following components; Housing, frame, matrix, shaft, drive belt, drive motor and seals.

Components of the Experimental Apparatus:

In addition to the Rotary Regenerator, the experimental apparatus consist of four air ducts used for hot air inlet and exit and cold air inlet and exit, electrical heater that can increase the temperature of the incoming air up to 75 °C, two fans for hot and cold air streams, connectors between the fan and the pulleys and speed regulator made of belts, pulleys and wheels. A very important component of the rotary type regenerative heat exchanger is matrix material since it is the main component that stores and transfers heat.

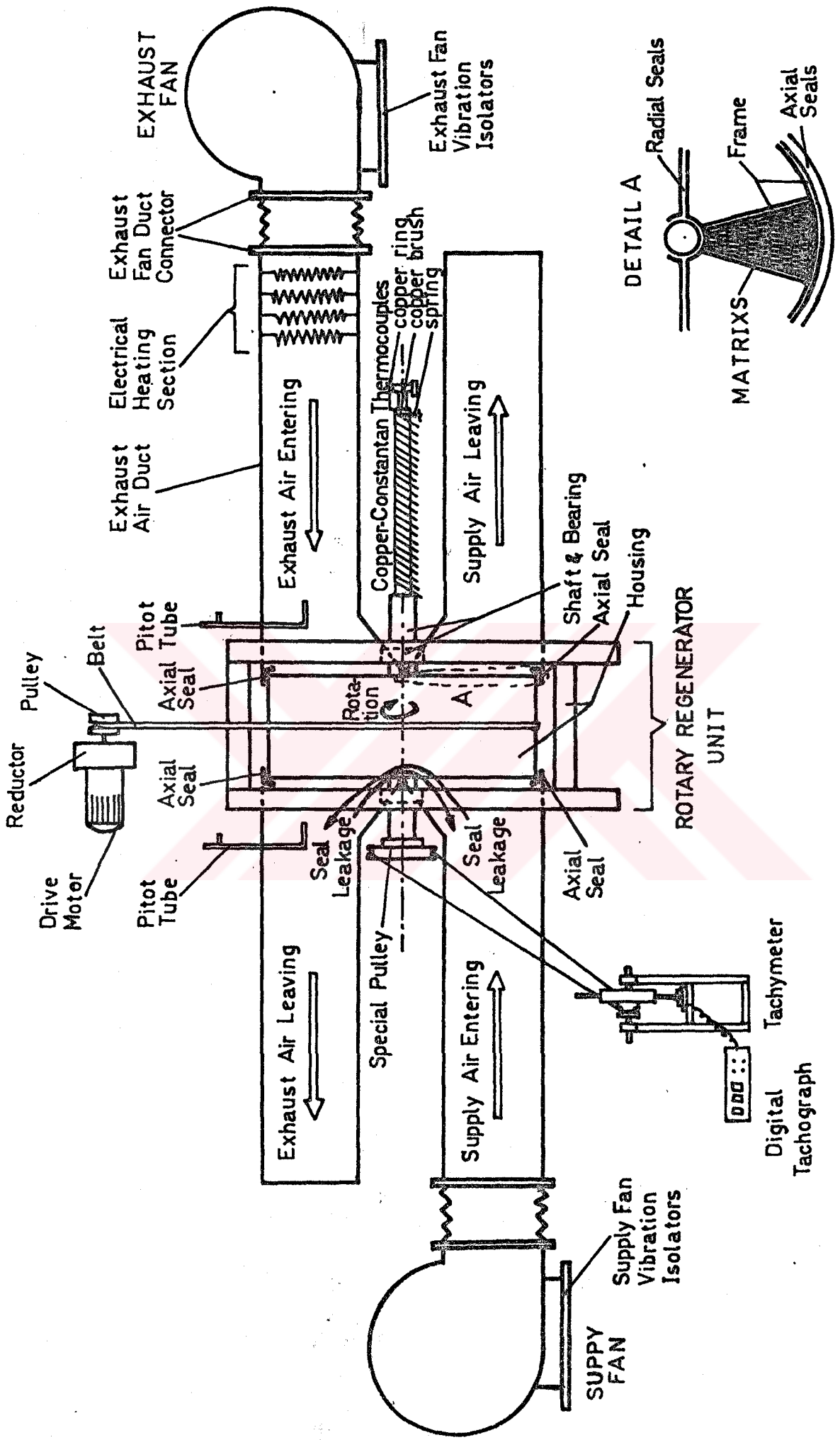


Figure 31. Schematic Diagram of the Rotary Regenerative Type Heat Exchanger Test Set-up

Matrix Material :

The material used for the construction of the matrix are mentioned in section 1.2 If the working temperature is not very high the material shown in the following tables (Table 3.1 and 3.2) are suitable as matrix material.

The composite material consists of different silicate based substances burnt together to form a composite. It is incombustible and extremely resistant to acid and basic environments as well as to marine atmospheres The Composite material contains no metal and that's why it is uncorrodable.

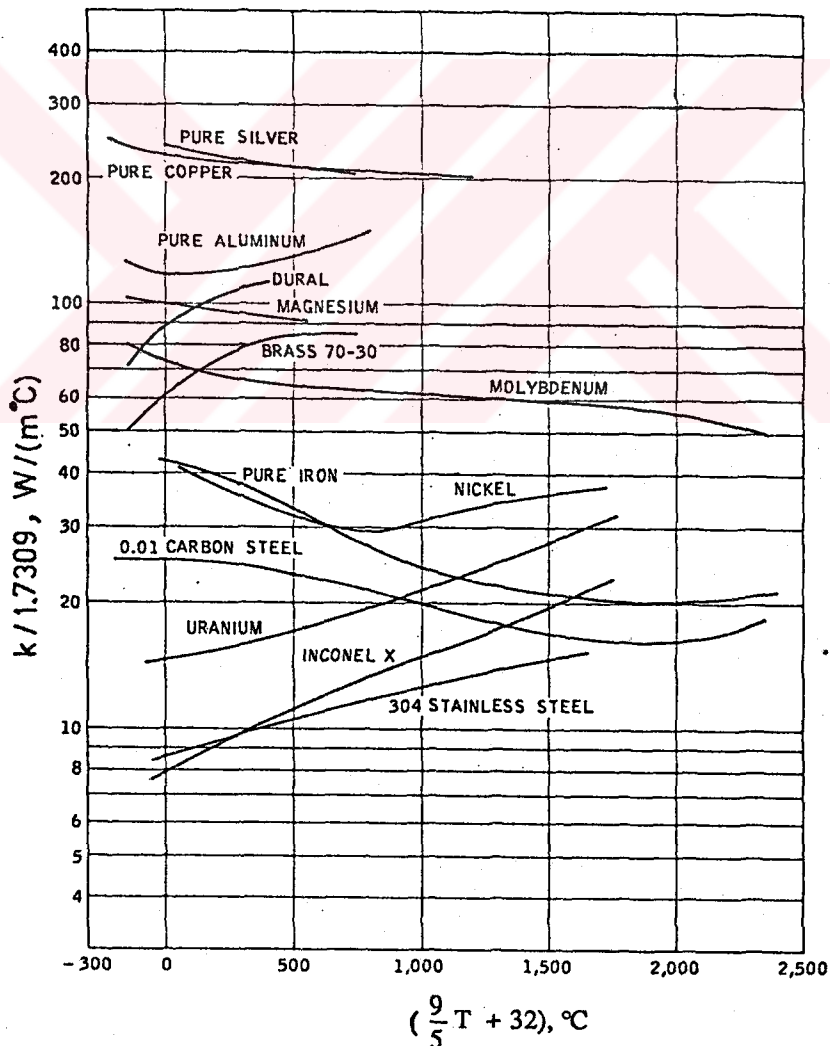


Figure 3.2 Thermal Conductivity of Some Metals [2].

Property	Temperature area °C	Kind of application
Hygroscopic	< 75	For comfort and moisture and cooling recovery. Big city environments, corrosive environments, sea-and coast climate.
Non-hygroscopic	<75, < 150, < 200	Industrial environments and/or higher temperatures, big city environments, corrosive environments, sea-and coast climate

Table 3.1 Matrix material made of composite material.

properties	Temperature area °C	Kind of application
Pure aluminium Non-hygroscopic	< 75	Exhaust air with solvents and/or dry dust. Atmosphere without risk for corrosion.
Pure aluminium Hygroscopic	< 75	Comfort. Atmosphere without risk for corrosion.
Al. alloy Hygroscopic	< 75	Comfort Atmospheres with small risk for corrosion.
Pure aluminium Non-hygroscopic	< 75	Exhaust air with solvents and/or dry dust. Industrial plants in atmospheres without risk for corrosion
Al. alloy Non-hygroscopic	< 75 < 130	Exhaust air with solvents and/or dry dust. Industrial plants with small risk for corrosion.

Table 3.2 Matrix material that contains aluminum.

In general as a matrix material corrosion-resistant high thermal conductivity sheets are used. The thickness of the sheet should be as small as possible for better heat transfer characteristics. In this thesis 0.35 mm thick galvanized sheet iron and 0.40 mm thick Aluminium sheet are used as matrix material.

HOUSING :

The housing of the regenerator is made of iron profiles and connections are made of bolts rather than welding. That makes the assembly and disassembly of the set-up quite practical. All sides of the regenerators are closed by means of corrosion resistant 1.5 mm galvanized sheet iron. The design is achieved in such a manner that an easy excess into the rotor of the regenerator becomes possible whenever a need occurs.

FRAME:

The frame is constructed by using 2.5 mm sheet iron flat bar (20x5) and steel center of it has twelve sections so that when it is loaded with the matrix material it has sufficient strength to resist centrifugal and other forces during the operation of the rotary heat exchanger.

In general, rotary heat exchangers with large dimensions should be designed by giving utmost consideration to the strength but in small rotary heat exchangers even a sheet iron surrounding the matrix becomes sufficient.

SHAFT AND BEARING :

The shaft of the rotor of the rotary heat exchanger is a multi-purpose one as far as its function is concerned. The steel made shaft is fixed to the frame by means of journal bearings (considering that the velocities are small) to eliminate vibration and noise. Both end of the shaft is designed such that it extends a considerable length beyond the bearing so that a digital revolution counter can be activated by means of a belt and pulley combination attached to the end of the shaft. Other end of the shaft which also extends beyond the other bearing is used to contain the thermocouples and the thermocouple brushes to connect the rotating and stationary thermocouples.

To rotate the rotary regenerator there are various possibilities. For large regenerators, usually, a gear system is necessary. For medium size regenerator a belt and pulley combination suffice. For small regenerators usually a friction wheel becomes sufficient to rotate. In this thesis a belt driven by a motor and wrapped around the drum is used to power the regenerator.

DRIVE MOTOR AND REDUCTOR :

To achieve various rotational speeds a belt pulley speed reductor is designed and constructed. Using a drive motor and the reductor which is explained in Appendix A in detail the regenerator speed can be made 0.5, 0.7, 1.0, 1.4, 2.1, 2.7, 3.5, 4.0, 5.4 and 7.0 rpm. Other rotational speeds are also possible by using suitable pulley of appropriate diameters.

SEALS :

To eliminate the mixing of hot and cold fluids with each other and also with the surroundings air, felt is used. It is used at the connections between the rotor and the air ducts. In addition, at the connectios of the air ducts, rubber gaskets are employed.

VIBRATION ISOLATION :

A 5 mm thick rubber is used to eliminate the transmission of vibration at the connections of motor drive, reductor, rotary regenerator, air ducts and fans.

DUCTS :

Four different ducts for hot air inlet, hot air exit, cold air inlet and cold air exit are connected to the regenerator. Two powerfull fans connected to the hot air inlet and cold air inlet ducts supply hot and cold air to the system. To achieve a streamlined flow in the ducts the outer surface of the ducts are given a circular geometry. To implement the thermocouple connections and revolution counter connection, sufficient space is left between the upper and lower ducts. In addition, baffles are used in the hot air duct to provide mixing and turbulance.

HEATERS :

Maximum design temperature of the hot air is fixed as 70 °C. To achieve that temperature electric heaters are placed at the hot air inlet. The power supplied to the heaters is regulated by means of a variac.

FANS :

Two power full fans with specifications given in Appendix A are used for hot and cold air.

SPECIFICATIONS OF THE ROTARY REGENERATOR DESIGNED

The followings briefs the specification of the rotary heat exchanger designed in this study.

$$\begin{aligned}\text{Total Volume} &= \text{Volume of Wheel} - \text{Volume of Hub} - \text{Volume of} \\ &\quad \text{Frame} \\ &= (\pi \times (25.25)^2 \times 20.2 - (\pi \times (2.7)^2 \times 20.2) - (12 \times \\ &\quad (25.25 - 2.7) \times 0.5 \times 20.2)) \\ &= 37\,264 \text{ cm}^3\end{aligned}$$

$$\text{Matrix Surface Area} = 25\,600 \text{ cm}^2 / \text{passage}$$

$$\text{Total Matrix Surface Area (G. Sheet Iron)} = 307\,200 \text{ cm}^2$$

$$\text{Total Matrix Surface Area (Aluminum Sheet)} = 307\,200 \text{ cm}^2$$

$$\text{Total Matrix Surface Area (Iron + Aluminum)} = 614\,400 \text{ cm}^2$$

$$\text{Total Volume of Matrix (G. Sheet Iron)} = 5430 \text{ cm}^3$$

$$\text{Total Volume of Matrix (Aluminum Sheet)} = 6620 \text{ cm}^3$$

$$\text{Total Volume of Matrix (Iron + Aluminum)} = 12\,050 \text{ cm}^3$$

$$\text{Total Mas of Matrix (G. Sheet Iron)} = 40.65 \text{ kg}$$

$$\text{Total Mass of Matrix (Aluminum Sheet)} = 16.50 \text{ kg}$$

$$\text{Total Mass of Rotary Type Regenerative Heat Exchanger}$$

$$= 40.65 + 16.50 + 30$$

$$= 87.15 \text{ kg}$$

$$\beta = \frac{\text{Total Matrix Surface Area}}{\text{Total Volume of Heat Exc.}} = \frac{30.72 \text{ m}^2}{0.037264 \text{ m}^3} = 825 \frac{\text{m}^2}{\text{m}^3} \text{ (G. Sheet Iron)}$$

$$\beta = \frac{\text{Total Matrix Surface Area}}{\text{Total Volume of Heat Exc.}} = \frac{61.44 \text{ m}^2}{0.037264 \text{ m}^3} = 1650 \frac{\text{m}^2}{\text{m}^3} \text{ (Iron + Aluminum)}$$

Heat Transfer Surface Area (A)

$$= 30.72 \text{ m}^2 \text{ (G. Sheet Iron)}$$

$$= 61.44 \text{ m}^2 \text{ (Iron + Aluminum)}$$

Frontal Area (A_{fr}) = 1844.7 cm²

Free Flow Area (A_o) = 1575.9 cm² (G. Sheet Iron)

$$(A_o) = 1248.2 \text{ cm}^2 \text{ (Iron + Aluminum)}$$

Cross - Sectional Area of the Matrix Wall

$$(A_{cr}) = 268.8 \text{ cm}^2 \text{ (G. Sheet Iron)}$$

$$(A_{cr}) = 596.5 \text{ cm}^2 \text{ (Iron + Aluminum)}$$

$$\text{Porosity } (\sigma) = \frac{A_o}{A_{fr}} = \frac{1575.9}{1844.7} = 0.85 \text{ (G. Sheet Iron)}$$

$$(\sigma) = \frac{A_o}{A_{fr}} = \frac{1248.2}{1844.7} = 0.68 \text{ (Iron+Aluminum)}$$

$$\text{Hydraulic Radius } (r_{hyd}) = \frac{A_o \cdot L}{A} = \frac{1575.9 \times 20.2}{307200} = 0.1036 \text{ cm}$$

$$= 1.036 \text{ mm (G. Sheet Iron)}$$

$$(r_{hyd}) = \frac{A_o \cdot L}{A} = \frac{1248.2 \times 20.2}{614400} = 0.04104 \text{ cm}$$

$$= 0.4104 \text{ mm (Iron + Aluminum)}$$

Hydraulic Diameter

$$(D_{\text{hyd}}) = 4 \cdot r_{\text{hyd}} = 4 \times 1.036 = 4.144 \text{ mm (G.Sheet Iron)}$$

$$(D_{\text{hyd}}) = 4 \cdot r_{\text{hyd}} = 4 \times 0.4104 = 1.642 \text{ mm (Iron+ Aluminum)}$$



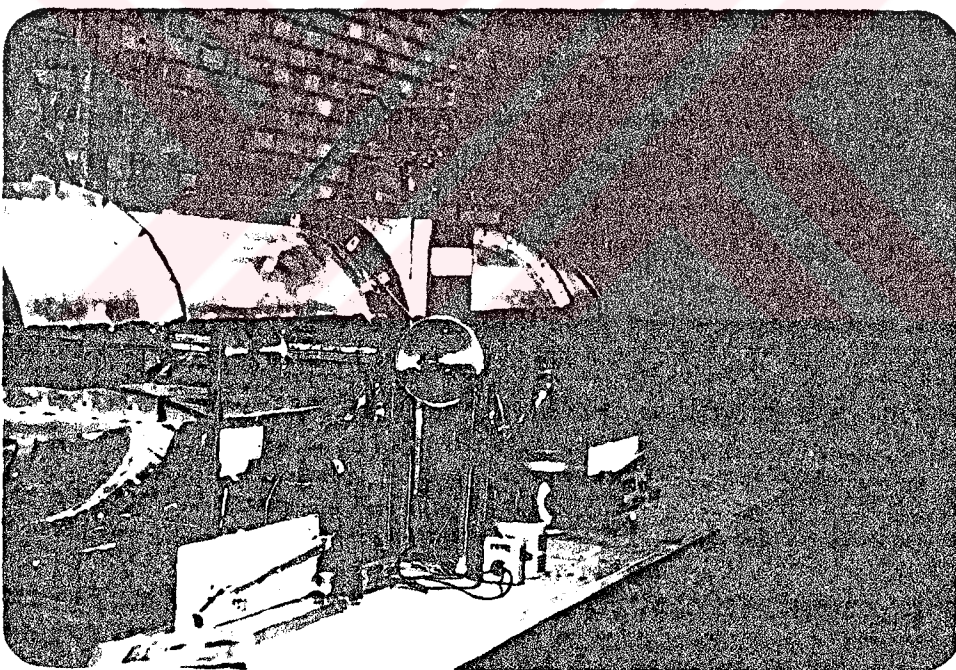
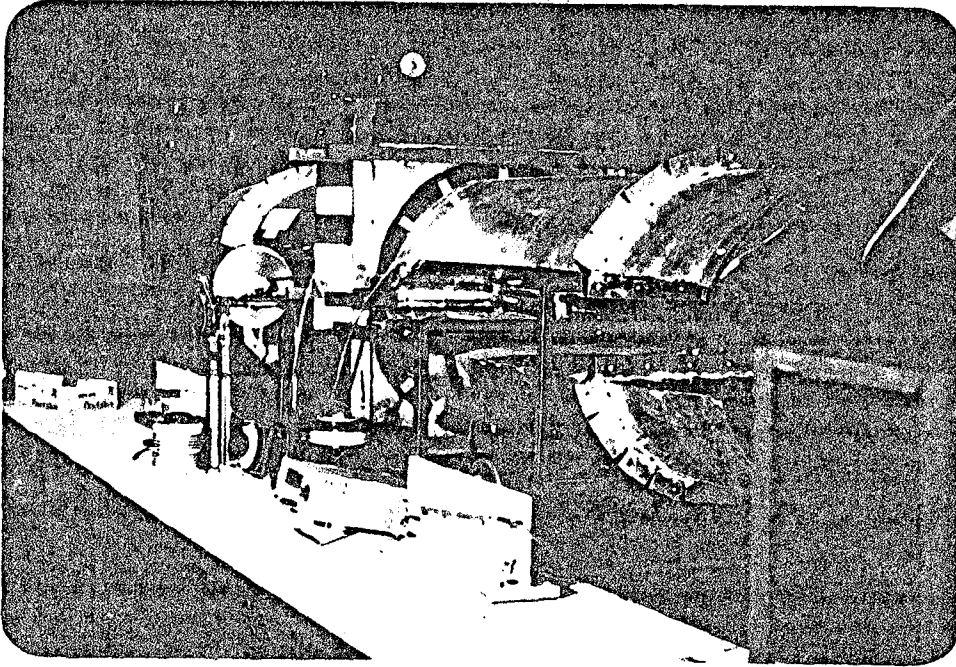


Figure 3.3. General Views of the Rotary Regenerator and the Test Set-up

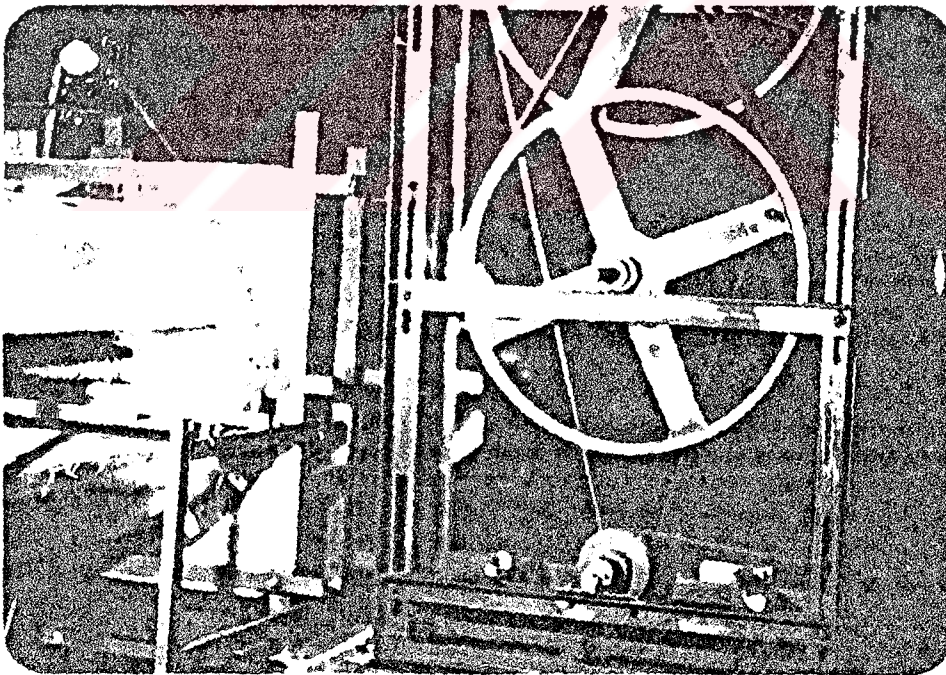
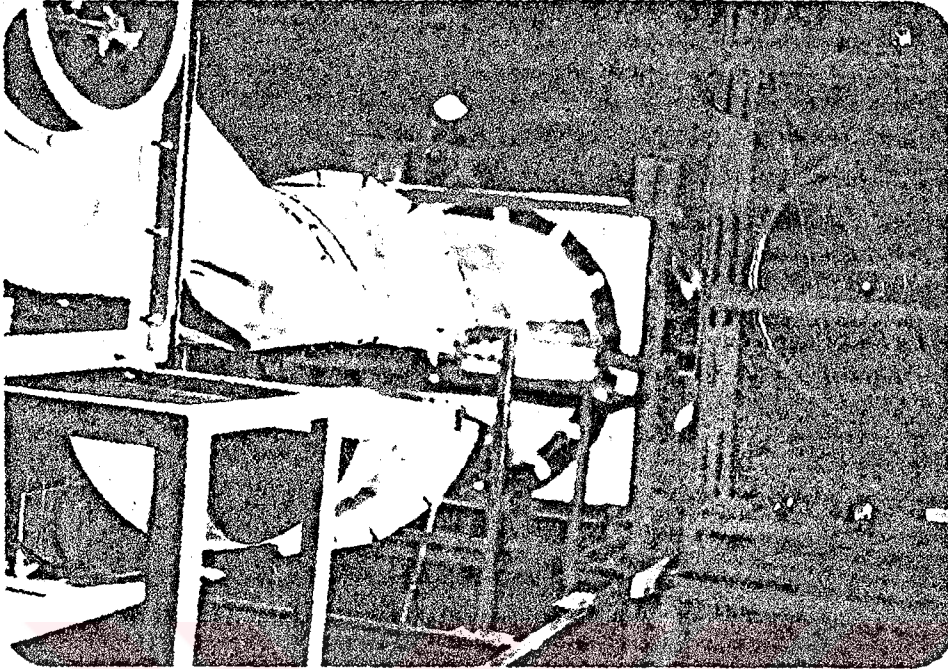


Figure 3.4. General Views of the Reductor and the Test Set-up.

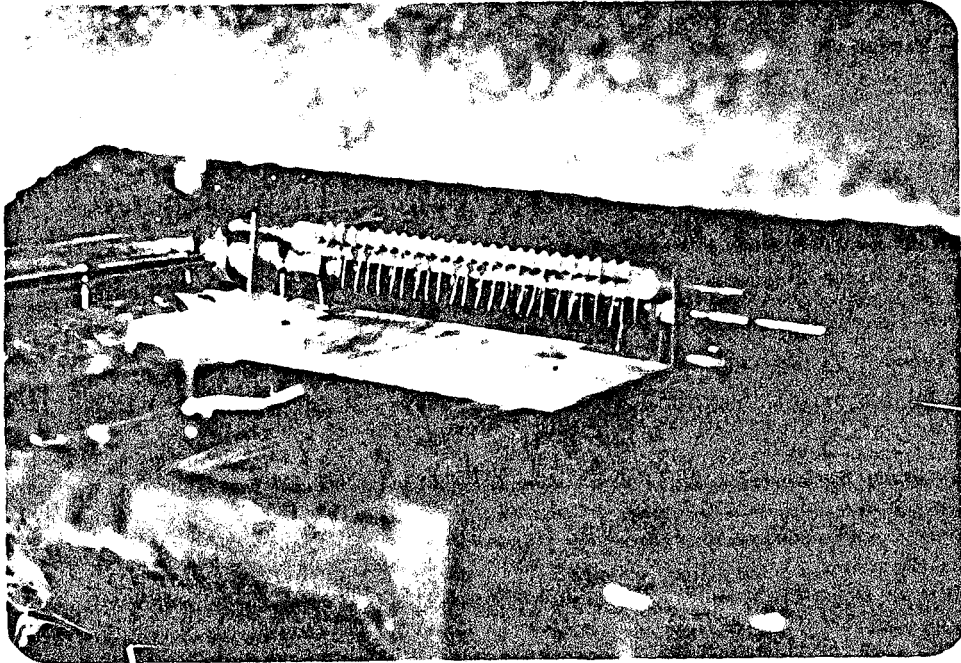


Figure 3.5 General View of the Copper-Constantan Thermocouples system (copper ring, copper brush, spring)



Figure 3.6. General View of the Digital Tachograph system

CHAPTER 4

EXPERIMENTAL PROCEDURE AND RESULTS

In this study a rotary type regenerative heat exchanger is designed, constructed and tested in the laboratory. The regenerator is designed to exchange heat from air to air but it can also be used for other fluids if certain precaution are taken. The main variables studies were the matrix material, flow rates of the cold and hot fluid (air) and the speed of the rotation of the rotor.

Two different material for the matrix are used. These are 0.35 mm galvanized sheet iron and 0.40 mm aluminum sheet for better performances of the regenerator it is advisable to use sheet material thinner that those used in this experiment. The sizes mentioned above are chosen since they are the thinnest material available in the market. Preperation of the matrix is done in laboratory by cutting the matrix material at suitable sizes and bending them in zig-zaggy shape at a length of 4 cm. Large surface area which is placed into the rotor required a long and cumbersome study to install it into rotor.

Galvanized sheet iron and aluminum sheet material are chosen on purpose since those is a wide variation in their thermal conductivity which is

one of the important heat transfer parameters in rotary heat exchangers. (Thermal conductivity of galvanized sheet iron is $k=73 \text{ W/(m}^\circ\text{C)}$ and the thermal conductivity of aluminum is $k=210 \text{ W/(m}^\circ\text{C)}$).

Flow rate measurements are made at the entrance of both fans (cold fluid and hot fluid). To achieve this, flanged tubes with varying diameters are employed. At the beginning of the tests, the flow measurements are planned to be made across the cross-section of the air channels. However it is found that such measurements are not very accurate because of the very low velocities which makes it very difficult to read on the manometers. Therefore it is decided to measure the flow rate of the hot and cold fluids at the small size flanged tubes at the inlet of the cold and hot air fans. By changing the diameter of the tubes the flow rates of both stream is changed and kept at fixed values during the experimental runs.

Diameters of the flanged tubes used at the inlet of the fans changed from the minimum value of 4.2 cm up to 20 cm. Four different diameters are used to change the flow rates of hot and cold air streams. Sufficiently long tubes are used to eliminate the entrance (boundary layer development regions) effects.

To measure the flow rate, pitot-tubes and inclined manometers are used to measure the small pressure heads. To take the variations in velocity across the cross-section into account, pitot tube measurements at various distances from the axis of the tube is taken. Then the flow rate of air is found by integrating across the cross-section of the tube. Details of the flow rate measurements are explained in appendix B.

Using the experimental data the velocity of the air in the tube is calculated by using the expression.

$$v = \sqrt{2.g.H_d \cdot \frac{\rho_{\text{water}}}{\rho_{\text{air}}}} \quad (\text{m/sec})$$

where;

v : velocity (m/sec)

g : gravitational acceleration (m/sec²)

H_d : dynamic pressure (m, water column)

ρ : density (kg/m³)

Using these velocities measured at known distances from the axis of the tube, a polynomial is obtained by fitting the experimental data by means of least square curve fitting technique. A typical velocity profile variation is shown in figure B.1 (Appendix B).

Flow rate is found by taking the following integral over the cross-section of the tube.

$$Q = \int_0^r v \cdot 2\pi r \cdot dr \quad (\text{m}^3/\text{sec})$$

To study the effect of the rotational speed on the performance of the regenerator, rotational speed of it is changed by means of a pulley and belt system. In the design phase of the experimental set up, two options are considered to change the rotational speed. These are a gear reduction system and pulley-belt system. Because of the high cost of the gear reduction system

pulley-belt system is favored although it is not as efficient, compact and practical as the gear reduction system. The A.C motor used has a comparatively large rotational speed and therefore a large reduction ratio is needed to reach reasonable regenerator rotational speeds. To achieve this large reduction, several combinations of belts and pulleys are used. By playing with these combinations various reduction ratios and therefore various rotational speeds are achieved. The highest possible reduction ratio that could be achieved was 1/300. Detailed information on the speed reduction is given in Appendix A.

To change the inlet temperature of the hot fluid heaters are placed at the entrance of the hot fluid channel. Totally eight separate heater element is used to adjust the inlet temperature of the hot fluid. Three of them are connected to 380 volt source, two of them to 220 volt source directly and three of them are connected to 220 volt source through a variac. Total power consumption of the heaters is 11 kw which makes it possible to increase the inlet temperature of the air up to 70°C (at average velocities). By adjusting the power through the variac and also by turning on of various combinations of heater it is possible to obtain the aimed temperatures at the inlet of the hot air channel.

Through the thermocouples placed in the air channels. It is found that during the operation of the regenerator large oscillations and locational variations of the temperature occur. Such oscillations and variation in the temperature makes the evaluation of the average fluid temperature extremely difficult and cause uncertainties in the heat load calculations. To eliminate

such effects two sets of mixing baffles at the inlet of the hot air into the rotor (just downstream of the heating elements) are employed. Measurements show that it is not necessary to employ similar baffles at the exit of hot fluid from the rotor and at the inlet and exit of the cold fluid to and from the rotor.

4.1.PROCEDURE

During the experiments, before the measurements are taken certain preparations are made to reach the right parameters. Hot and cold air fans are turned on. The electric heaters are adjusted to the planned power. At the inlet of the fans the flanged tubes with the required diameters are installed. The pulley and belt system is arranged to give the right rotational speed and the electric motor is turned on. The temperature measuring system is prepared. Cold junction flask is filled with the ice cubes and water and sufficient time is allowed to reach steady state. The entire system is allowed to run around an hour so that all the measurements reach steady state. Once it is believed that the apparatus is running at steady state measurements are taken. The following data is taken:

1. Ambient temperature to calculate the mass flow rate is measured by using a thermometer.

2. At the inlet of the cold air duct the inlet temperature of the cold air is measured by means of four thermocouple junctions placed there to average the local variations across the cross-section. The inlet temperature of the cold air is taken as the average of the four thermocouple readings.

3. The cold air exit temperature is averaged by means of the eight thermocouples distributed across the cross-section of the duct at the cold air exit.

4. Hot air inlet and exit temperatures are averaged by means of nine thermocouple junctions distributed across the cross-section of the duct at the inlet and exit.

5. Temperature of the matrix material is measured by means of specially designed thermocouple system, the detail of which is seen in Figure 4.1. Since the rotor is rotating with the thermocouple junctions or them and the rest of the measuring system is stationary the connection is achieved by means of (24) copper rings and brushes. After passing through the copper rings and brushes thermocouples continue through the axis of the shaft of the rotor and then reach the matrix. Thermocouple junctions are placed at various locations on the matrix to obtain a complete temperature distribution picture of it. The location of the thermocouple junctions are shown in Figure 4.1. The signals obtained from these thermocouples are recorded on a recorder.

6. Rotational speed is measured by means of tachymeter.

4.2. EVALUATION OF THE EXPERIMENTAL DATA

Mass flow rate of the hot and cold fluids are obtained from the following relation;

$$\dot{m} = Q \cdot \rho \text{ (kg/sec)}$$

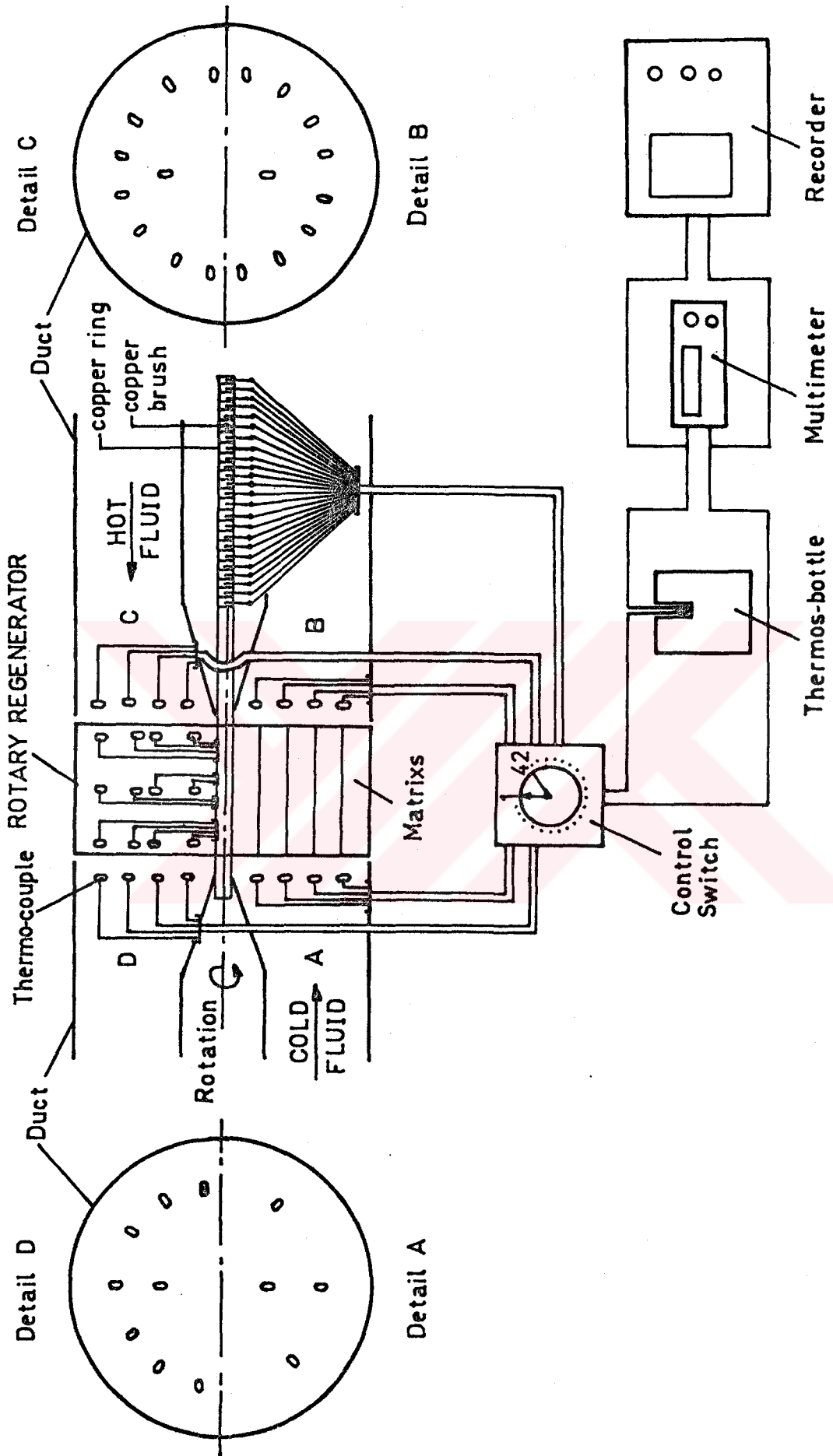


Figure.4.1. Schematic Diagram of Thermo-couple System

Where;

Q = volume flow rate (m^3/sec)

(it is obtained by integrating the velocity distribution at the inlet flanged tubes)

ρ = density (kg/m^3)

(at the inlet of the flanged tubes)

Heat capacity rate of the cold and hot sides can be obtained by,

$$C_c = (\dot{m} \cdot c_p)_{\text{cold}}$$

(it is taken as C_{min} in this study)

Where;

C_c = heat capacity rate of the cold side ($\text{W}/^\circ\text{C}$)

c_p = specific heat of fluid at constant pressure ($\text{J}/\text{kg}^\circ\text{C}$)

(it is calculated at the mean temperature of the cold fluid in the regenerator.)

$$C_h = (\dot{m} \cdot c_p)_{\text{hot}}$$

(is taken as C_{max} in this study)

Where;

C_h = heat capacity rate of hot side ($\text{W}/^\circ\text{C}$)

c_p = specific heat of fluid at constant pressure (J/kg°C)

(it is calculated at the mean temperature of the hot fluid in the regenerator.)

Heat Capacity rate ratio of the fluids can be found as

$$C^* = \frac{C_{\min}}{C_{\max}} = \frac{C_{\text{cold}}}{C_{\text{hot}}} \text{ (dimensionless)}$$

The effectiveness of the regenerator is defined as the ratio of the actual heat transfer to the maximum possible heat transfer

Then, the effectiveness can be found by using the expression

$$\varepsilon = \frac{C_c (T_{c,o} - T_{c,i})}{C_{\min} (T_{h,i} - T_{c,i})} \text{ (dimensionless)}$$

Since $C_c = C_{\min}$ one gets;

$$\varepsilon = \frac{T_{c,o} - T_{c,i}}{T_{h,i} - T_{c,i}}$$

Which gives the effectiveness .

The number of heat transfer unit is obtained from the following expression

$$NTU = \frac{1}{\frac{C_{\min}}{(hA)_h} + \frac{C_{\min}}{(hA)_c}} \text{ (dimensionless)}$$

Heat transfer coefficient at the surface of the matrix material depend on the flow velocity and thermal properties and the detail of this calculation is given in the Appendix C.

Since in this study it is taken that ;

$$A_C = A_H$$

$$h_C = h_H$$

Therefore expression of NTU simplifies to

$$NTU = \frac{(hA)_C}{2.C_{\min}}$$

Where;

$$A_{\text{total}} = A_C + A_H$$

then;

$$NTU = \frac{h \cdot A_t}{4.C_{\min}}$$

Another important parameter in regenerator analysis is the heat capacity rate of rotating matrix and can be calculated as;

$$C_r = M_W \cdot c_W \cdot N \quad (W/^\circ C)$$

Where;

M_W = total mass of the matrix (kg)

c_W = specific heat of the matrix material (J /kg °C)

N = rotational speed of the rotor (rev. /sec)

Matrix heat capacity rate ratio then becomes,

$$C_r^* = \frac{C_r}{C_{\min}}$$

Sample evaluation of experimental data is given in Appendix D.

4.3. RESULTS

The results of the experimental measurements are presented in figures 4.2 - 4.15.

In figure 4.2, variation of the regenerator effectiveness is shown as a function of the number of heat transfer units, for various matrix heat capacity rate ratio. Since the flow rates of hot and cold fluids are taken equal in these experiments C^* becomes unity. In the experiments heat capacity rate ratio is changed by changing the flow rates of hot and cold fluids by equal amount and also by changing the rotational speed of the regenerator. The material used in the matrix for these experiments is galvanized sheet iron. To see the effect of heat transfer surface area on the performance of the regenerator the same experiments are repeated by installing additional matrix material (aluminum) into the rotar. The total matrix surface area is increased from the previous value of 30.72 m² to 61.44 m². The resulting graph is shown in figure 4.3.

Figure 4.4 shows the variation of regenerator effectiveness as a function of number of heat transfer unit for various heat capacity rate ratio (=Cmin/Cmax). Matrix heat capacity rate ratio is kept constant at the value of 13.

The matrix material in that figure was galvanized sheet iron. In figure 4.5 the same graph is redrawn by using the data obtained from the experiments in which the matrix surface area is doubled.

Figure 4.6 presents the results of the performance experiment of the regenerator with 30.72 m^2 heat transfer surface area (galvanized sheet iron) to show the variation of the effectiveness of the regenerator as a function of the number of heat transfer units. The figure presents data obtained at a fixed ($=2.7 \text{ rpm}$) rotational speed. Therefore the horizontal axis represents the matrix heat capacity rate ratio also. The aim of this figure is to present the effect of heat capacity rate ratio at constant rotational speed.

Figures 4.7 and 4.8 show the variation of the regenerator effectiveness as a function of the heat capacity rate ratio for galvanized sheet iron matrix and galvanized sheet iron plus aluminum matrix respectively.

Figures 4.9 and 4.10 show the effect of matrix heat capacity rate ratio on the effectiveness of the regenerator for a given number of heat transfer units for different matrix heat transfer surface area.

To see the effect of rotational speed alone on the effectiveness of the regenerator, in figure 4.11, regenerator effectiveness is graphed versus rotational speed for a fixed value of number of heat transfer units.

Figures 4.12 and 4.13 show the temperature distribution in the matrix and the hot and cold fluids as a function of the axial and angular position of the rotor of the regenerator. In those figures z^* represent the nondimensional axial distance (nondimensionalized with the rotor length) and its origin is the

inlet of the cold fluid, t^* is the normalized angular position (normalized by 2π). In figure 4.12 theoretical calculation of the Reference (33) is also shown for comparison purposes. Figure 4.13 shows the same behavior as the Figure 4.12 except Cr^* and NTU values are greatly reduced to show their effect on the temperature distribution and also the difference between the matrix and fluid temperatures.

Figures 4.14 and 4.15 show the temperature distribution in the hot and cold fluid just at the exit of the rotor as a function of nondimensional angular position of the rotor. In figures 4.14 and 4.15 theoretical calculation of the Reference (34) is also shown for comparison purposes.

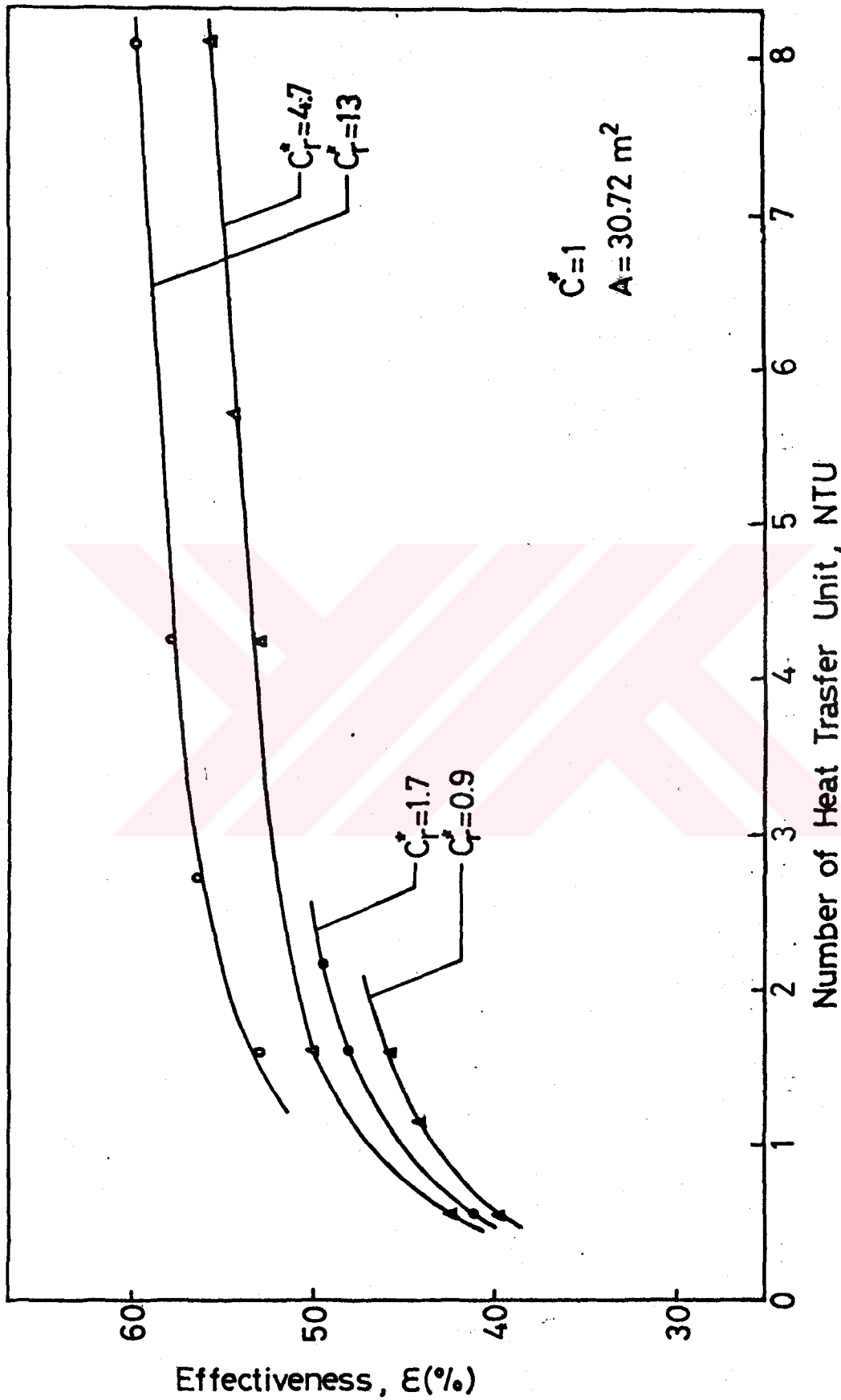


Figure 4.2. Rotary Regenerator Effectiveness (ϵ) as a Function of C_r^* and NTU for $C^* = 1$ and Galvanized Sheet Iron.

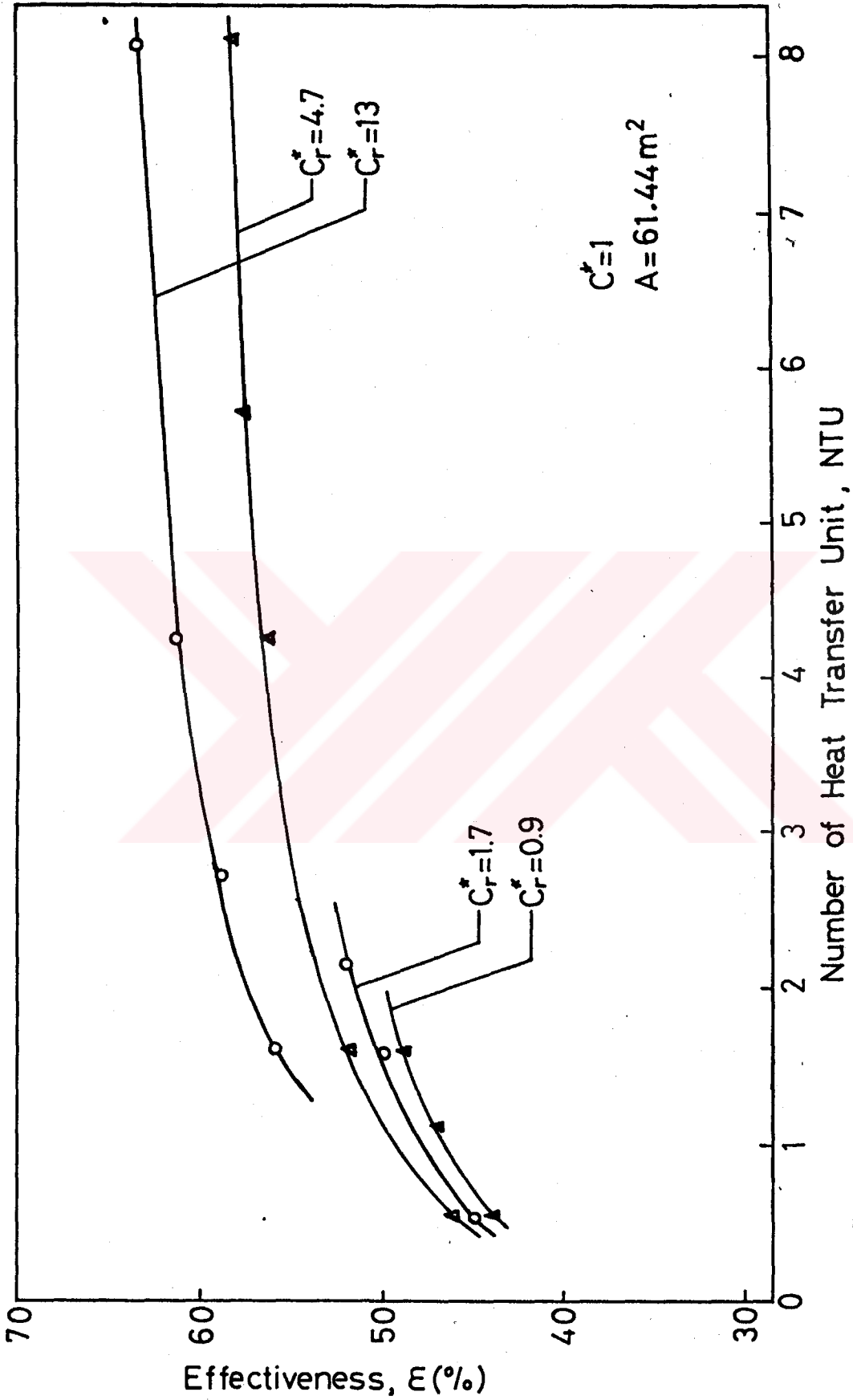


Figure 4.3. Rotary Regenerator Effectiveness (ϵ) as a Function of C_r^* and NTU for $C^* = 1$ and Galvanized Sheet Iron+Aluminum Sheet.

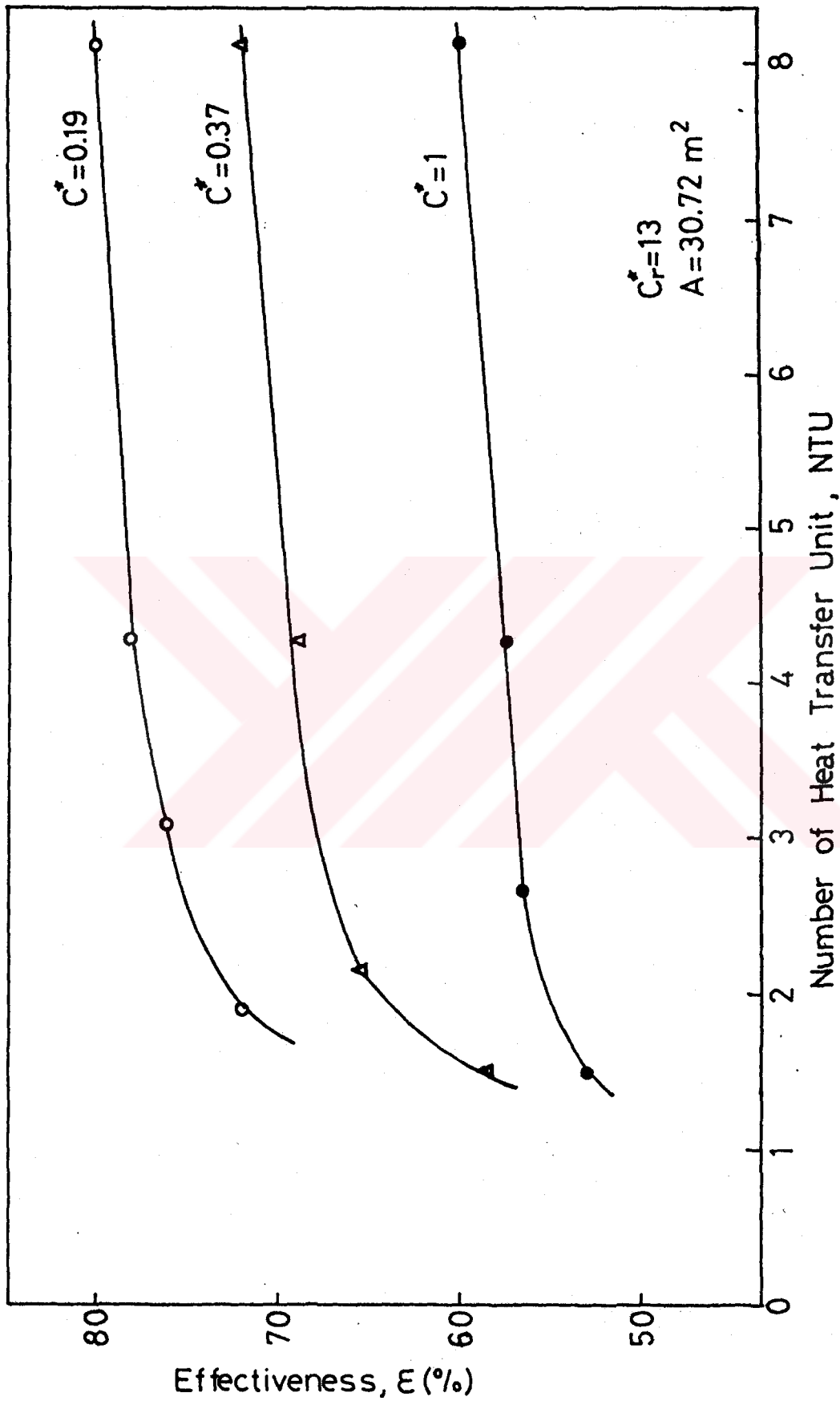


Figure 4.4. Rotary Regenerator Effectiveness (ϵ) as a Function of C^* and NTU for $C_r^* = 13$ and Galvanized Sheet Iron.

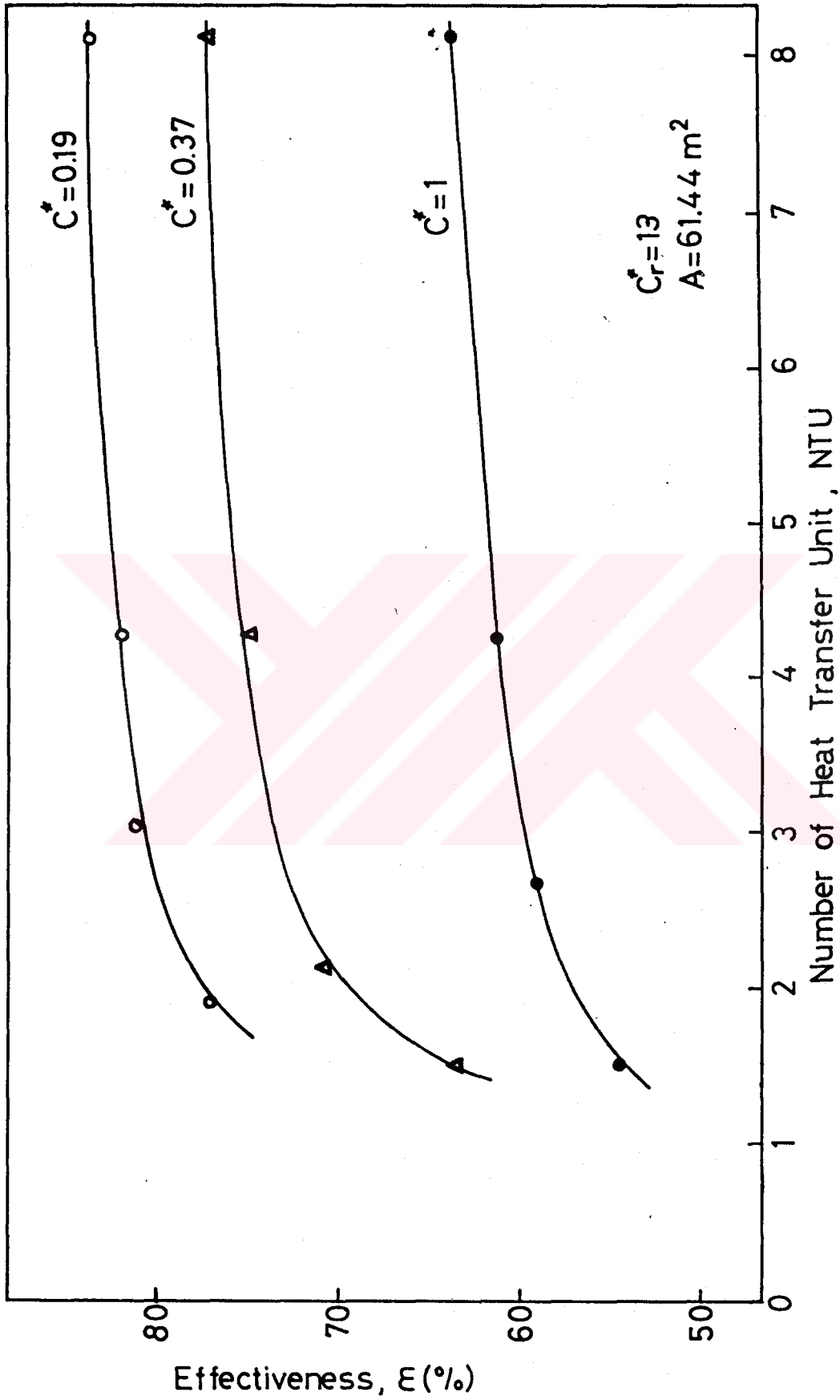


Figure 4.5. Rotary Regenerator Effectiveness (ϵ) as a Function of C^* and NTU for $C_r = 13$ and Galvanized Sheet Iron+Aluminum Sheet.

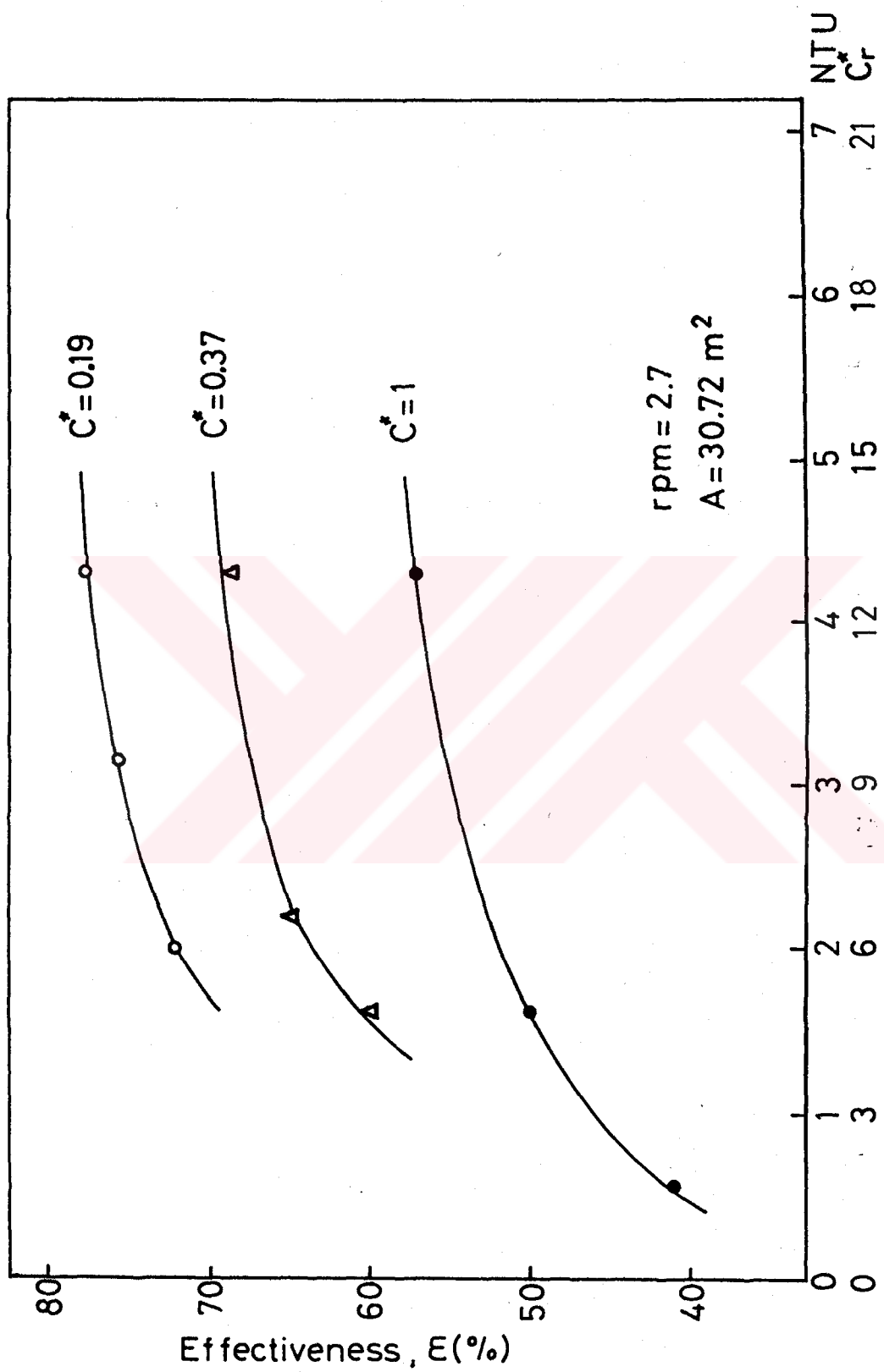


Figure 4.6. Rotary Regenerator Effectiveness (ϵ) as a Function of C^* , C_r^* , and NTU for $\text{rpm} = 2.7$ and Galvanized Sheet Iron.

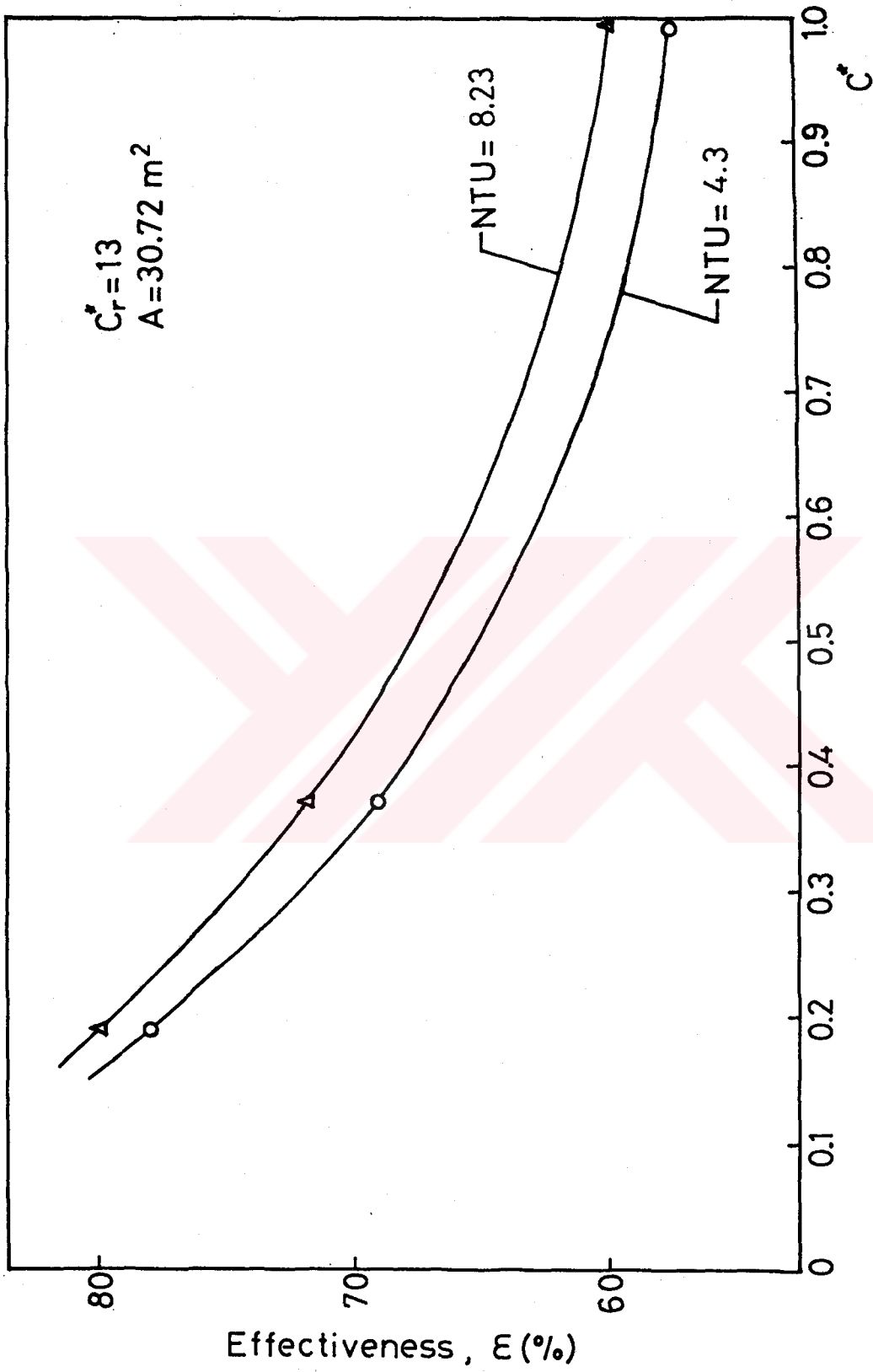


Figure 4.7. Rotary Regenerator Effectiveness (ϵ) as a Function of C^* and NTU for $C_r^* = 13$ and Galvanized Sheet Iron.

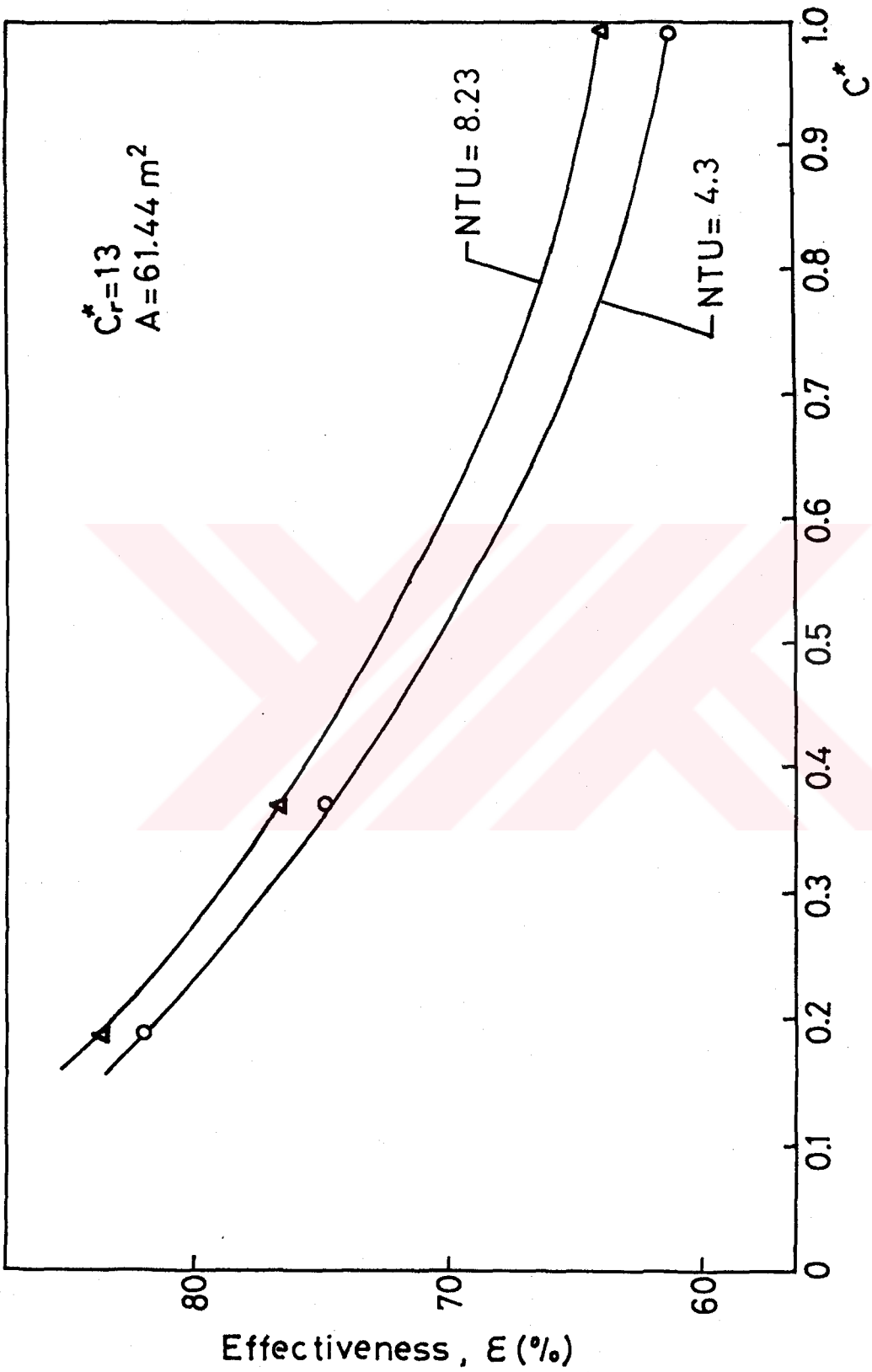


Figure 4.8. Rotary Regenerator Effectiveness (ϵ) as a Function of C^* and NTU for $C_r^*=13$ and Galvanized Sheet Iron+Aluminum Sheet.

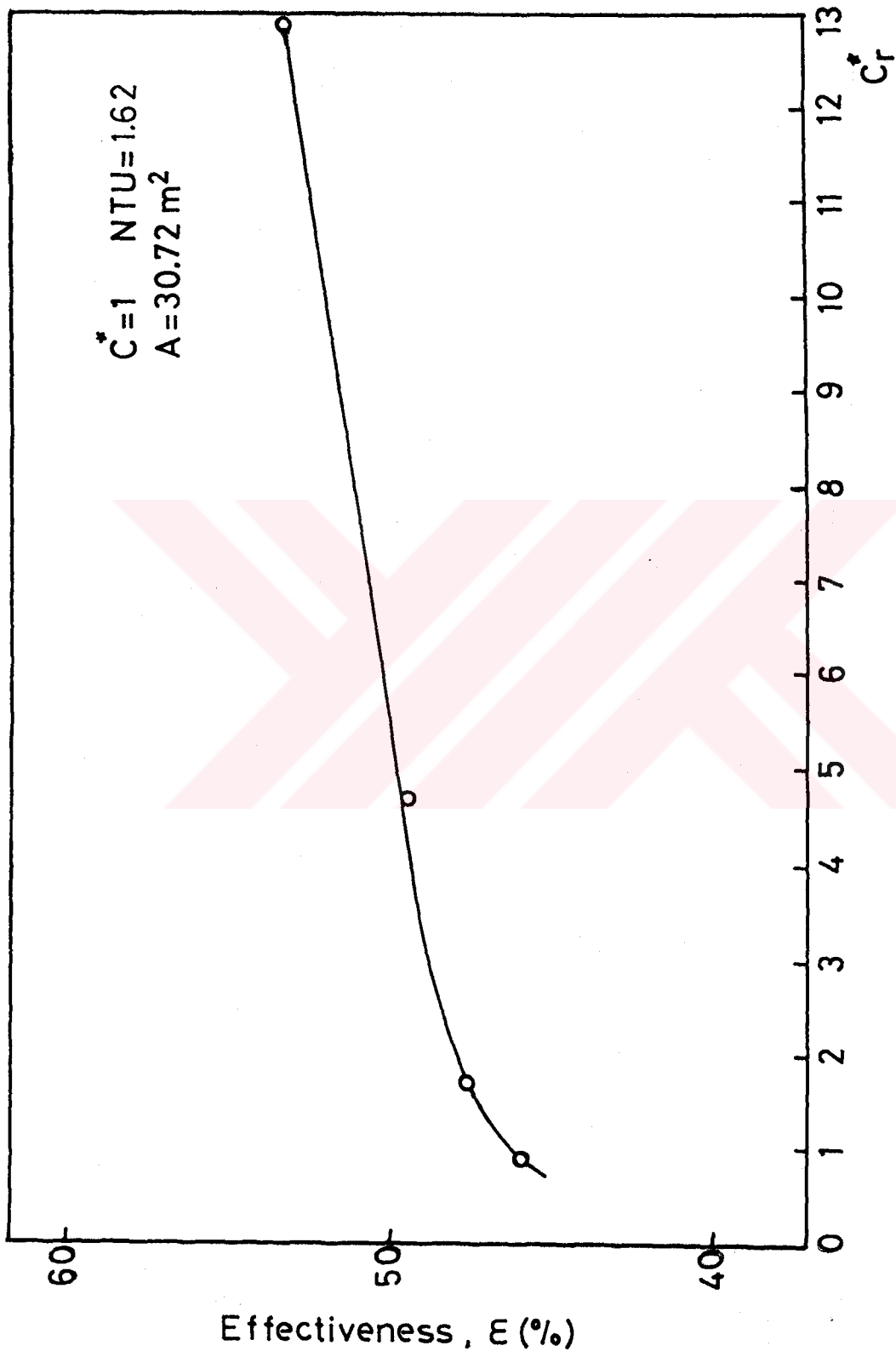


Figure 4.9. Rotary Regenerator Effectiveness (ϵ) as a Function of C_r^* for $C_r^* = 1$, $NTU = 1.62$ and Galvanized Sheet Iron.

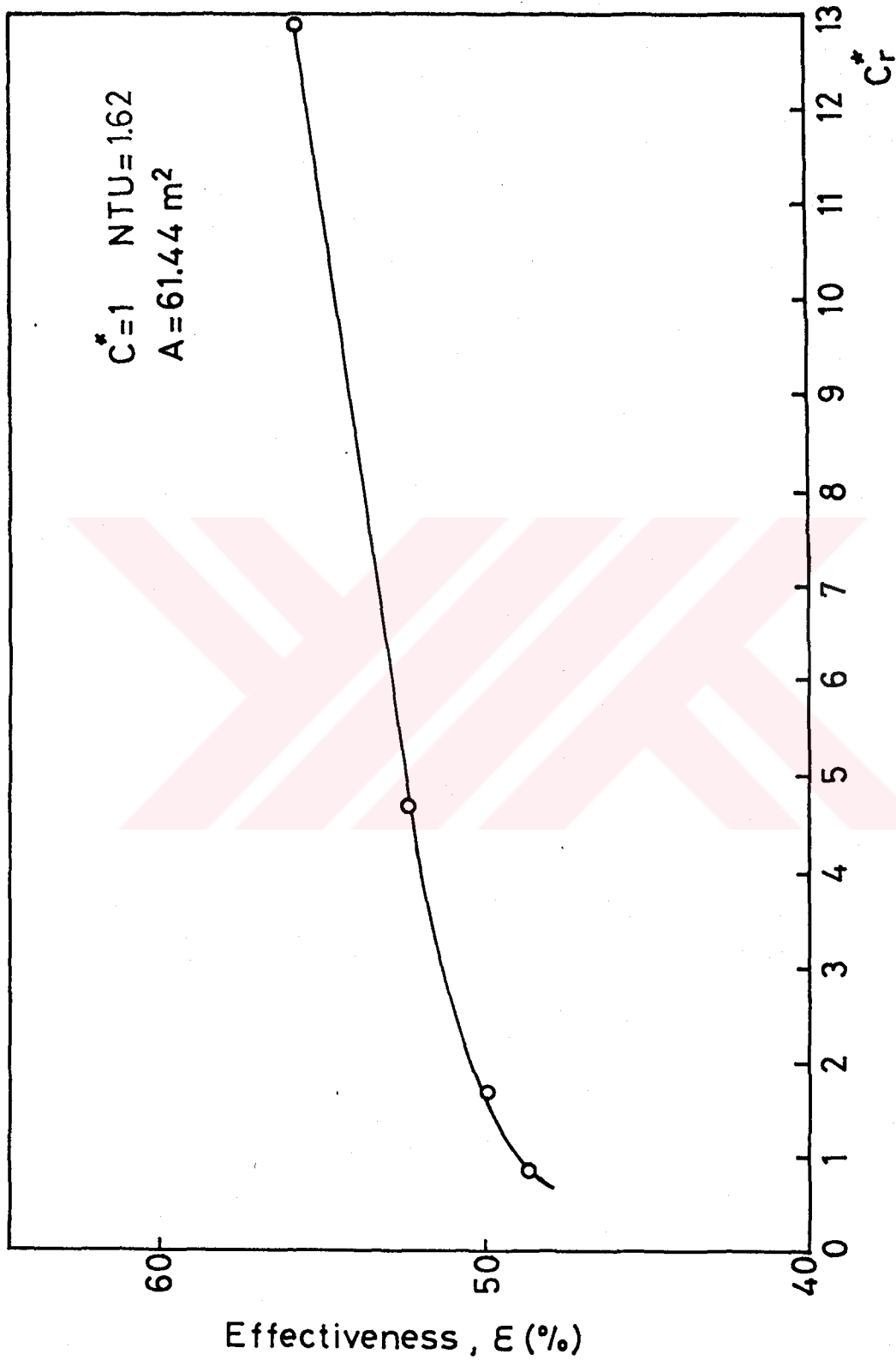


Figure 4.10. Rotary Regenerator Effectiveness (ϵ) as a Function of C_r^* for

$C^* = 1$, $NTU = 1.62$

and Galvanized Sheet Iron+ Aluminum Sheet.

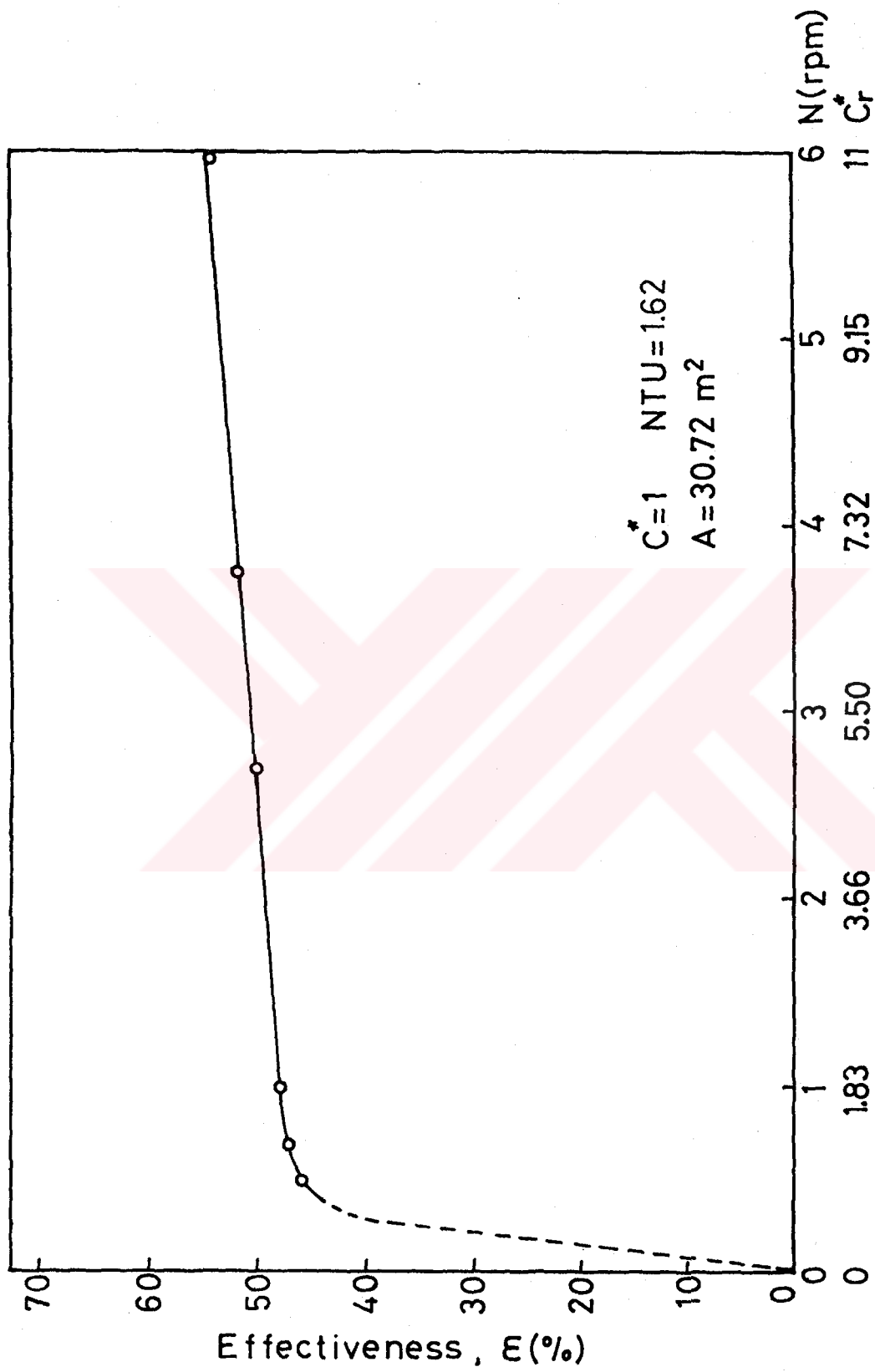


Figure 4.11. Rotary Regenerator Effectiveness (ϵ) as a Function of N, C_r^* for

$C^* = 1, NTU = 1.62$ and Galvanized Sheet Iron.

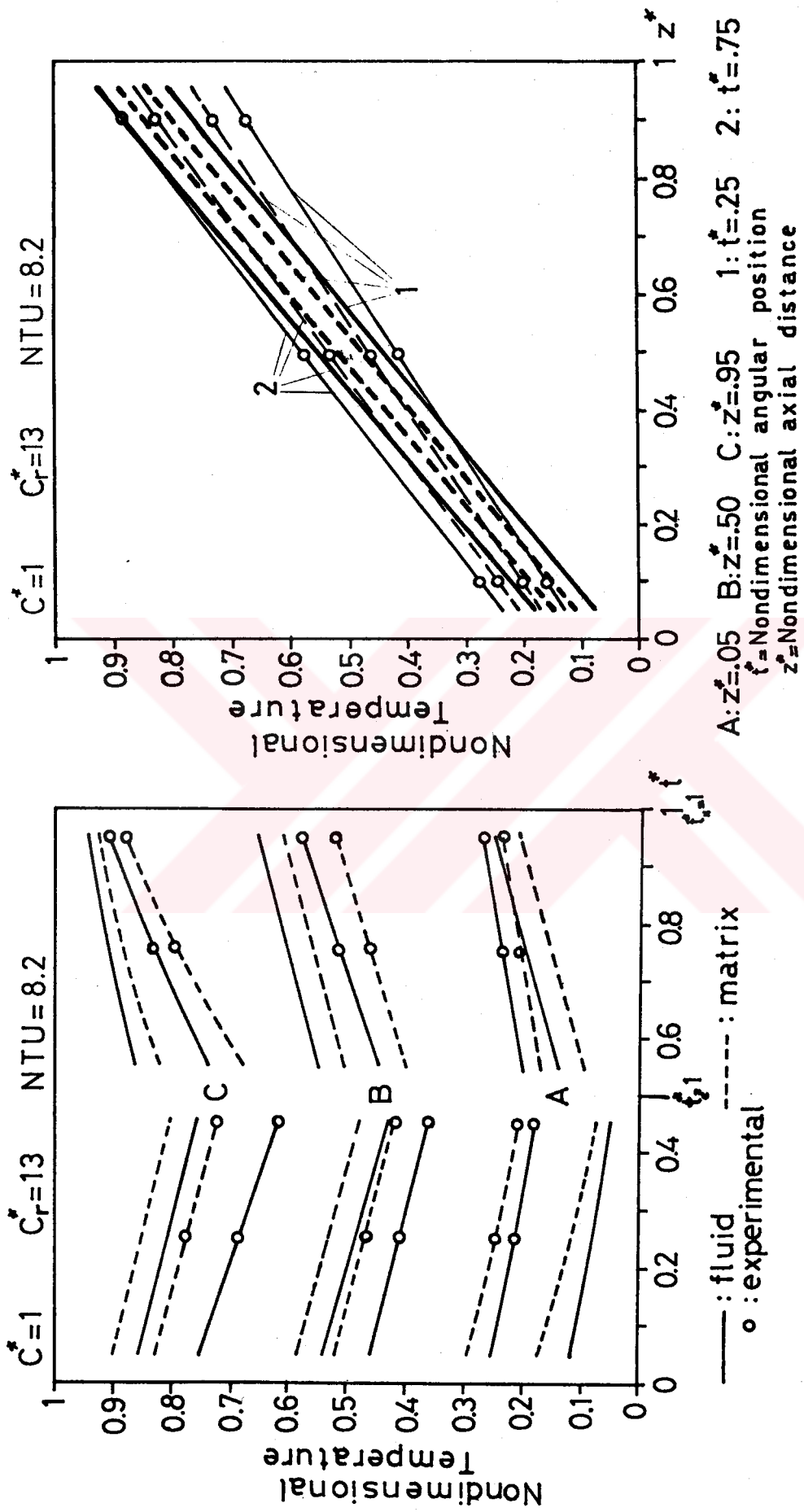


Figure 4.12. Temperature Distributions in the Rotary Regenerator for $C^* = 1$,

$C_r^* = 13$, $NTU = 8.2$ and Galvanized Sheet Iron.

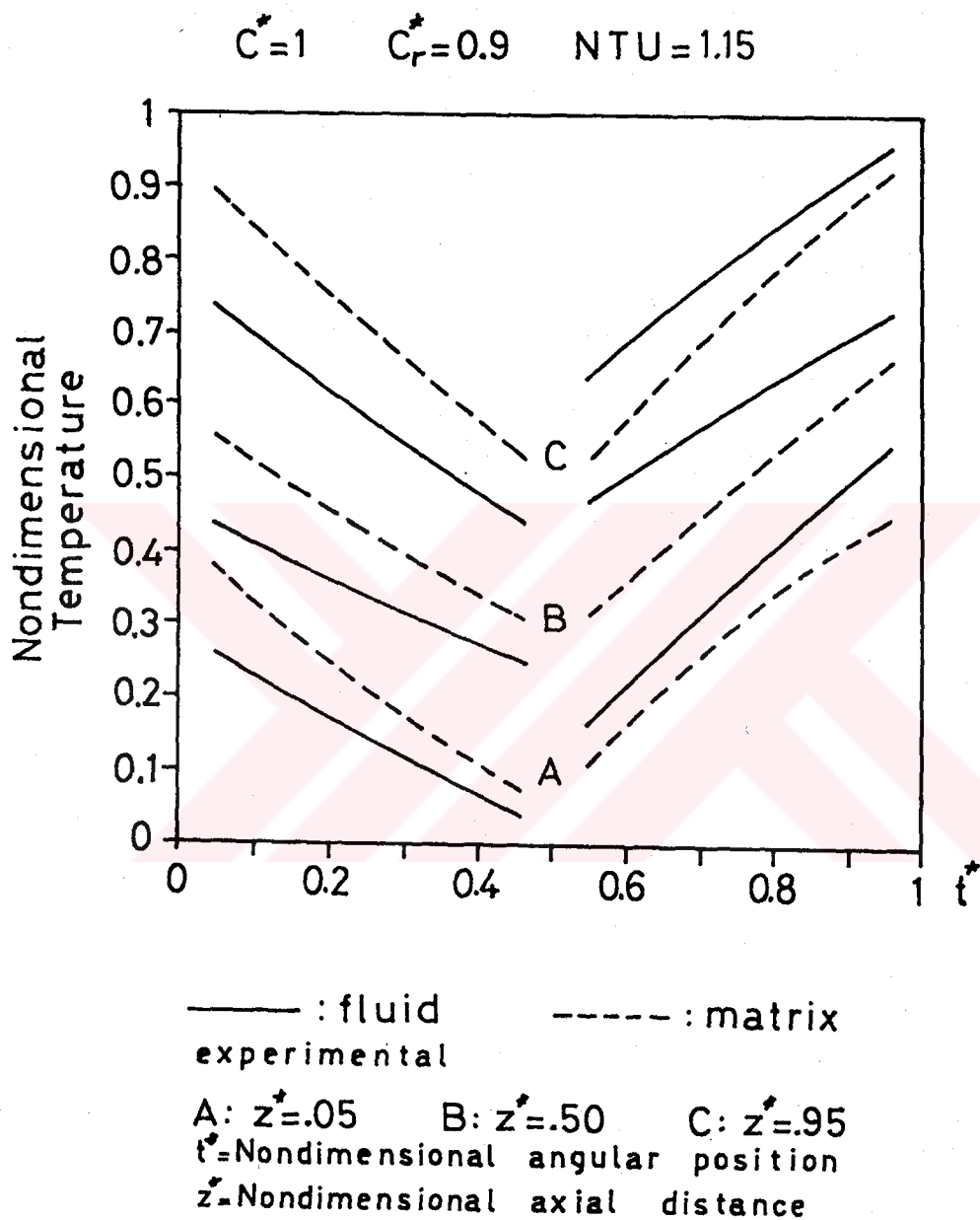


Figure 4.13. Temperature Distributions in the Rotary Regenerator for $C^* = 1, C_r^* = 0.9, NTU = 1.15$ and Galvanized Sheet Iron.

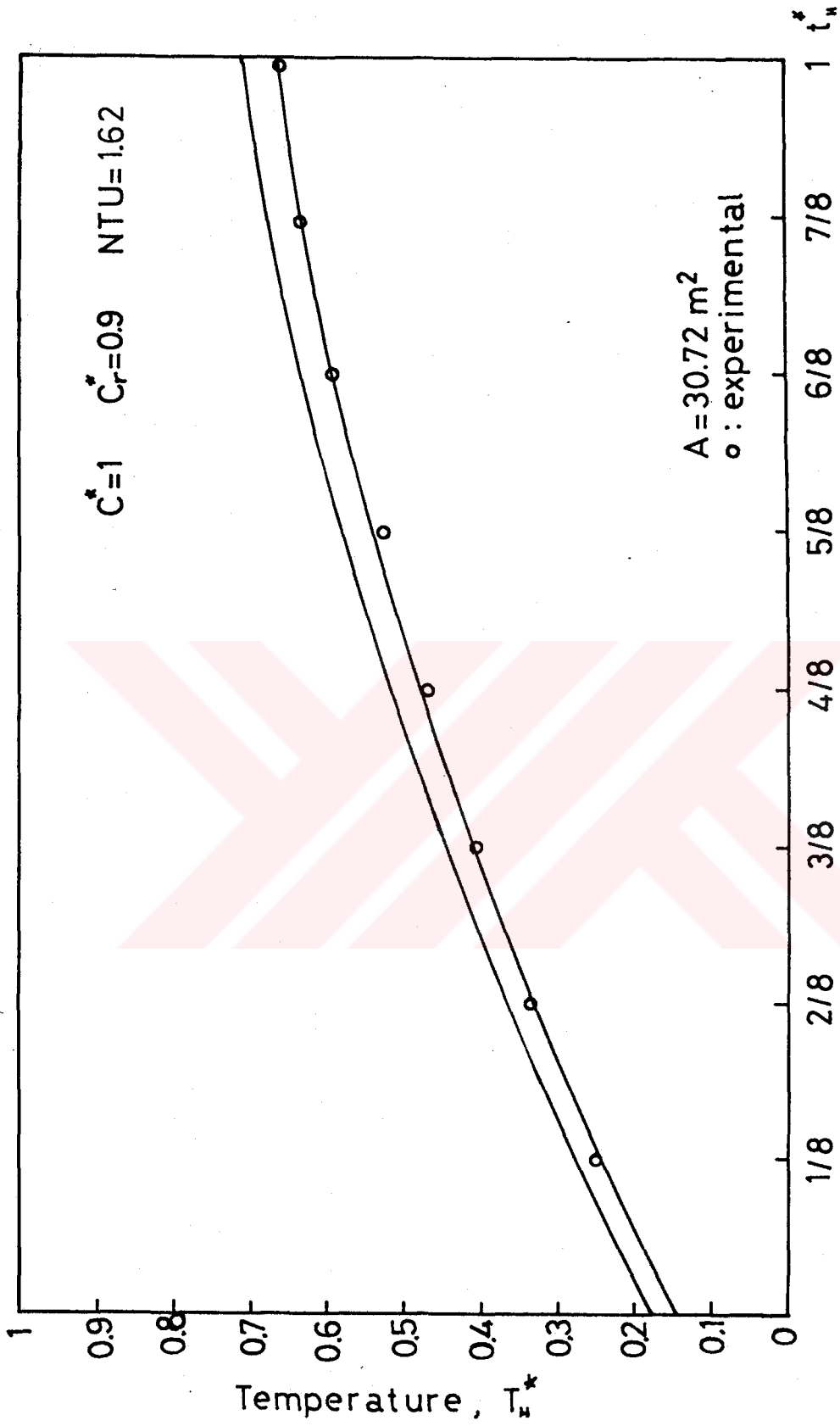


Figure 4.14. Temperature Distributions of the Hot Fluid at the Exit of the Rotary Regenerator for $C^*=1$, $C_r^*=0.9$, $NTU=1.62$ and Galvanized Sheet Iron.

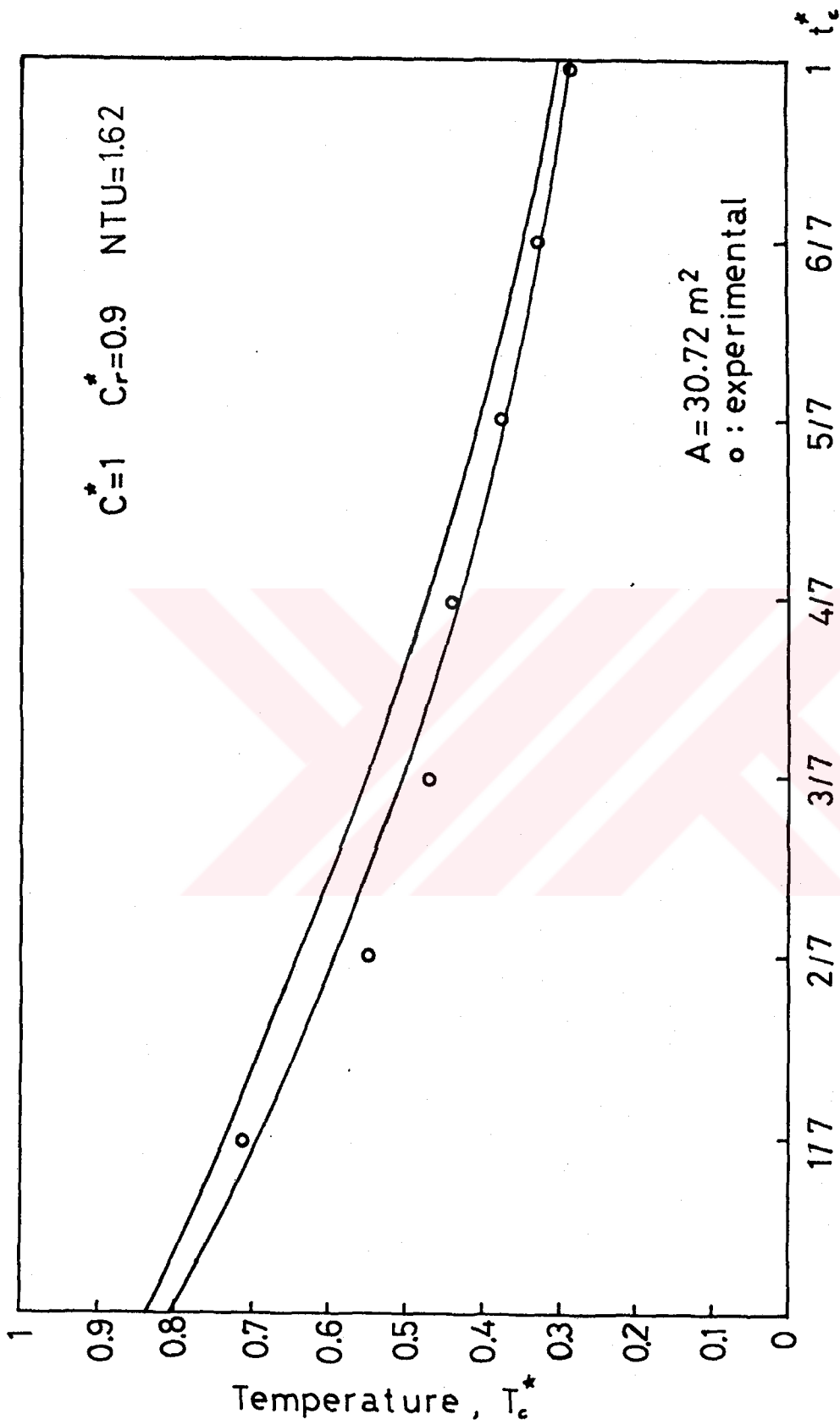


Figure 4.15. Temperature Distributions of the Cold Fluid at the Exit of the Rotary Regenerator for $C^* = 1$, $C_r^* = 0.9$, $NTU = 1.62$ and Galvanized Sheet Iron.

CHAPTER 5

DISCUSSION AND CONCLUSION

In this study a rotary type regenerative heat exchanger is designed, constructed and tested. The rotor of the regenerator is filled with zigzaggy shaped matrix material made of aluminum sheet and galvanized sheet iron. This matrix geometry, by no means, is the best design as far as the heat transfer characteristics are concerned. Nevertheless it is chosen because of the easiness of the manufacturing. The heat transfer surface area density achieved in this study is $825 \text{ m}^2/\text{m}^3$ for galvanized sheet iron matrix and $1650 \text{ m}^2/\text{m}^3$ for the galvanized sheet iron and aluminum matrix. This surface area density can be made even larger to achieve higher effectiveness if it is designed. Financial limitations and the production difficulties were the factors that forced the designers to keep this parameter at modest values.

In the performance analysis tachometer is used to measure the rotational speed, pitot tube and inclined manometer for fluid velocity measurements and thermocouples for temperature measurements are

employed. Measurement equipment used in this study proved sufficient in general, in this study except for recording the temperatures the recorders used is found to be a little bit insufficient to record the measurements. Therefore it is suggested to use a more sensitive recorders in the future work.

Figures 4.2 and 4.3 show an almost linear variation of effectiveness with number of heat transfer units and effectiveness increases with an increase in the matrix heat capacity rate ratio. Comparison of figures 4.2 and 4.3 show that increase in the surface area of the matrix increases the effectiveness of the rotary regenerator. It should be kept in mind that the increase in the surface area of the matrix increases the pressure drop across the rotary regenerator since the free flow area decreases (The free flow area in galvanized sheet iron matrix is 85 % whereas it decrease down to 68 % in the galvanized sheet iron and aluminum matrix).

In figures 4.4 and 4.5 the effect of number of heat transfer unit or effectiveness of the regenerator, this time at fixed value of heat capacity rate ratio, is observed.

Again, for most part of the curves, the relation is almost linear and effectiveness increases with an increase in the number of heat transfer units. Comparison of 4.4 and 4.5 show that increase in the surface area of the matrix, again, have an increasing effect on the effectiveness.

Figure 4.6 is drawn to isolate the variations in the value of NTU from rotational effects for a fixed value of rotational speed a continuous increase in the value of effectiveness with an increase in number of heat transfer units is observed.

To show the sole effect of the matrix heat capacity rate ratio on the effectiveness figures 4.9 and 4.10 are drawn. Effectiveness increases directly with an increase in matrix heat capacity rate ratio as it is observed in the figures. Again, comparison of the figures show that larger matrix heat transfer area gives a larger effectiveness at the same matrix heat capacity rate ratio.

Figure 4.12 shows the angular and axial variations of the matrix and fluid temperatures in the rotor. The curves with small circular on them shows the experimental results obtained by the rotating thermocouple junctions in the matrix. Broken lines represent the matrix temperature. The matrix temperature is nondimensionalized by the maximum temperature difference in the rotary regenerator which is equal to the difference of the inlet temperatures of the hot and cold fluid. The reference temperature in the nondimensionalizing procedure is taken as the inlet temperature of the cold fluid. That is, the nondimensional temperature becomes zero at the cold fluid inlet and unity at the hot fluid inlet. In the bottom figure of Figure 4.12 axial variation of the temperature of the matrix and fluid are observed. Since t^* represents the angular location in the direction of rotation starting from the edge of the cold fluid, the lower four curves show the experimental and theoretical results for the cold fluid and the matrix in touch with the cold fluid whereas the upper four curves belong to the hot region. Figures show that the slope of the experimental curves are smaller compared to the theoretical ones. The reason for this discrepancy is believed to be due to the neglect of the axial conduction in the theoretical calculations. The existence of the axial conduction makes the axial temperature distribution has a tendency of pure uniform temperature

distribution. A similar argument can be made for the upper figure. The discrepancy is basically due to the assumptions made in the theoretical model.

Figure 4.13 shows the drastic change in the slope of the temperature distribution curves as the system parameters is changed.

In the figures 4.14 and 4.15 the large variations at the exit of both hot and cold fluid is shown. This results shown the necessity of some kind of mixing process if the heated or cooled fluid will be used in any thermodynamic process afterwards. Another important result that one gets from these figures is that large temperature difference at the exit and the mixing that takes afterwards results in loss in exergy and should be eliminated with additional, considerations in the design of the rotary heat exchangers.

Variation of the temperature of the hot fluid as a function of angular position in figure. 4.14 can be explained as follows. At smaller angular position the matrix temperature is lower and therefore larger cooling of the hot fluid and consequently smaller exit temperature of the hot fluid occurs. Similar arguments also apply to figure 4.15 for the cold fluid exit temperature.

5.1. CONCLUSIONS

Following conclusions can be obtained from the results of this study:

1. In general effectiveness of the rotary type heat exchanger increases with an increase in the number of heat transfer units.
2. Matrix heat capacity rate ratio, therefore, the rotational speed of the

rotor increases the effectiveness of the rotary type regenerative heat exchanger.

3. Increase in the surface area of the matrix increases the effectiveness of the rotary type regenerative heat exchanger.

4. Large variations in the exit temperatures of the hot and cold fluids occur in this type of heat exchangers.

5. In rotary type regenerative heat exchanger it is possible to reach large values of effectiveness with comparatively smaller pressure drops in contrast to ordinary heat exchangers.

5.2. RECOMMENDATIONS

The set-up designed and constructed in this study is used to study the effectiveness of a rotary heat exchanger. The same set-up can be used for the following future investigations.

1. Existing set-up is suitable to study simultaneous mass and heat transfer by making minor changes on the rotor design.

2. Existing set-up can be used to study the effect of various parameter in rotary type of heat exchangers such as matrix geometry, porosity, matrix material etc.

LIST OF REFERENCES

1. Shah, Ramesh K. "Classification of Heat Exchangers", in Heat Exchangers-Thermal-Hydraulic Fundamentals and Design, edited by S. Kakaç, A.E. Bergles, and F. Mayinger, New York, Hemisphere Publishing Corp., 1981.
2. Kays, W.M. and A.L. London. Compact Heat Exchangers, 2 nd ed. New York, Mc Graw-Hill Book Company, 1964.
3. Stecher, P.G. "Heat Wheels", in Industrial and Institutional Waste Heat Recovery, New Jersey, USA : Noyes Data Corporation, 1979.
4. Iliffe, C.E. "Thermal Analysis of the Contra-Flow Regenerative Heat Exchanger", Journal Institution of Mechanical Engineers, 1948, vol. 159, p. 363.
5. Compage, J.E. and A.L. London. "The periodic-Flow Regenerator-A Summary of Design Theory", Journal of Heat Transfer Transaction, of the ASME, July, 1953, p. 779.
6. "Air-to-Air Heat Recovery Equipment" in ASHRAE Equipment Handbook & Product Directory, 1975.

7. Jakob, M. Heat Transfer, New York, John Wiley and Sons Inc., 1957, Vol. II, pp. 261-341.
8. Coppage, J.E. and A.L. London, "The Periodic-Flow Regenerator- A Summary of Design Theory", Journal of Heat Transfer Transactions of the ASME, 1953, vol. 75, pp. 779-787.
9. Harper, D.B. and W.M. Rohsenow, "Effect of Rotary Regenerator Performance on Gas-Turbine- Plant Performance", Journal of Heat Transfer Transactions of the ASME, 1953, Vol. 75, pp. 759-765.
10. Lambertson, T. J. "Performance Factors of a Periodic-Flow Heat Exchanger", Journal of Heat Transfer Transactions of the ASME, 1958, vol. 80, pp. 586-591.
11. Bahnke, G.D. and C.P. Howard, "The Effect of Longitudinal Heat Conduction on Periodic-Flow Heat Exchanger Performance", Journal of Engineering for Power Transactions of the ASME, April 1964, pp. 105-120.
12. London, A.L., D.F. Sampsel and J.G. Gowan, "The Transient Response of Gas Turbine Plant Heat Exchangers-Additional Solutions for Regenerators of the Periodic-Flow and Direct-Transfer Types", Journal of Engineering for Power Transactions of the ASME, April 1964, pp. 127-135.
13. Holmberg, R. B. "Heat and Mass Transfer in Rotary Heat Exchangers with Nonhygroscopic Rotor Materials", Journal of Heat Transfer Transactions of the ASME, 1977, vol. 99, pp. 196-202.

14. Holmberg, R. B. "Combined Heat and Mass Transfer in Regenerators with Hygroscopic Materials", *Journal of Heat Transfer Transactions of the ASME*, 1979, vol. 101, pp. 205-210.
15. Leersum, J. G. and C.W. Ambrose "Comparisons between Experiments and a Theoretical Model of Heat and Mass Transfer in Rotary Regenerators with Nonsorbing Matrices", *Journal of Heat Transfer Transactions of the ASME*, May 1981, vol. 103, pp. 189-195.
16. London, A.L. "Laminar Flow Gas Turbine Regenerators-The Influence of Manufacturing Tolerances", *Journal of Engineering for Power Transactions of the ASME*, January 1970, pp. 46-56.
17. Vigor, C.W. and W. Leibring "Metal Peeling for Production of Stainless Steel Foil for Gas Turbine Regenerators", *Journal of Heat Transfer Transactions of the ASME*, 1973, vol. 82, pp. 435-440.
18. Mondt, J.R. "Effects of Nonuniform Passages on Deepfold Heat Exchanger Performance", *Journal of Engineering for Power Transactions of the ASME*, October 1977, pp.657-663.
19. Rapley, C.W. and A.I.C. Webb "Heat Transfer Performance of Ceramic Regenerator Matrices with Sine-Duct Shaped Passages", *International Journal of Heat & Mass Transfer*, 1983, vol. 26, pp. 805-814.
20. London, A.L. "Heat Exchangers, Part I-Design Theory", *Mechanical Engineering*, May 1964, pp. 47-51.

21. London, A.L. "Heat Exchangers, Part II- Surface Geometry", Mechanical Engineering, June 1964, pp. 31-34.
22. London, A.L. "Heat Exchangers, Part III-Applications", Mechanical Engineering, July 1964, pp.33-36.
23. Szabo, B.S. "The Economics of Heat Recovery Systems", Air Conditioning, Heating and Ventilating, June 1967, pp. 59-64.
24. Dunkle, R.V. and I.L. Maclaine-Cross, B.E. "Theory and Design of Rotary Regenerators for Air Conditioning", Mechanical & Chemical Engineering Transactions, May 1970, pp. 1-6.
25. London, A.L., M.B.O. Young and J.H. Stang, "Glass-Ceramic Surfaces, Straight Triangular Passages-Heat Transfer and Flow Friction Characteristics", Journal of Engineering for Power Transactions of the ASME, October 1970, pp. 381-389.
26. Kern, J. "Heat Transfer in a Rotary Heat Exchanger", International Journal of Heat & Mass Transfer, 1974, vol. 17, pp. 981-990.
27. Brandemuehl, M.J., P.J. Banks "Rotary Heat Exchangers With Time Varying or Nonuniform Inlet Temperatures", November 1984, vol. 106, pp. 750-758.
28. Bluck, E.V.D., J.W. Mitchell and S.A. Klein "Design Theory for Rotary Heat and Mass Exchangers-I. Wave Analysis of Rotary Heat and Mass Exchangers with Infinite Transfer Coefficients", International Journal Heat & Mass Transfer, 1985, vol. 28, pp. 1575-1586.

29. Bulck, E.V.D., J.W. Mitchell and S.A. Klein "Design Theory for Rotary Heat and Mass Exchangers-II. Effectiveness-Number of Transfer Units Method for Rotary Heat and Mass Exchangers", International Journal Heat & Mass Transfer, 1985, vol. 28, pp. 1587-1595.
30. Romie, F.E. "Transient Response of Rotary Regenerators", Journal of Heat Transfer Transactions of the ASME, November 1988, vol. 110, pp. 836-840.
31. Skiepko, T. "The Effect of Matrix Longitudinal Heat Conduction on the Temperature Fields in the Rotary Heat Exchanger", International Journal of Heat & Mass Transfer, 1988, vol. 31, pp. 2227-2238.
32. Atthey, D.R. "An Approximate Thermal Analysis for a Regenerative Heat Exchanger", International Journal of Heat & Mass Transfer, 1988, Vol. 31, pp. 1431-1441.
33. Bae, Young Lib. "Performance of Rotary Regenerative Heat Exchanger-A Numerical Simulation", A Doctor's Thesis, Oregon State University, June 1987.
34. Sönmez, Murat. "Modelling and Optimization of a Rotary Regenerative Type Waste-Heat Heat Exchanger", a Master's Thesis, Middle East Technical University, March 1986.

APPENDICES



APPENDIX A

SPECIFICATIONS OF INSTRUMENTS

Table A.1. Specifications of Alarko Model Supply (Cold) Fan.

Type	: FLE 28
Capacity	: 1800 m ³ /h
Pressure	: 50 mm. water column.
Motor	: 5.5 HP (4 KW), 1420 rpm.

Table A.2. Specifications of Alarko Model Exhaust (Hot) Fan.

Type	: FLE 28
Capacity	: 1800 m ³ /h
Pressure	: 50 mm. water column.
Motor	: 1.5 HP (1.1 KW), 1380 rpm.

Table A.3. Specifications of Gamak Model Electric Motor of Reductor.

Type	: 380 V, 0.91 A
Power	: 0,5 HP (0.37 KW)
Revolution	: 1410 rpm.

Table A.4. Specifications of Reductor.

Pulleys : 600 mm (2)
180 mm (1)
125 mm (2)
60 mm (5)

Reductions

Ratios : 1/4, 1/6, 1/20, 1/23, 1/33, 1/40, 1/48, 1/100, 1/144, 1/208,
1/300.

**Table A.5. Specifications of Keithley Instruments Model 179
A DC Voltmeter Digital Multimeter.**

Range : 200 mV, 2V, 20V, 200V, 1200V

Accuracy : 0,04 % of Reading + 3 digit on 200 mV range

0,04 : of Reading + 1 digit on the other ranges

Input Resistance : 10 megaohms + 01 %

Setting Time : 1 second to within 1 digit of final reading

Table A.6 Specifications of Electrical Heaters.

Power (Variac)	: 1700 Watt (3 x 220 volt)
Power (direct)	: 8000 Watt (3 x 380 volt)
Power (direct)	: 1300 Watt (2x 220 volt)
Total Power	: 11000 Watt

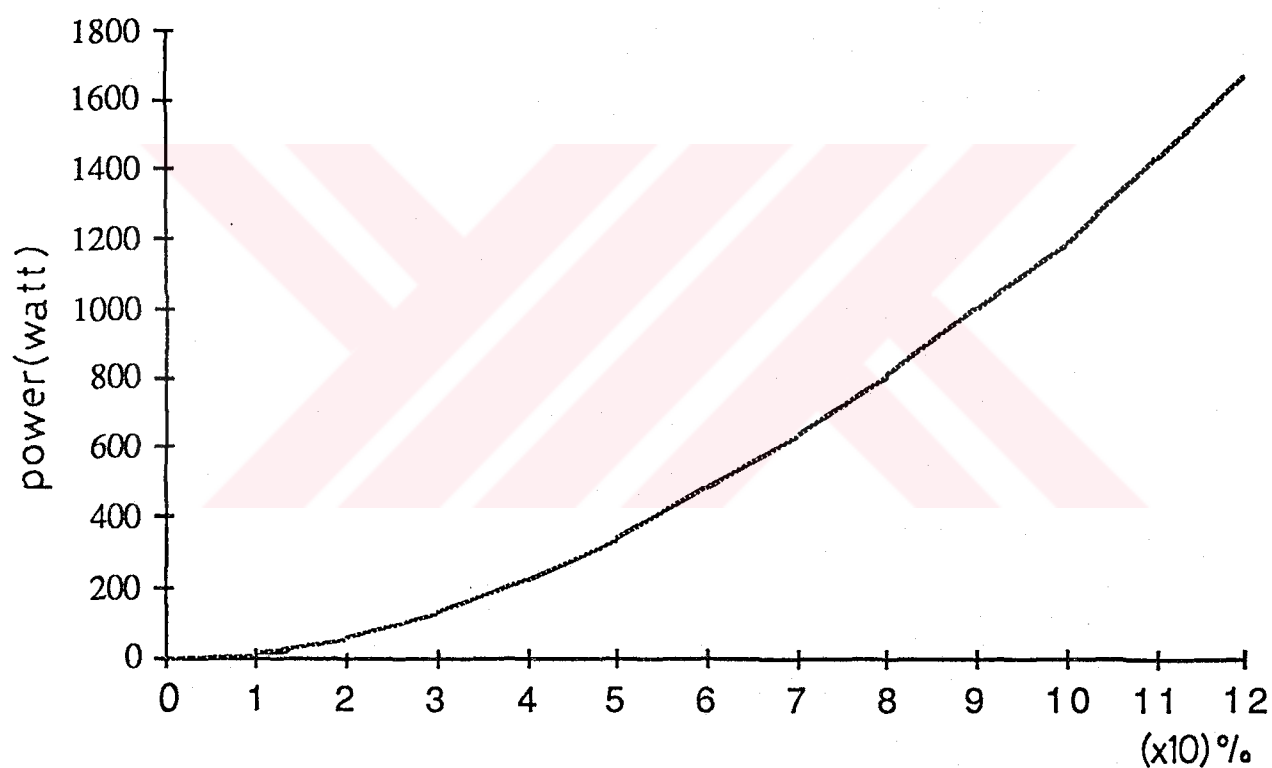


Figure A.1. Power Distribution of the Variac.

**Table A.7. Specifications of Gould Brush Mark-250 Type
Chart Recorder**

Chart Speed (2 ranges)	:	0.02, 0.05, 0.1, 0.2, 0.5, 1.0 sec/div 0.02, 0.05, 0.1, 0.2, 0.5, 1.0 min/div
Chart Speed Accuracy	:	Sprocketed drive, line synchronized speed error non-cumulative
Trace Presentation	:	Rectilinear
Trace Width	:	0.01 inch, nominal
Chart Description	:	
Width	:	6 inches overall
Divisions	:	5.0 divisions in 4 1/2 inches
Power Input (AC)	:	115 ± 10 % volts, 60 cps, 125 Watts 230 ± 10 % volts, 50 cps, 185 Watts 115 ± 10 % volts, 50 cps, 125 Watts
Signal Input	:	
Impedance	:	50 kohms
Sensitivity	:	2.5 volts for center to edge deflection
Signal Output	:	
Noise	:	Less than 0.1 % of full scale
Non-Linearity	:	0.5 % of full scale

APPENDIX B

CALCULATION OF FLOW RATE

A sample calculation of flow rate is shown below. In a typical the following dynamic heads at various axial distances in a $\varnothing 8$ cm. diameter tube are measured using a pitot tube and inclined manometer.

(from center)	r= 0 cm	$H_D = 2''$ (vertical value)
	r= 1 cm	$H_D = 1.6''$
	r= 2 cm	$H_D = 1.2''$
	r= 3 cm	$H_D = 0.5''$
	r= 4 cm	$H_D = 0''$

From these data the velocity can be found by using the following expression;

$$v = \sqrt{2 \cdot g \cdot H_D \cdot \frac{\rho_{\text{water}}}{\rho_{\text{air}}}} \quad (\text{m/sec})$$

where;

g: gravitational acceleration (m/sec^2)

H_D : dynamic head (m,water column)

ρ : density (kg/m^3)

$r=0$ cm $v=28$ m/s

$r=1$ cm $v=26$ m/s

$r=2$ cm $v=22$ m/s

$r=3$ cm $v=14$ m/s

$r=4$ cm $v=0$ m/s

By least square curve fitting of the data above the velocity of the fluid can be found as a function of the radial distance as:

$$v = 28.00 - 4.23r + 2.93r^2 - 1.48r^3 + 0.14r^4$$

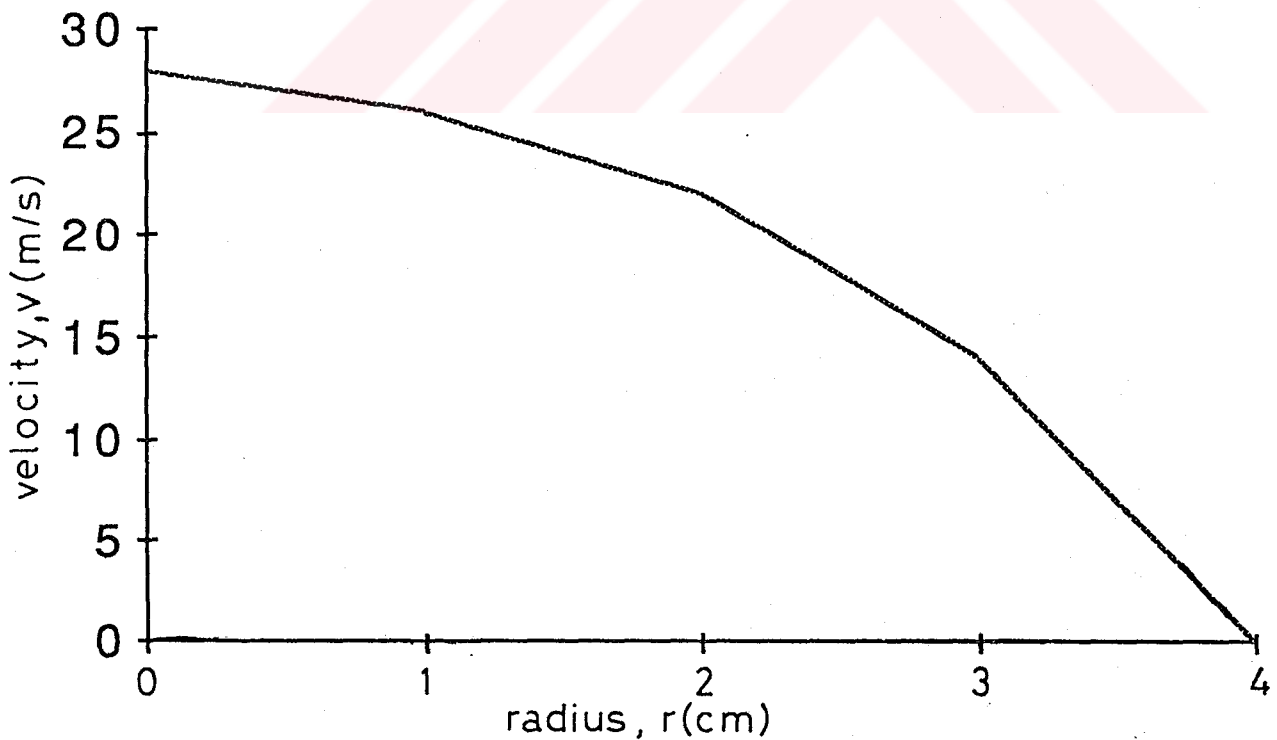


Figure B.1. Distribution of the Velocity in the Inlet Tube

To find the volume flow rate of the fluid following integral is taken:

$$Q = \int_0^r v \cdot 2\pi r \cdot dr$$

$$Q = \int_0^{0.04} (28.00 - 4.23r + 2.93r^2 - 1.48r^3 + 0.14r^4) \cdot 2\pi r \cdot dr$$

$$Q = 2\pi \left(\frac{28.00}{2} r^2 - \frac{4.23}{3} r^3 + \frac{2.93}{4} r^4 - \frac{1.48}{5} r^5 + \frac{0.14}{6} r^6 \right) \Big|_0^{0.04}$$

$$Q = 0.139 \text{ (m}^3\text{/s)}$$

$$Q = 500 \text{ (m}^3\text{/h)}$$

APPENDIX C

CALCULATION OF THE CONVECTION HEAT TRANSFER COEFFICIENT

Mass velocity is calculated from the following expression;

$$G = \frac{\dot{m}}{A_o} = \frac{Q \cdot \rho_{air}}{A_o} \text{ (kg/m}^2\text{.sec)}$$

Where;

G: mass velocity (kg/m².sec)

\dot{m} : mass flow rate (kg/sec)

A_o : free flow area (m²)

Reynolds number can be found from the following expression;

$$Re = \frac{D_{hyd} \cdot G}{\mu}$$

Where;

Re: Reynolds number (dimensionless)

D_{hyd} : hydraulic diameter (m)

μ : dynamic viscosity (kg/m.sec)

Pressure drop across the rotary regenerator are given in the following tables;

Re	87	124	165	226	261	323
$\Delta P(N/m^2)$	1.7	2.5	3.4	4.7	5.5	6.7
Re	353	433	610	897	1200	
$\Delta P(N/m^2)$	7.4	9.1	12.8	18.8	25.6	

TABLE C.1. Pressure Drop Across the Rotary Regenerator for the Matrix Geometry of the Galvanized Sheet Iron Rotor.

Re	43	62	82	113	130	161
$\Delta P(N/m^2)$	3.1	4.1	5.5	7.6	8.8	10.8
Re	176	216	305	448	600	
$\Delta P(N/m^2)$	11.8	14.6	20.6	30.3	41.2	

TABLE C.2. Pressure Drop Across the Rotary Regenerator for the Matrix Geometry of the Galvanized Sheet Iron+Aluminum Sheet Rotor.

Fanning friction factor is calculated as;

$$f_f = \frac{\Delta P \cdot \rho \cdot D_{hyd}}{2 \cdot L \cdot G^2}$$

where;

f_f : Fanning friction factor

ρ : density (kg/m^3)

L: length of the rotary regenerator (m)

ΔP : Pressure drop of rotary regenerator (N/m^2)

To find Fanning friction factor, the following figures obtained by experimental measurement are used;

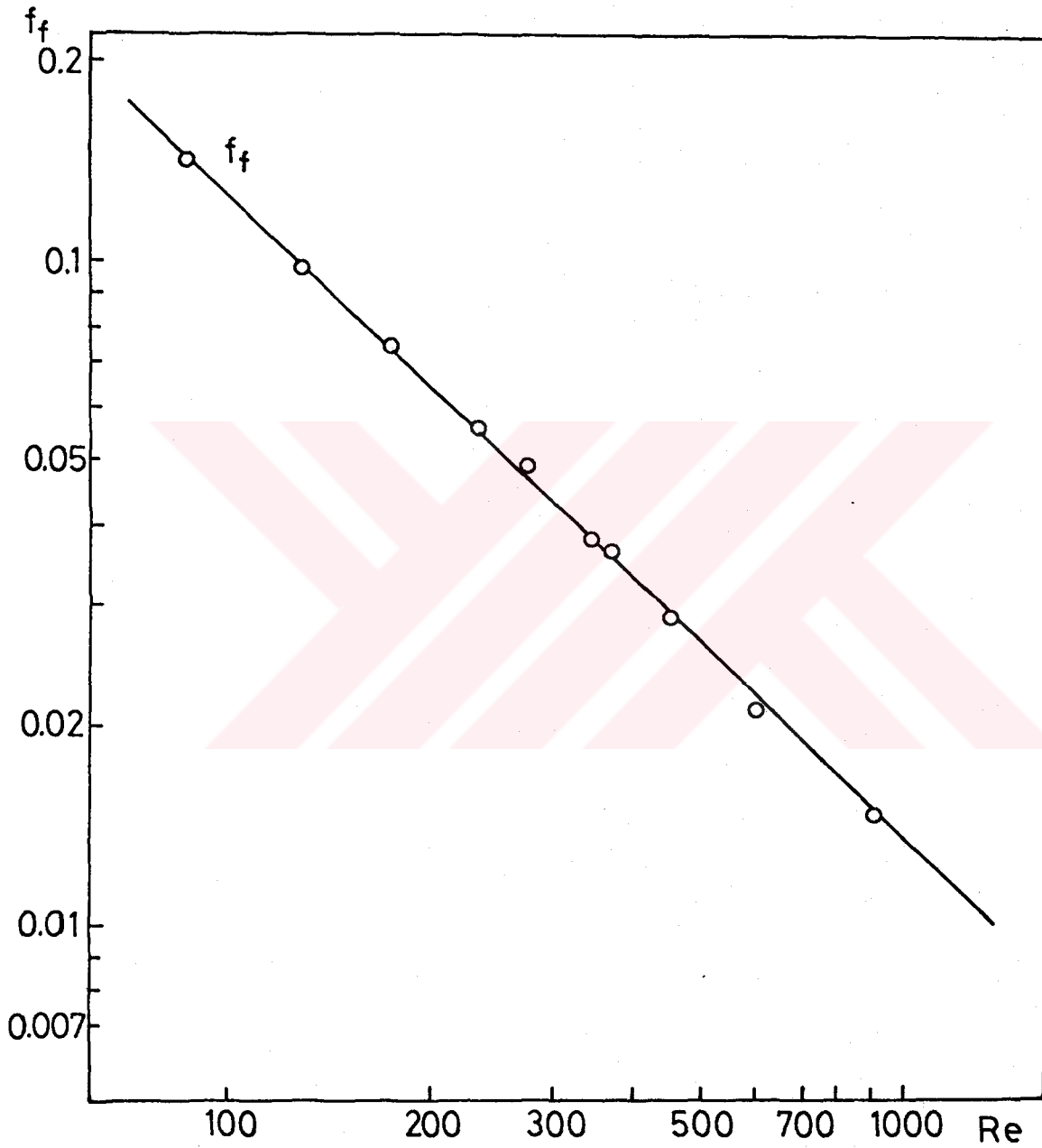


Figure C.1. Fanning Friction Factor as a Function of Reynolds Number for the Matrix Geometry of the Galvanized Sheet Iron Rotor.

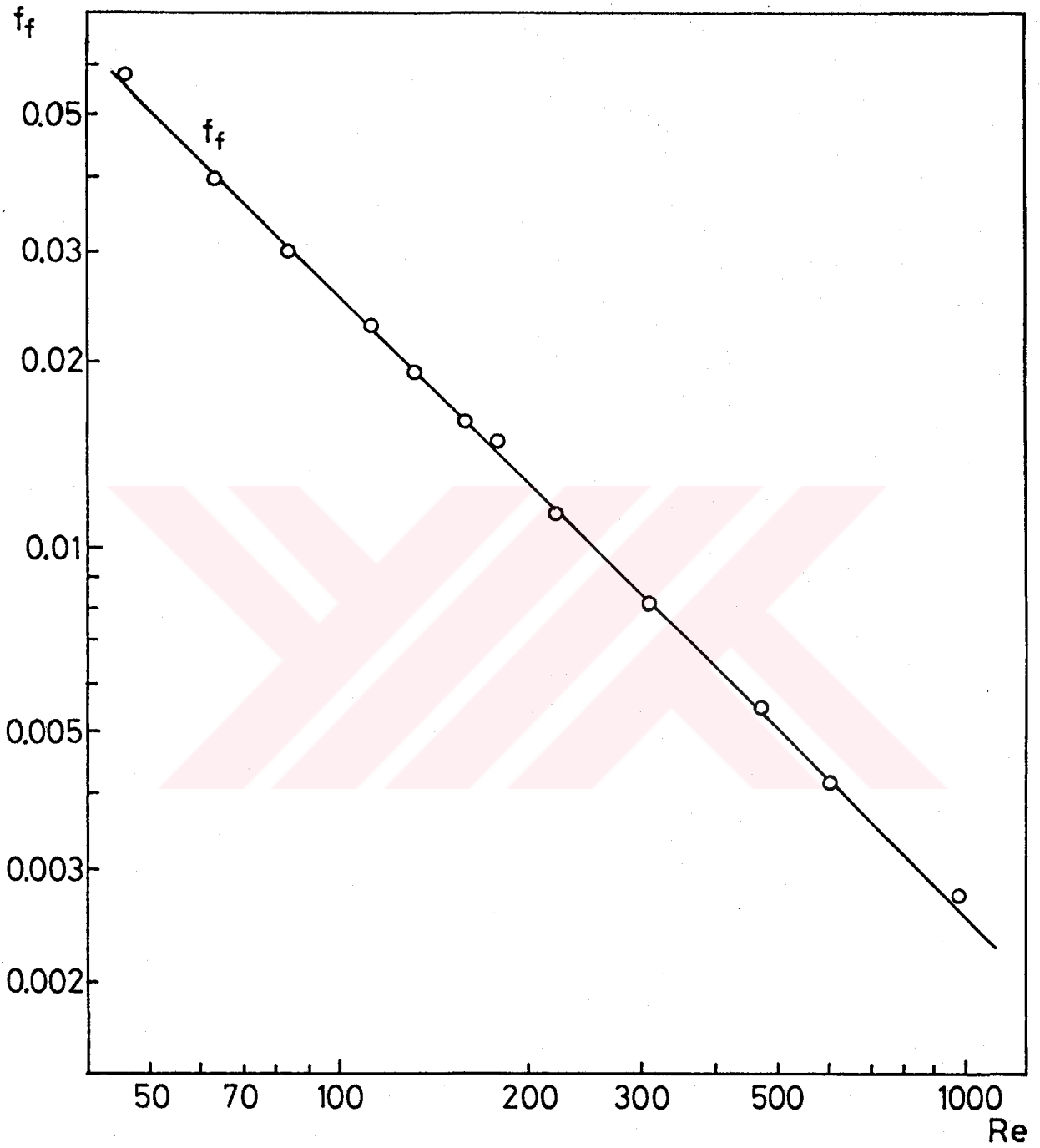


Figure C.2. Fanning Friction Factor as a Function of Reynolds Number for the Matrix Geometry of the Galvanized Sheet Iron+ Aluminum Sheet Rotor.

In this study, fully developed turbulent flow is considered in the regenerator.

Stanton number can be calculated by using Reynolds Colburn Analogy;

$$St = \frac{1}{2} f_f \cdot Pr^{-2/3}$$

Where;

St :Stanton number (dimensionless)

Pr: Prandtl number (dimensionless)

Then, heat transfer coefficient is given by

$$St = \frac{h}{G \cdot c_p}$$

$$h = St \cdot G \cdot c_p$$

Where;

h= convection heat transfer coefficient (W/m²°C)

c_p= specific heat of fluid at constant pressure (J/kg°C)

APPENDIX D

A SAMPLE EVALUATION OF EXPERIMENTAL DATA

A sample evaluation of experimental data is shown below. Volume flow rates were calculated for two fans in Appendix B.

$$Q = 0.139 \text{ (m}^3\text{/sec)}$$

$$\text{for } T_{\text{ambient}} = 25.6 \text{ (}^\circ\text{C)}$$

$$\rho = 1.1826 \text{ (kg/m}^3\text{)}$$

was obtained by using air tables.

then, mass flow rate of hot and cold fluids were obtained from the following relation;

$$\dot{m} = Q \cdot \rho$$

$$\dot{m} = 0.139 \times 1.1826 = 0.1644 \text{ (kg/sec)}$$

Temperature data was obtained as;

$$T_{c,i} = 28.39 \text{ (}^\circ\text{C) (mean temperature)}$$

$$T_{c,o} = 42.07 \text{ (}^\circ\text{C) (mean temperature)}$$

$$T_{h,i} = 54.20 \text{ (}^\circ\text{C) (mean temperature)}$$

$$T_{h,o} = 40.54 \text{ (}^\circ\text{C)} \text{ (mean temperature)}$$

Specific heat of fluid at constant pressure of hot and cold side were obtained following relation;

$$\frac{T_{c,i} + T_{c,o}}{2} = \frac{28.39 + 42.07}{2} = 35.23 \text{ (}^\circ\text{C)}$$

$$(c_p)_c = 1006.254 \text{ (J/kg }^\circ\text{C)} \quad \text{for } 35.23 \text{ }^\circ\text{C}$$

$$\frac{T_{h,i} + T_{h,o}}{2} = \frac{40.54 + 54.20}{2} = 47.37 \text{ (}^\circ\text{C)}$$

$$(c_p)_H = 1007.059 \text{ (J/kg }^\circ\text{C)} \quad \text{for } 47.37 \text{ }^\circ\text{C}$$

Then, heat capacity rate of the cold and hot side were obtained by,

$$C_c = C_{\min} = \dot{m}_c \cdot c_p = 0.1644 \times 1006.254 = 165.428 \text{ (W/}^\circ\text{C)}$$

$$C_H = C_{\max} = \dot{m}_H \cdot c_p = 0.1644 \times 1007.059 = 165.560 \text{ (W/}^\circ\text{C)}$$

Heat capacity rate ratio of fluids was obtained from the following expression;

$$C^* = \frac{C_{\min}}{C_{\max}} = \frac{C_c}{C_H} = \frac{165.428}{165.560} = 1$$

The effectiveness of the rotary regenerator was calculated as;

$$\epsilon = \frac{T_{c,o} - T_{c,i}}{T_{h,i} - T_{c,i}} = \frac{42.07 - 28.39}{54.20 - 28.39} = 0.53$$

Method of the calculation of the convection heat transfer coefficient is shown in Appendix C.

Convection heat transfer coefficient was calculated from the following expression;

$$G = \frac{\dot{m}}{(A_o)_c} = \frac{0.1644}{0.0787} = 2.0890 \text{ (kg/m}^2\text{sec)}$$

$$Re = \frac{D_{hyd} \cdot G}{\mu} = \frac{4.144 \cdot 10^{-3} \times 2.0890}{2 \cdot 10^{-5}} = 433$$

ΔP data was obtained as;

$$\Delta P = 9.1 \text{ (N/m}^2\text{)} \quad \text{for } Re = 433$$

Fanning friction factor was calculated as;

$$f_f = \frac{\Delta P \cdot \rho \cdot D_{hyd}}{2 \cdot L \cdot G^2}$$

$$f_f = \frac{9.1 \times 1.1826 \times 4.144 \cdot 10^{-3}}{2 \times 0.202 \times (2.0890)^2} = 0.025295$$

$$St = \frac{1}{2} f_f \cdot Pr^{-2/3}$$

$$St = \frac{1}{2} \times 0.025295 \times (0.705)^{-2/3} = 0.01597$$

$$h = St \cdot G \cdot c_p = 0.01597 \times 2.0890 \times 1006.254$$

$$h = 33.6 \text{ (W/m}^2\text{ }^\circ\text{C)}$$

The number of heat transfer unit was obtained from the following expression;

$$NTU = \frac{h.A}{4.C_{\min}} = \frac{33.6 \times 30.7}{4 \times 165.428} = 1.56$$

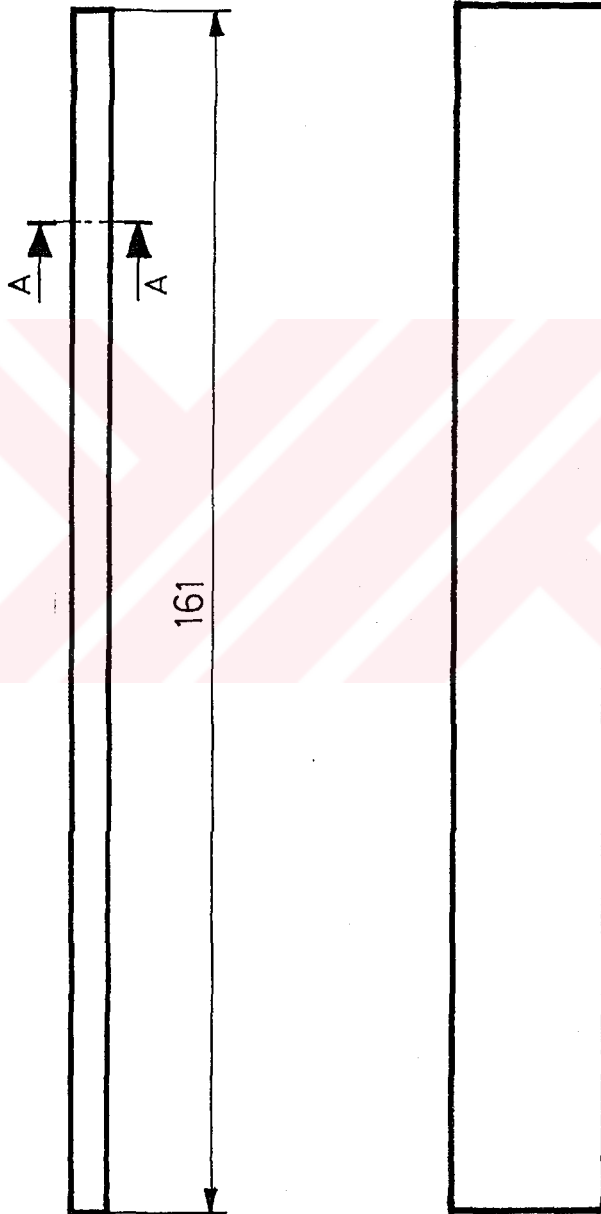
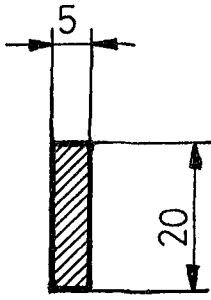
Heat capacity rate of rotating matrix was calculated as;

$$C_r = M_w \cdot C_w \cdot N = 40.65 \times 450 \times 0.118 = 2150.2 \text{ (W/}^\circ\text{C)}$$

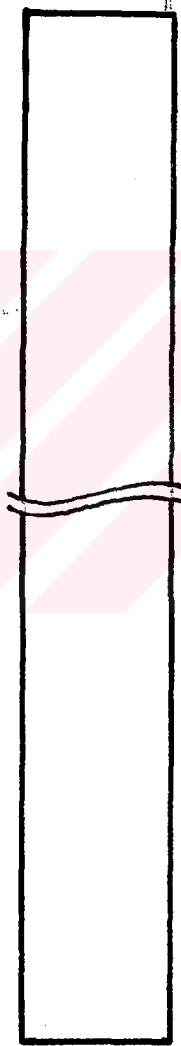
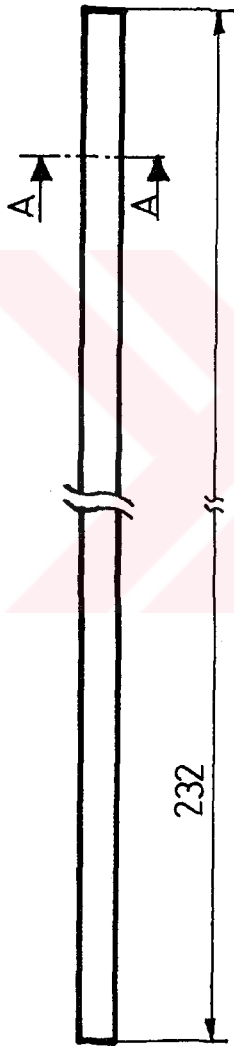
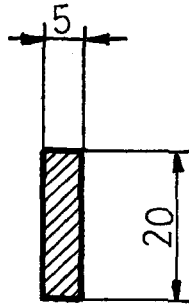
Then, the matrix heat capacity rate ratio was calculated as;

$$C_r^* = \frac{C_r}{C_{\min}} = \frac{2150.2}{165.4} = 13$$

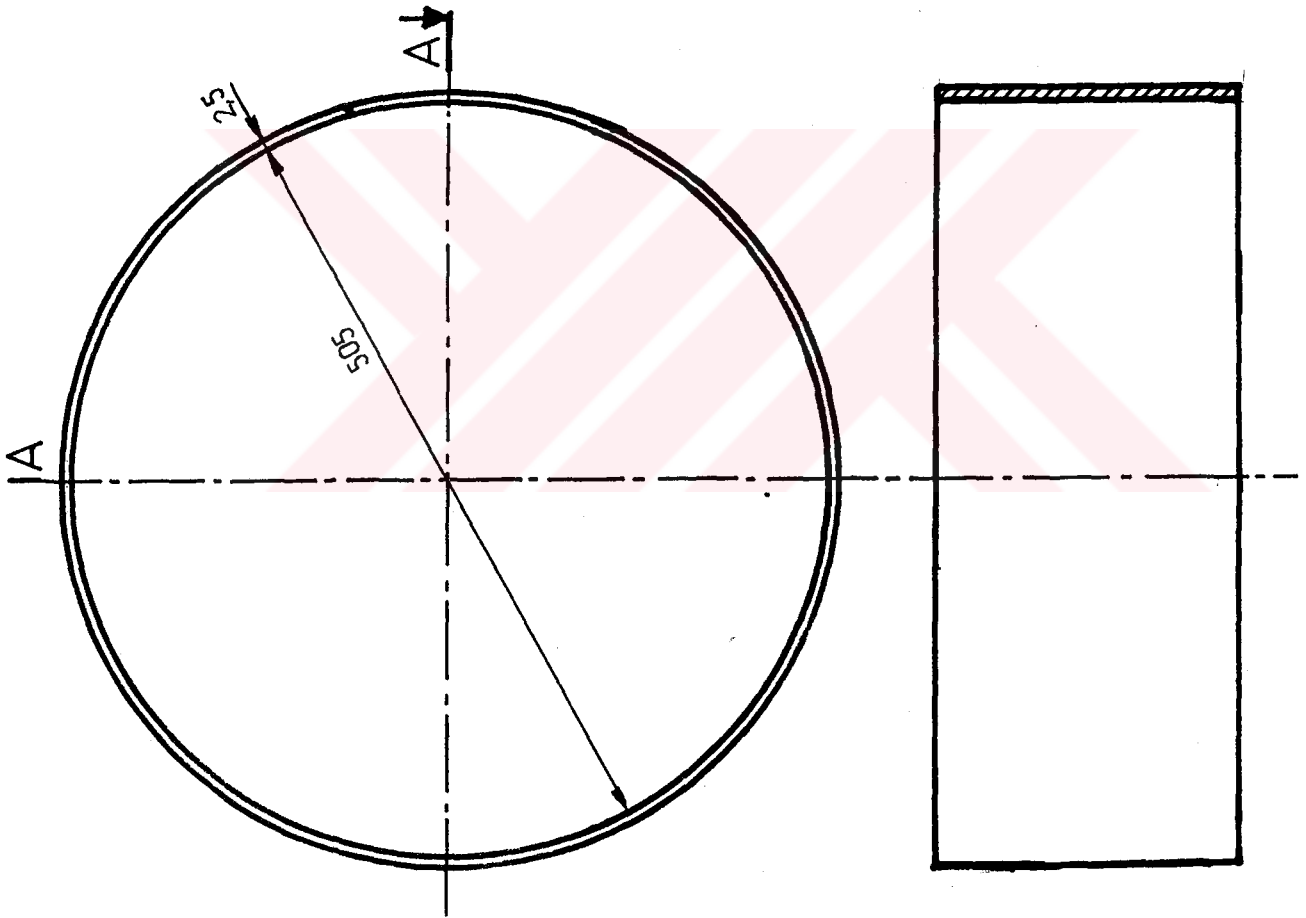
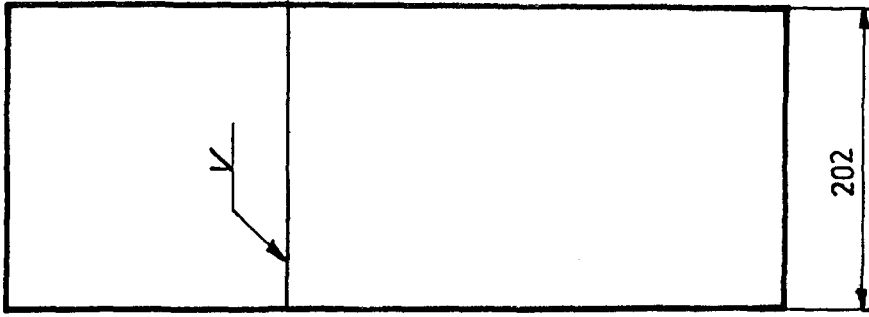
APPENDIX E
ENGINEERING DRAWINGS OF THE ROTARY TYPE
REGENERATIVE HEAT EXCHANGER



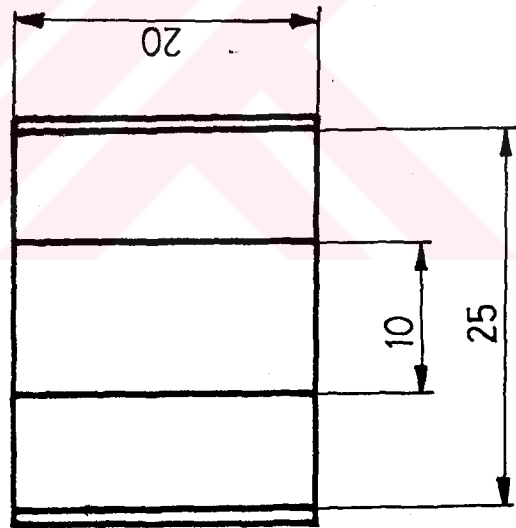
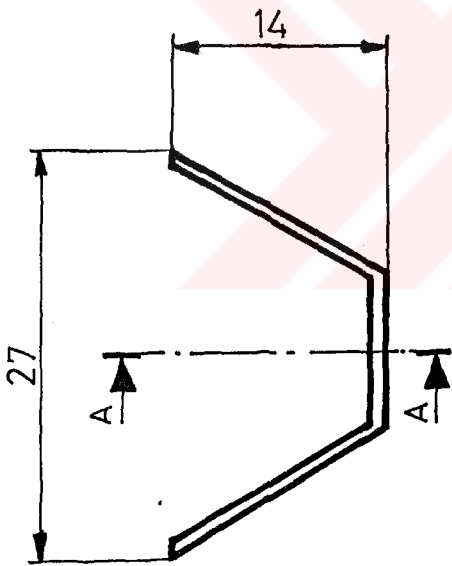
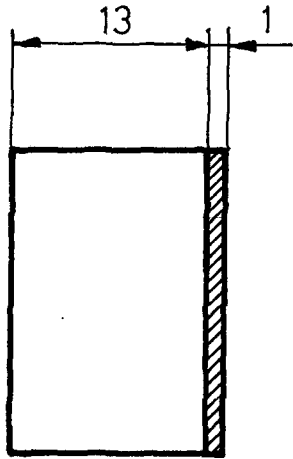
DESIGNED BY	Mehmet TARAKCI	QUAN:	Frame of R.R.H.E.	METU	
DRAWN BY	Mehmet TARAKCI	2		Mech. Eng. Dpt.	
SUPERVISOR	Prof. Dr. Cemil YAMALI	SCALE		DRAWING NO	1
MATERIAL	20x5 Flat Bar	1 / 1			



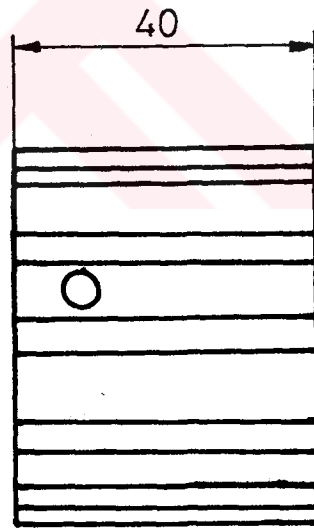
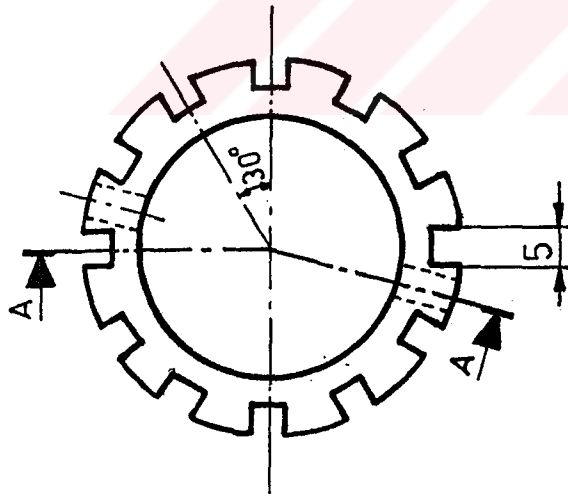
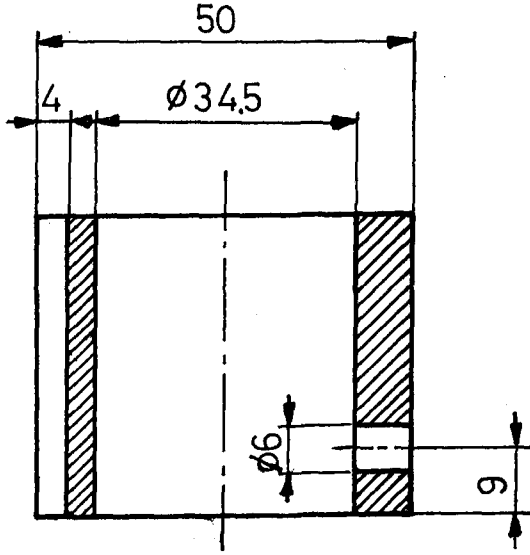
DESIGNED BY	Mehmet TARAKCI	QUAN.	Frame of R.R.H.E.	METU	
DRAWN BY	Mehmet TARAKCI	24		Mech. Eng. Dpt.	
SUPERVISOR	A.Prof.Dr.Cemil YAMALI	SCALE		DRAWING NO	2
MATERIAL	20x5 Flat Bar	1/1			



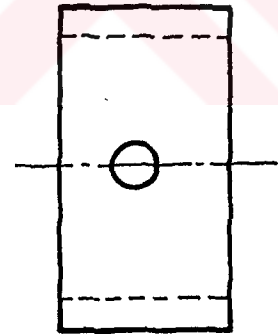
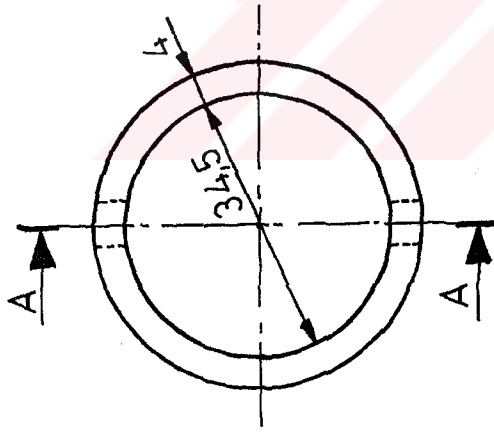
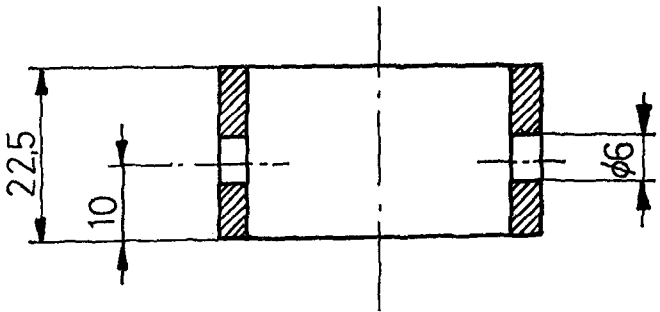
DESIGNED BY	MEHMET TARAKCI	QUAN. 1	Frame Drum of R.R.H.E.	METU	
DRAWN BY	Mehmet TARAKCI			Mech. Eng. Dpt.	
SUPERVISOR	A.P.Dr. Cemil YAMALI	SCALE 1 / 5		DRAWING NO	3
MATERIAL	2.5mm. Sheet Iron				



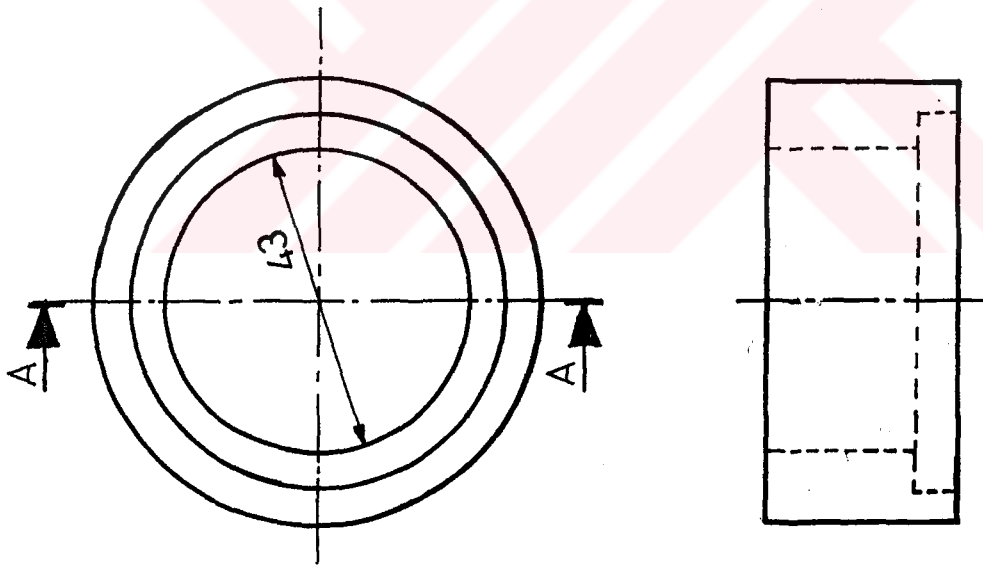
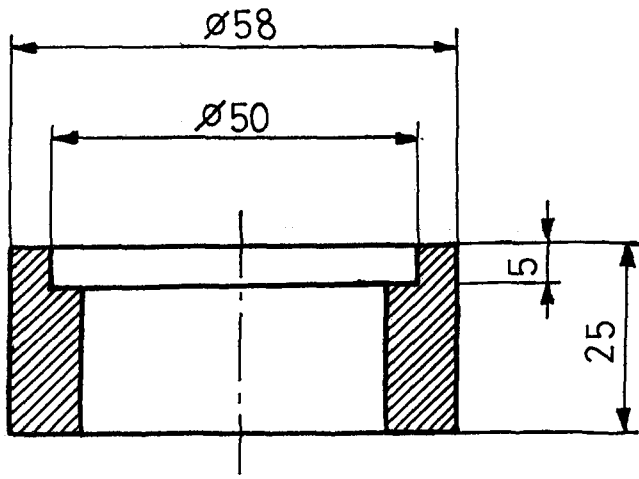
DESIGNED BY	Mehmet TARAKCI	QUAN.	Pulley of Drum	METU	
DRAWN BY	Mehmet TARAKCI	24		Mech. Eng. Dpt.	
SUPERVISOR	Prof. Dr. Cemil YAMALI	SCALE		DRAWING NO	4
MATERIAL	1mm. Sheet Iron	2/1			



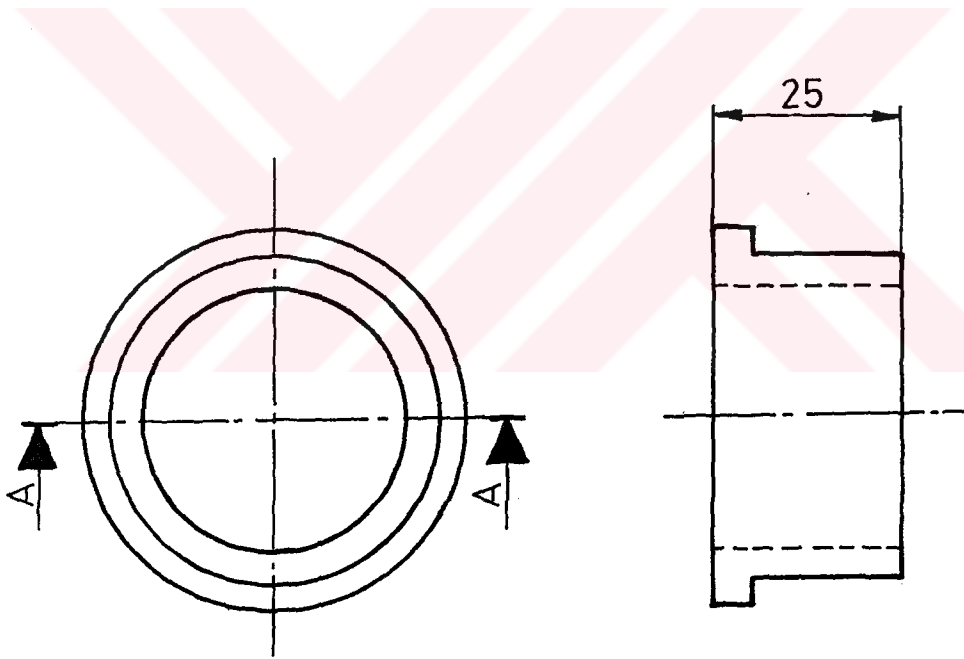
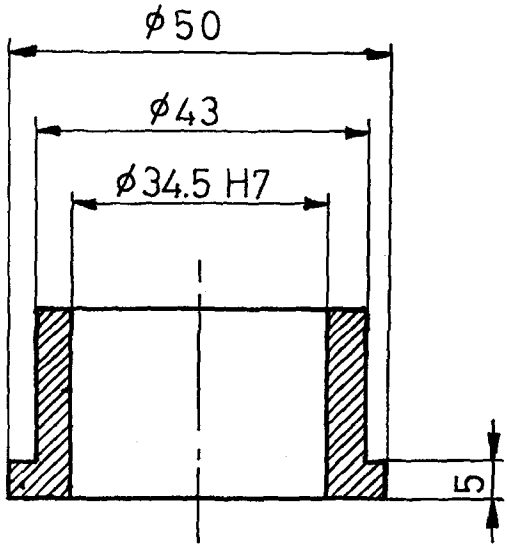
DESIGNED BY	Mehmet TARAKÇI	QUAN.	Frame of R.R.H.E.	METU	
DRAWN BY	Mehmet TARAKÇI			2	Mech. Eng. Dpt.
SUPERVISOR	A.P. Dr. Cemil YAMALI	SCALE		DRAWING NO	5
MATERIAL	ST 42	1/1			



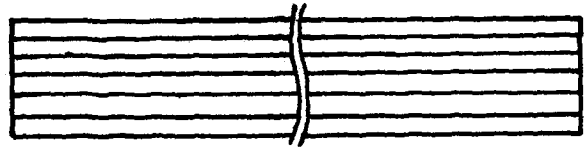
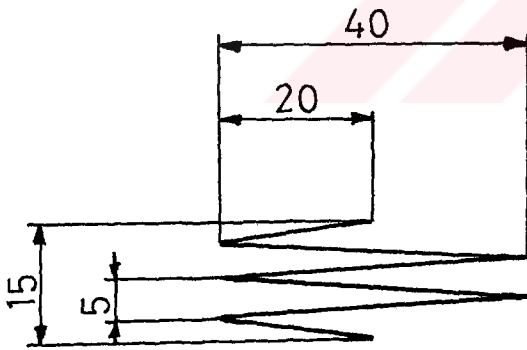
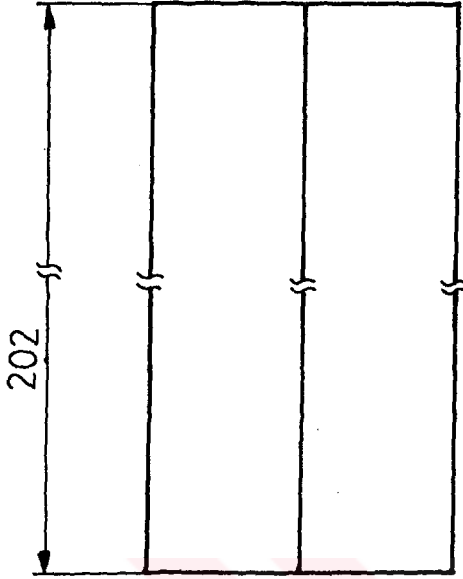
DESIGNED BY	Mehmet TARAKÇI	QUAN. 2	Frame Bearing neck of R.R.H.E.	METU	
DRAWN BY	Mehmet TARAKÇI			Mech. Eng. Dpt.	
SUPERVISOR	A.P. Dr. Cemil YAMALI	SCALE 1/1		DRAWING NO	6
MATERIAL	ST 42				



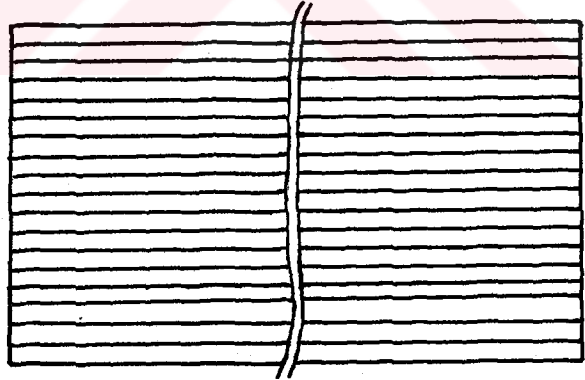
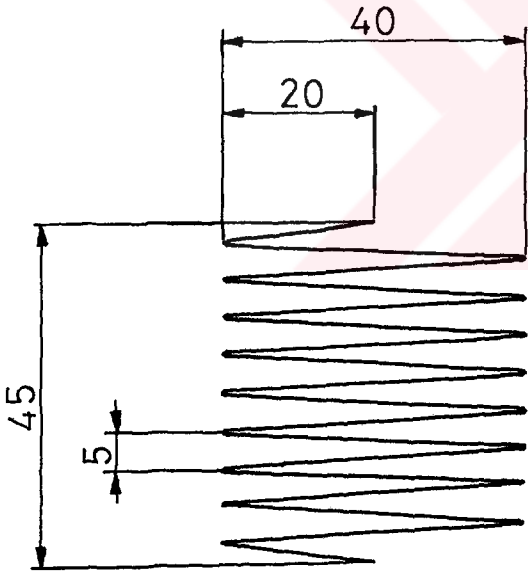
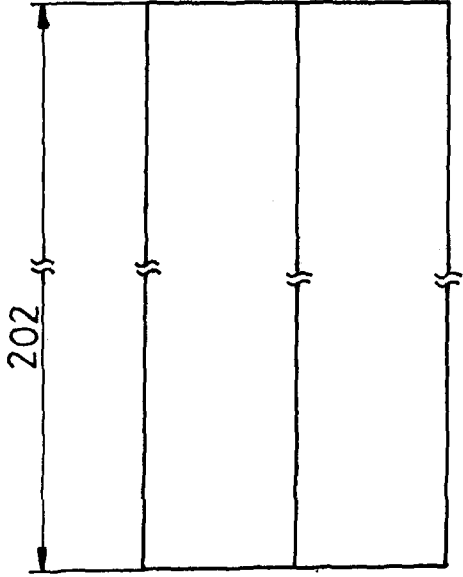
DESIGNED BY	Mehmet TARAKÇI	QUAN. 2	Bearing of R.R.H.E.	METU Mech. Eng. Dpt.	
DRAWN BY	Mehmet TARAKÇI			SCALE 1/1	DRAWING NO
SUPERVISOR	Assoc.PDr.Cemil YAMALI				
MATERIAL	ST 60				



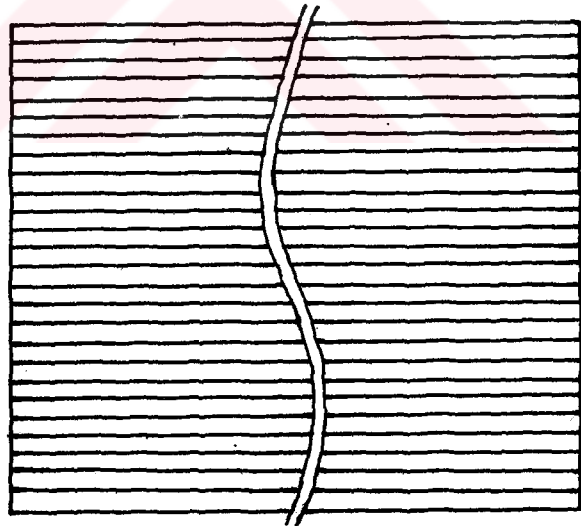
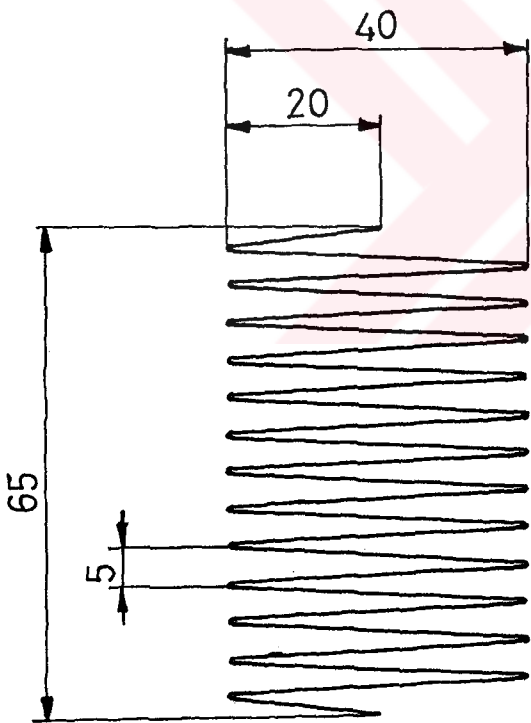
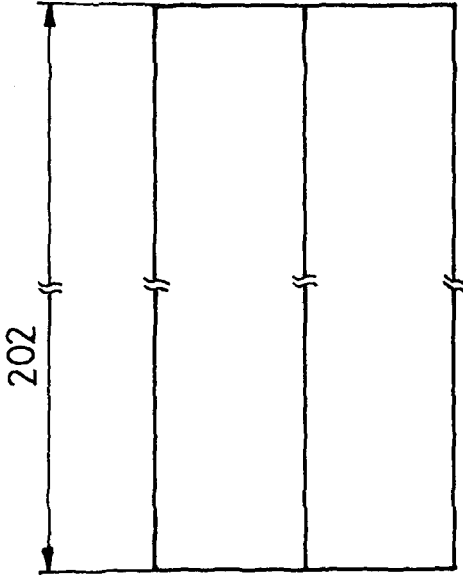
DESIGNED BY	Mehmet TARAKCI	QUAN.	2	Bearing Bronze of R.R.H.E.	METU	
DRAWN BY	Mehmet TARAKCI				Mech. Eng. Dpt.	
SUPERVISOR	Assoc.Prof.Dr.Cemil YAMALI	SCALE	1/1		DRAWING NO	8b
MATERIAL	BRONZE					



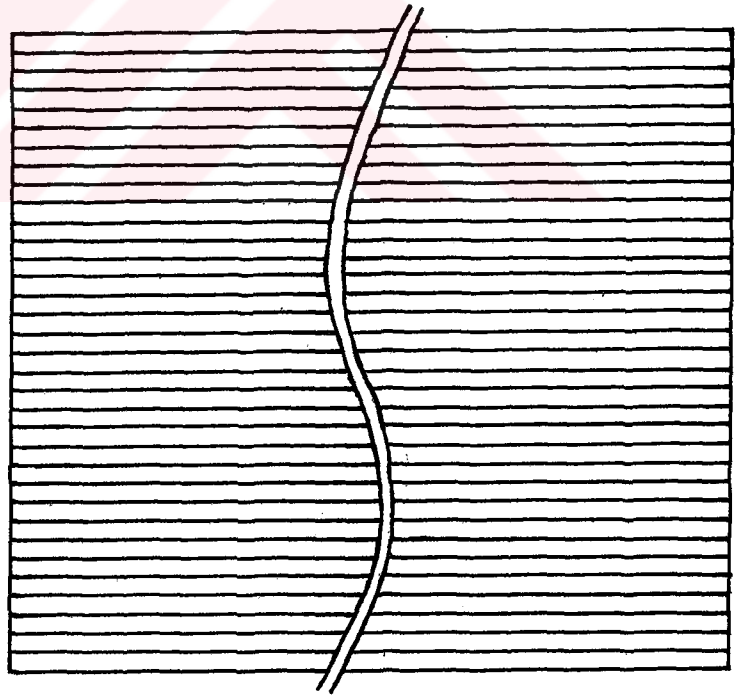
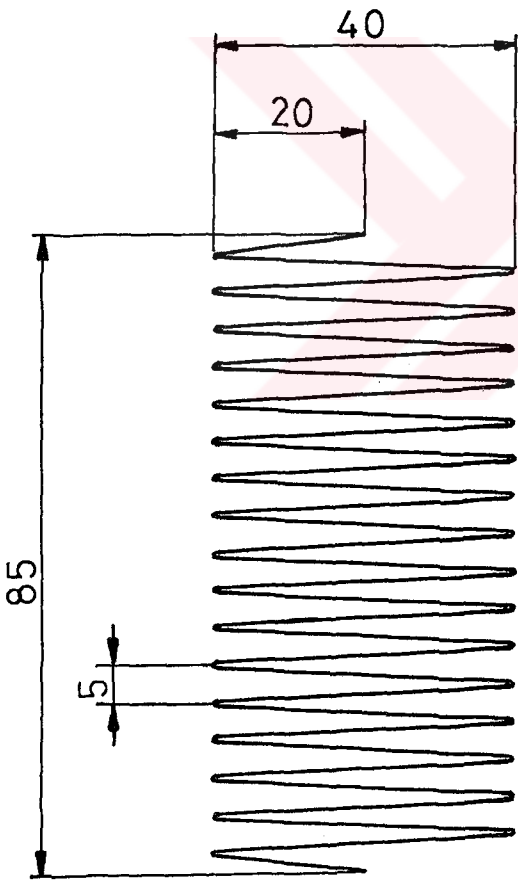
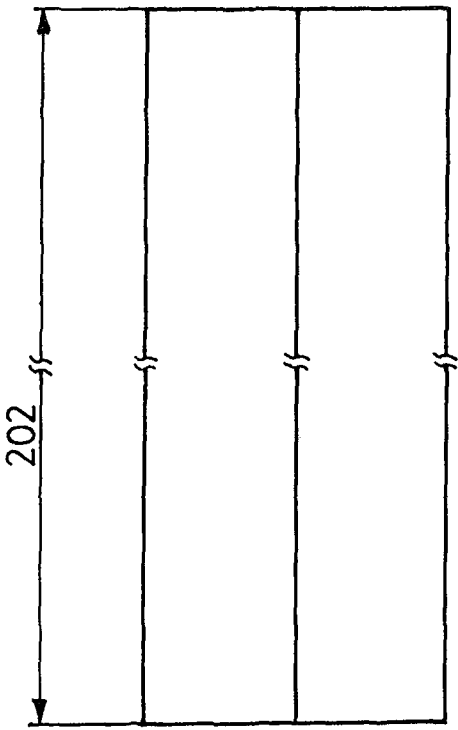
DESIGNED BY	Mehmet TARAKÇI	QUAN. 12	Matrix (1. Step)	METU	
DRAWN BY	Mehmet TARAKÇI			Mech..Eng. Dpt.	
SUPERVISOR	AssocProf.Dr.Cemil YAMALI	SCALE 1/1		DRAWING NO	9
MATERIAL	0.35 Galvanized Sheet Iron				



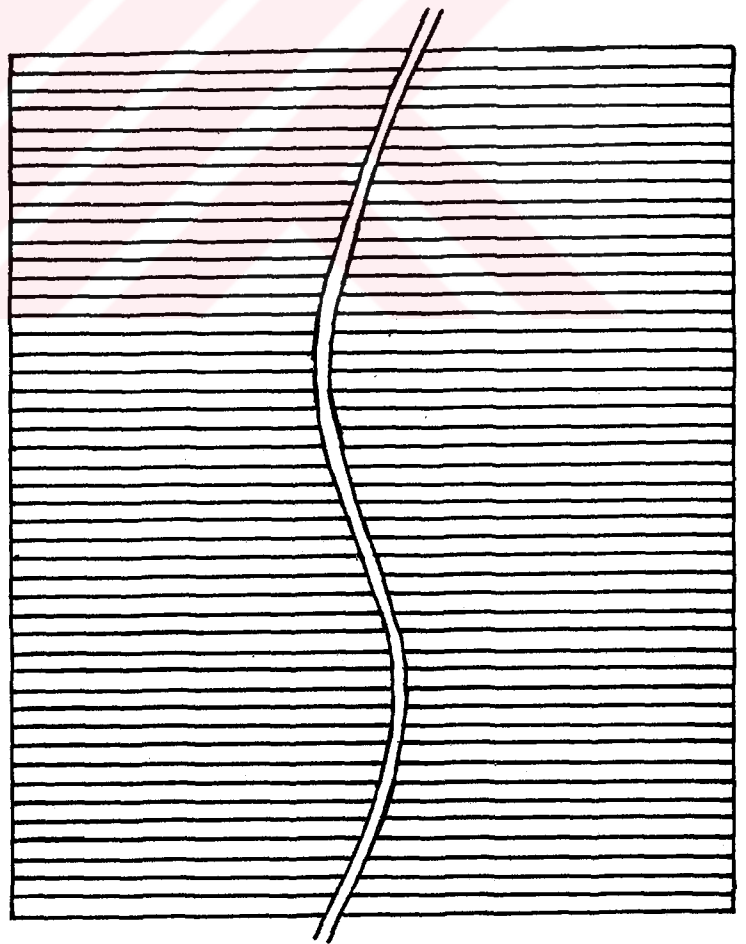
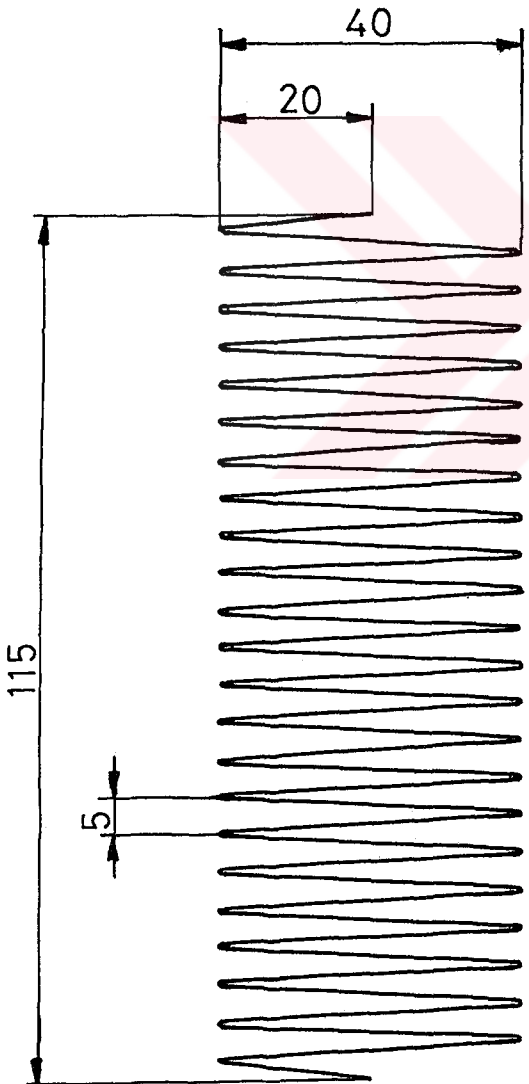
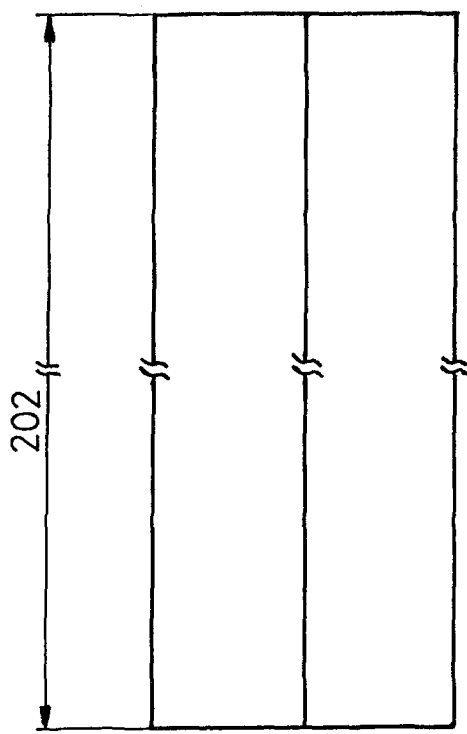
DESIGNED BY	Mehmet TARAKÇI	QUAN. 12	Matrix (2. Step)	METU	
DRAWN BY	Mehmet TARAKÇI			Mech. Eng. Dpt.	
SUPERVISOR	Assoc.Prof. Dr.Cemil YAMALI	SCALE 1 / 1		DRAWING NO	10
MATERIAL	0.35mm Galvanized Sheet Iron				



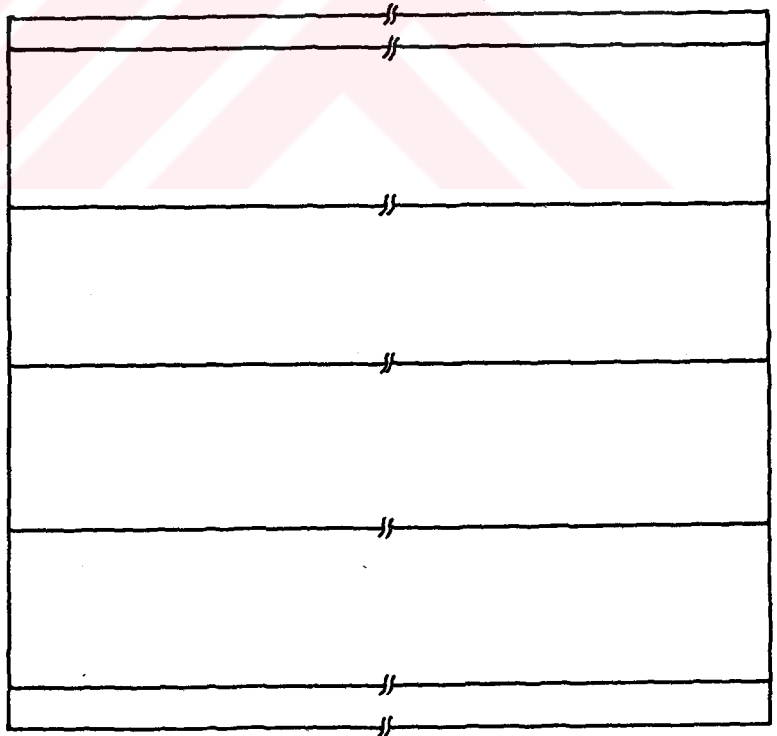
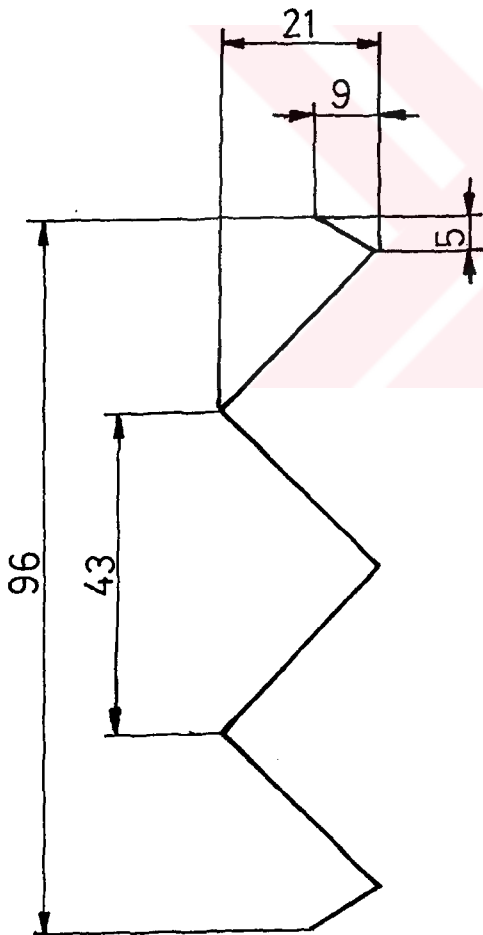
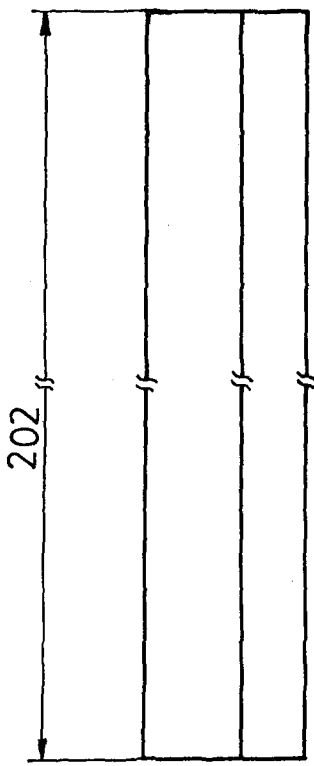
DESIGNED BY	Mehmet TARAKÇI	QUAN.	Matrix (3. Step)	METU	
DRAWN BY	Mehmet TARAKÇI			12	Mech. Eng. Dpt.
SUPERVISOR	Assoc.Prof.Dr.Cemil YAMALI	SCALE		DRAWING NO	11
MATERIAL	0,35mm Galvanized Sheet Iron	1/1			



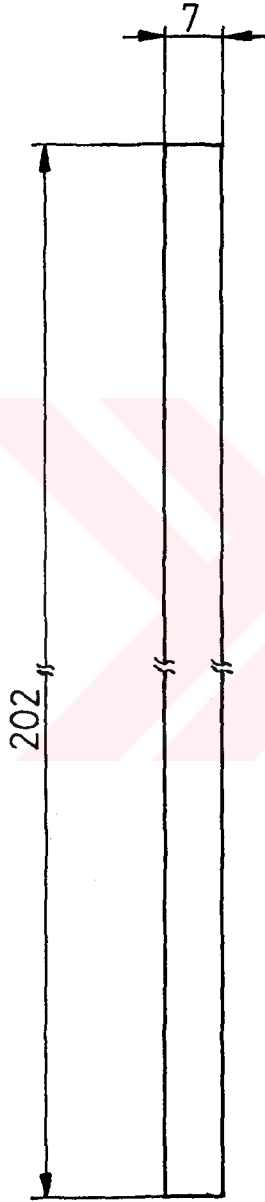
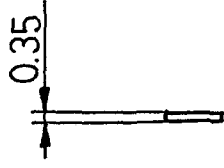
DESIGNED BY	Mehmet TARAKCI	QUAN.	Matrix (4. Step)	METU	
DRAWN BY	Mehmet TARAKCI	12		Mech. Eng. Dpt.	
SUPERVISOR	Assoc. Prof. Dr. Cemil YAMALI	SCALE	1/1	DRAWING NO	12
MATERIAL	0.35mm Galvanized Sheet Iron				



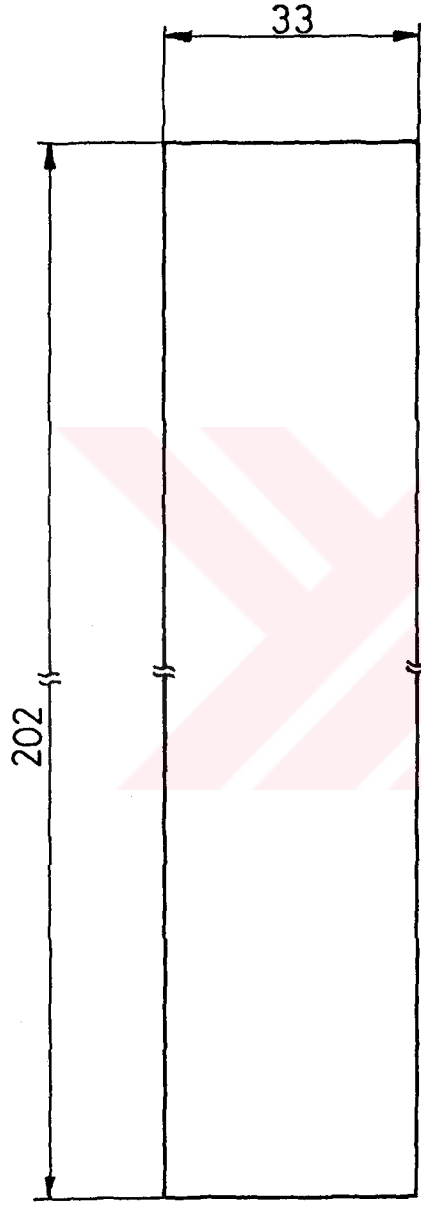
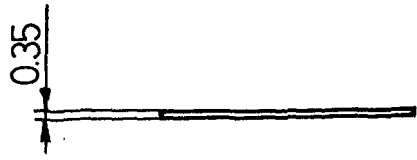
DESIGNED BY	Mehmet TARAKÇI	QUAN.	Matrix (5. Step)	METU	
DRAWN BY	Mehmet TARAKÇI	12		Mech. Eng. Dpt.	
SUPERVISOR	Assoc.Prof. Dr. Cemil YAMALI	SCALE	DRAWING NO	13	
MATERIAL	0.35mm Galvanized Sheet Iron	1/1			



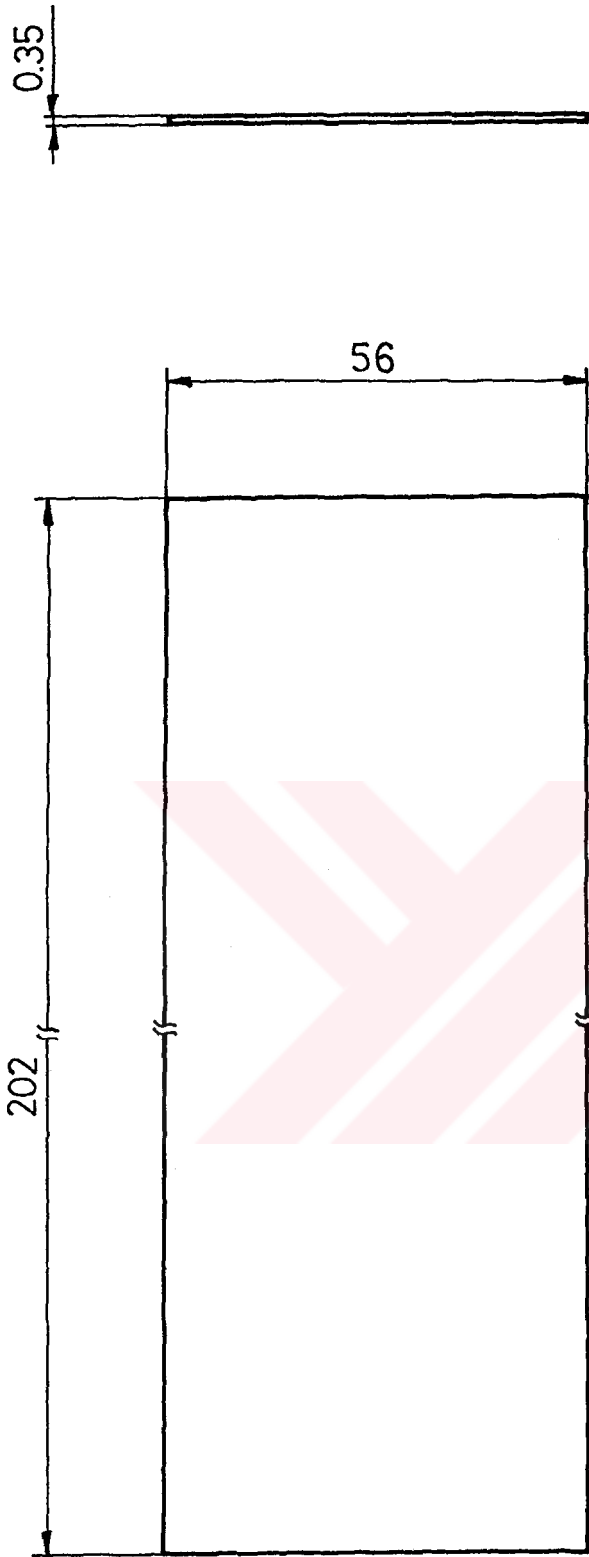
DESIGNED BY	Mehmet TARAKCI	QUAN.	Matrix (6. Step)	METU	
DRAWN BY	Mehmet TARAKCI	12		Mech. Eng. Dpt.	
SUPERVISOR	Assoc Prof Dr Cemil YAMALI	SCALE	1/1	DRAWING NO	14
MATERIAL	0.35mm Galvanized Sheet Iron				



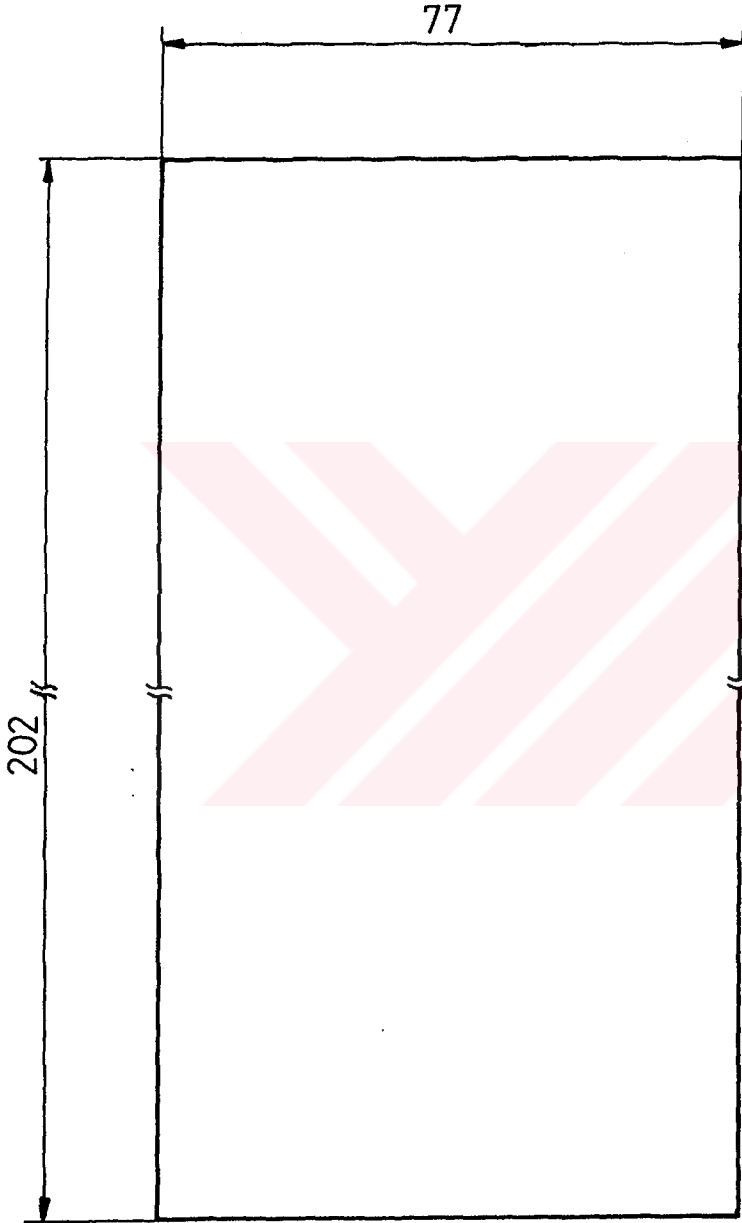
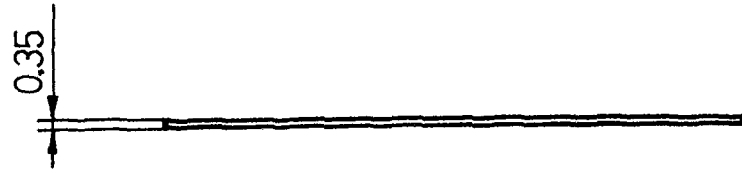
DESIGNED BY	Mehmet TARAKCI	QUAN.	Flat Matrix (1. Step)	METU	
DRAWN BY	Mehmet TARAKCI	12		Mech. Eng. Dpt.	
SUPERVISOR	Assoc.Prof.Dr.Cemil YAMALI	SCALE		DRAWING NO	15
MATERIAL	0.35mm Galvanized Sheet Iron	1/1			



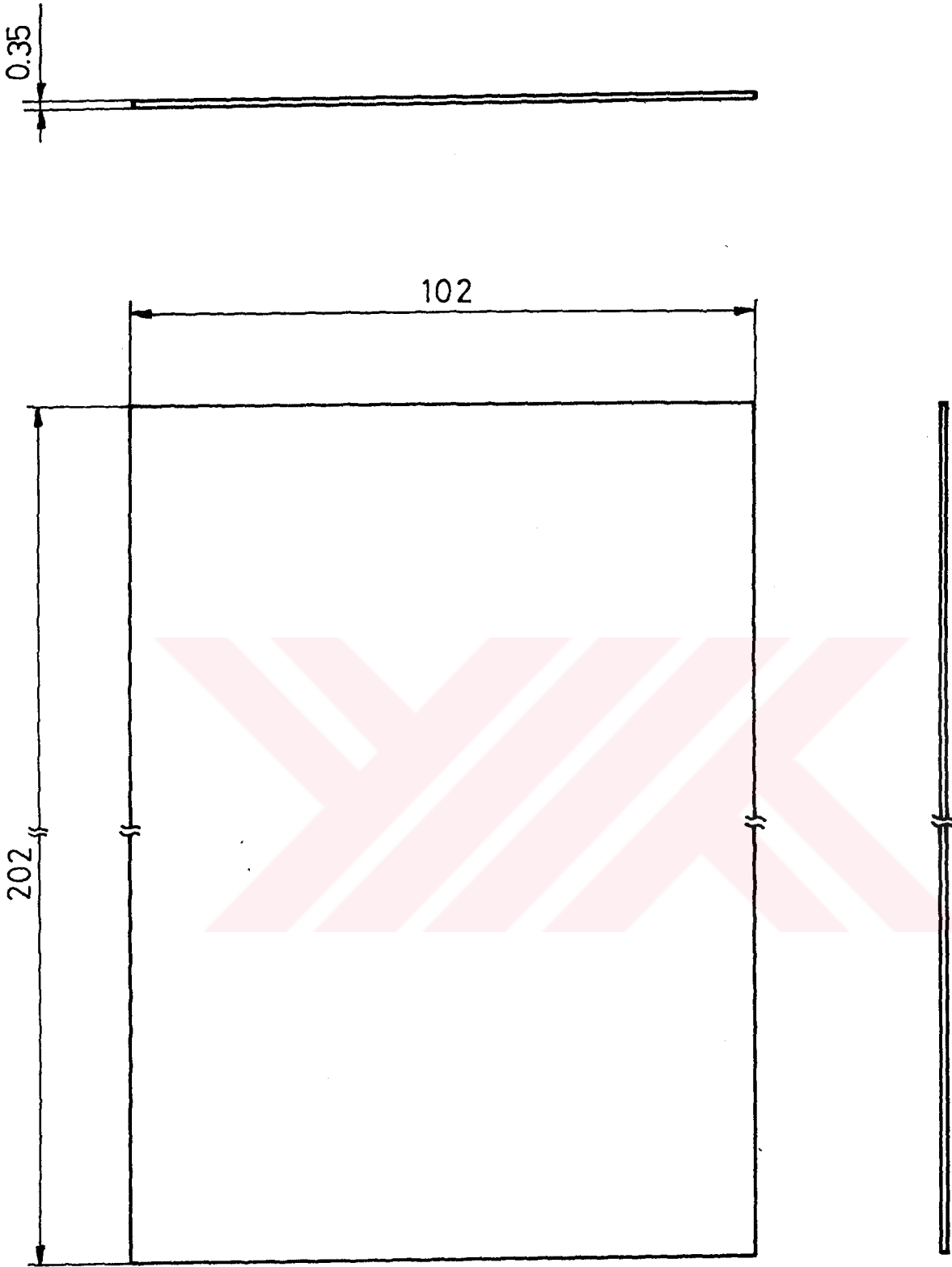
DESIGNED BY	Mehmet TARAKÇI	QUAN 12	Flat Matrix (2. Step)	METU Mech. Eng. Dpt.	
DRAWN BY	Mehmet TARAKÇI				
SUPERVISOR	Assoc.Prof.Dr.Cemil YAMALI	SCALE 1/1		DRAWING NO	16
MATERIAL	0.35mm Galvanized Sheet Iron				



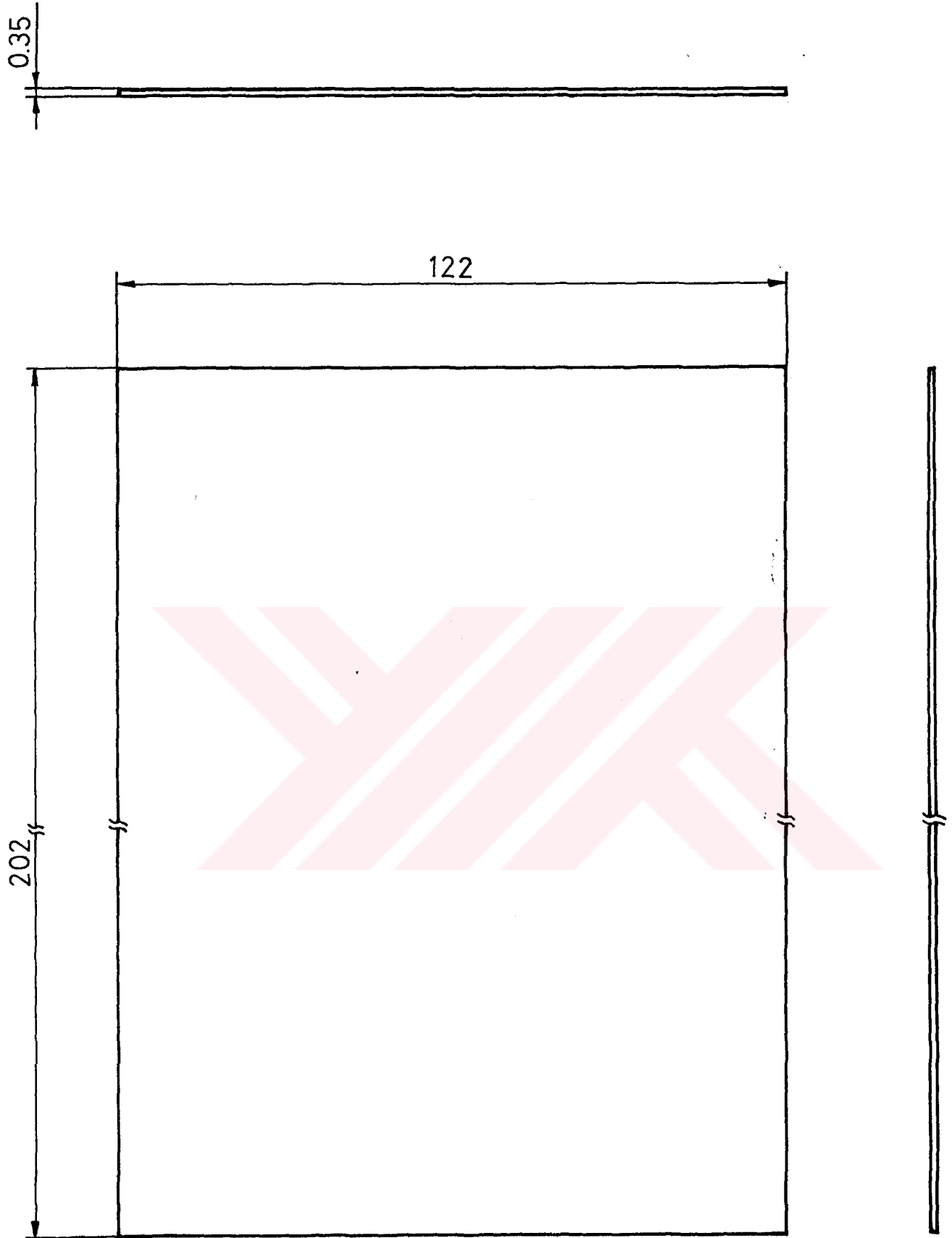
DESIGNED BY	Mehmet TARAKÇI	QUAN.	Flat Matrix (3. Step)	METU	
DRAWN BY	Mehmet TARAKÇI	12		Mech. Eng. Dpt.	
SUPERVISOR	Assoc.Prof.Dr.Cemil YAMALI	SCALE		DRAWING NO	17
MATERIAL	0.35mm Galvanized Sheet Iron	1/1			



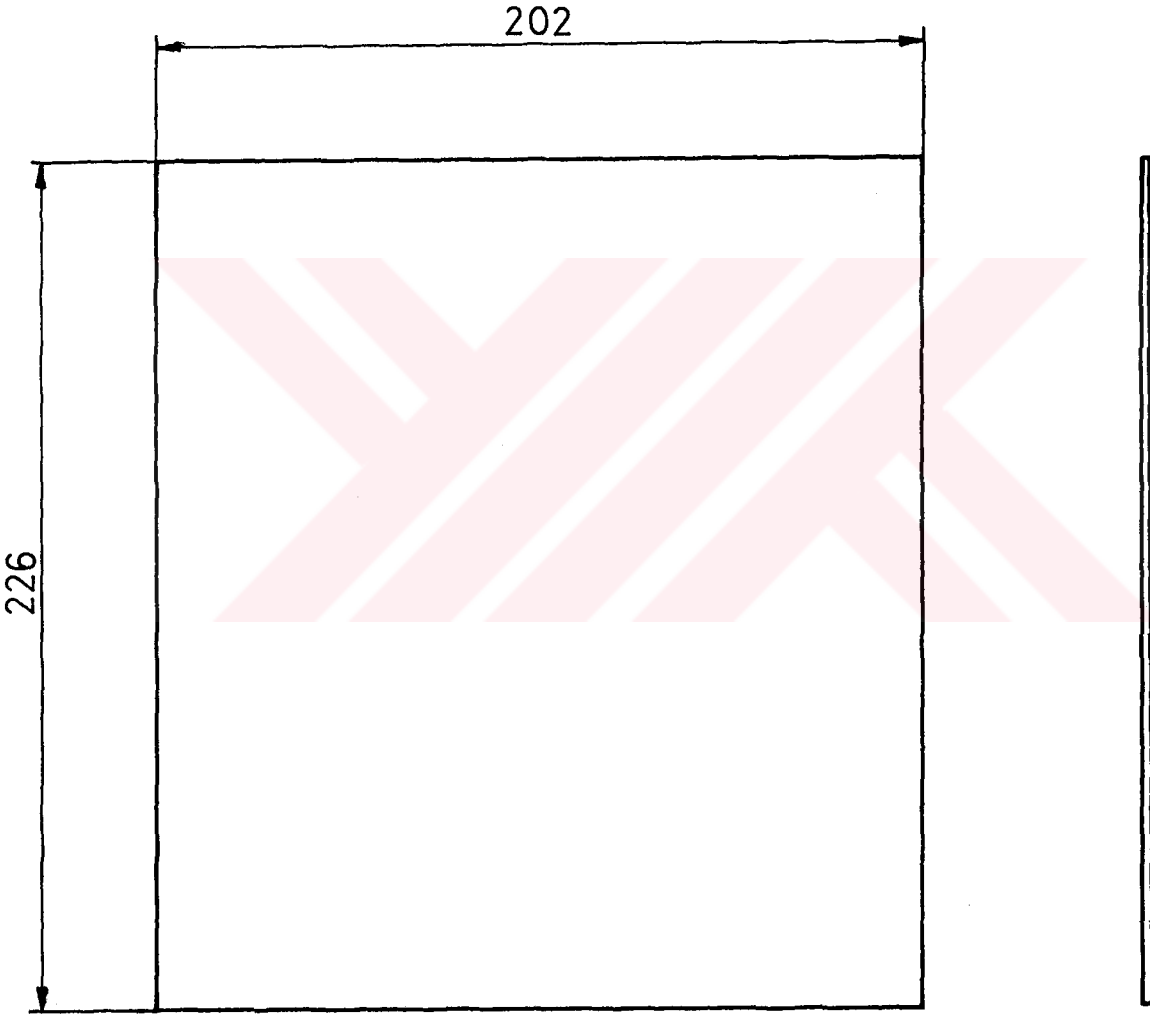
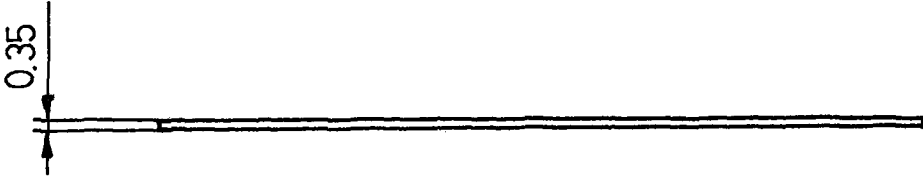
DESIGNED BY	Mehmet TARAKÇI	QUAN.	Flat Matrix (4. Step)	METU	
DRAWN BY	Mehmet TARAKÇI	12		Mech. Eng. Dpt.	
SUPERVISOR	Assoc Prof Dr Cemil YAMALI	SCALE		DRAWING NO	18
MATERIAL	035mm Galvanized Sheet Iron	1/1			



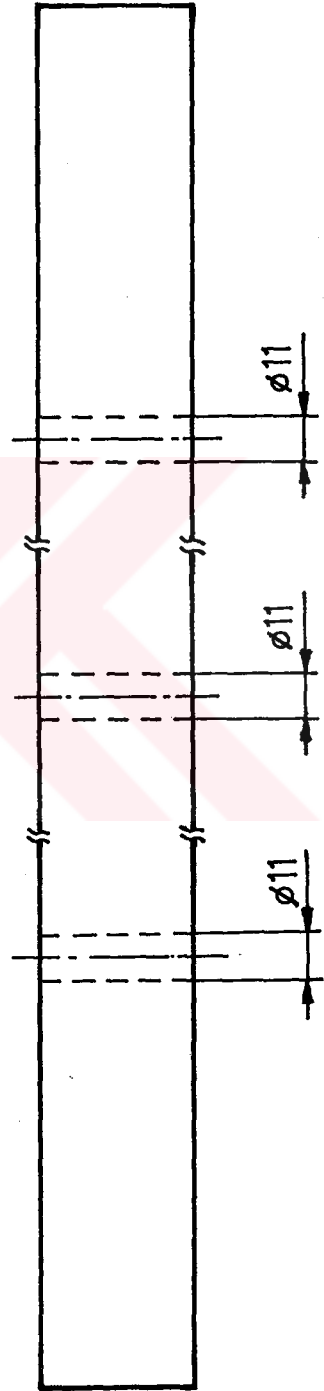
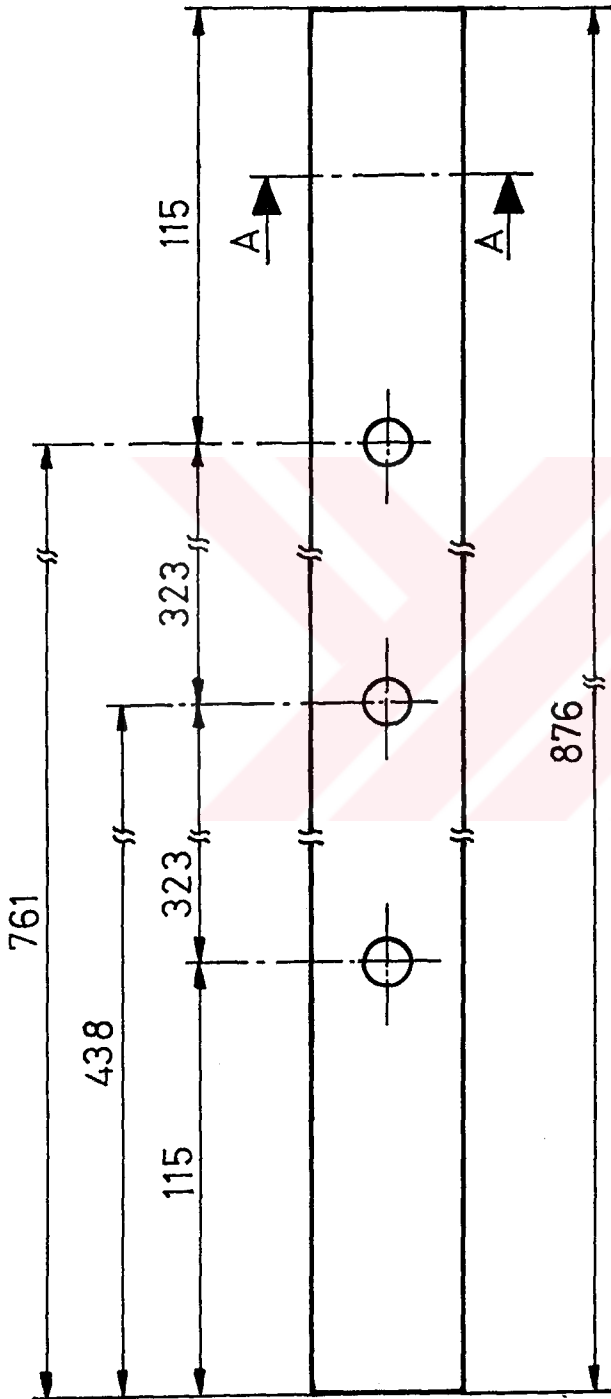
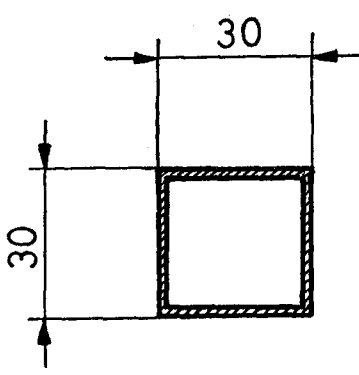
DESIGNED BY	Mehmet TARAKÇI	QUAN.	Flat Matrix (5. Step)	METU	
DRAWN BY	Mehmet TARAKÇI	12		Mech. Eng. Dpt.	
SUPERVISOR	Assoc Prof Dr Cemil YAMALI	SCALE		DRAWING NO	19
MATERIAL	0.35mm Galvanized Sheet Iron	1/1			



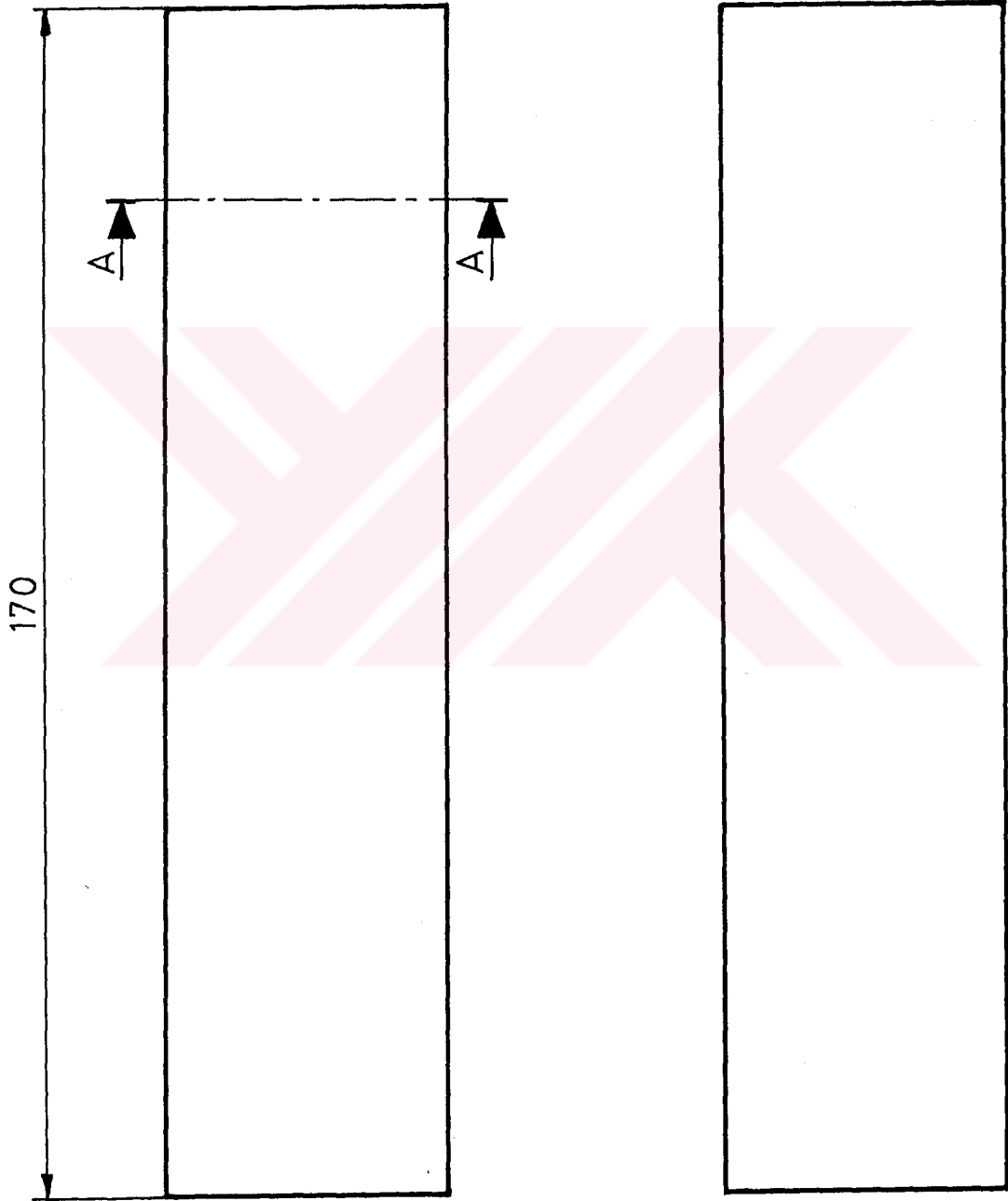
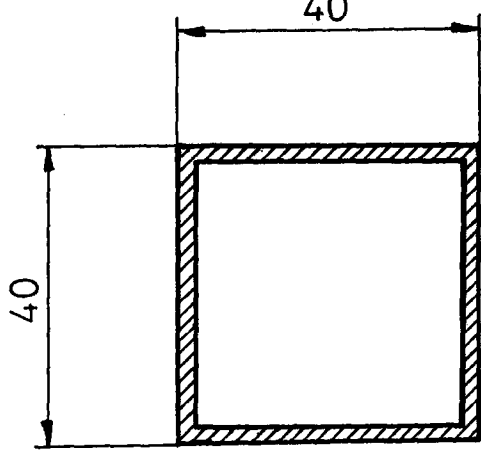
DESIGNED BY	Mehmet TARAKÇI	QUAN.	Flat Matrix (6. Step)	METU	
DRAWN BY	Mehmet TARAKÇI	12		Mech. Eng. Dpt.	
SUPERVISOR	Assoc.Prof.Dr.Cemil YAMALI	SCALE		DRAWING NO	20
MATERIAL	0,35mmGalvanized Sheet Iron	1/1			



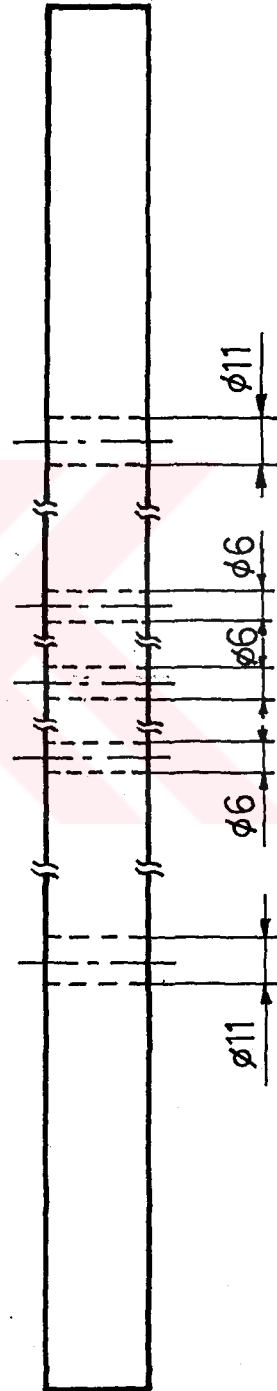
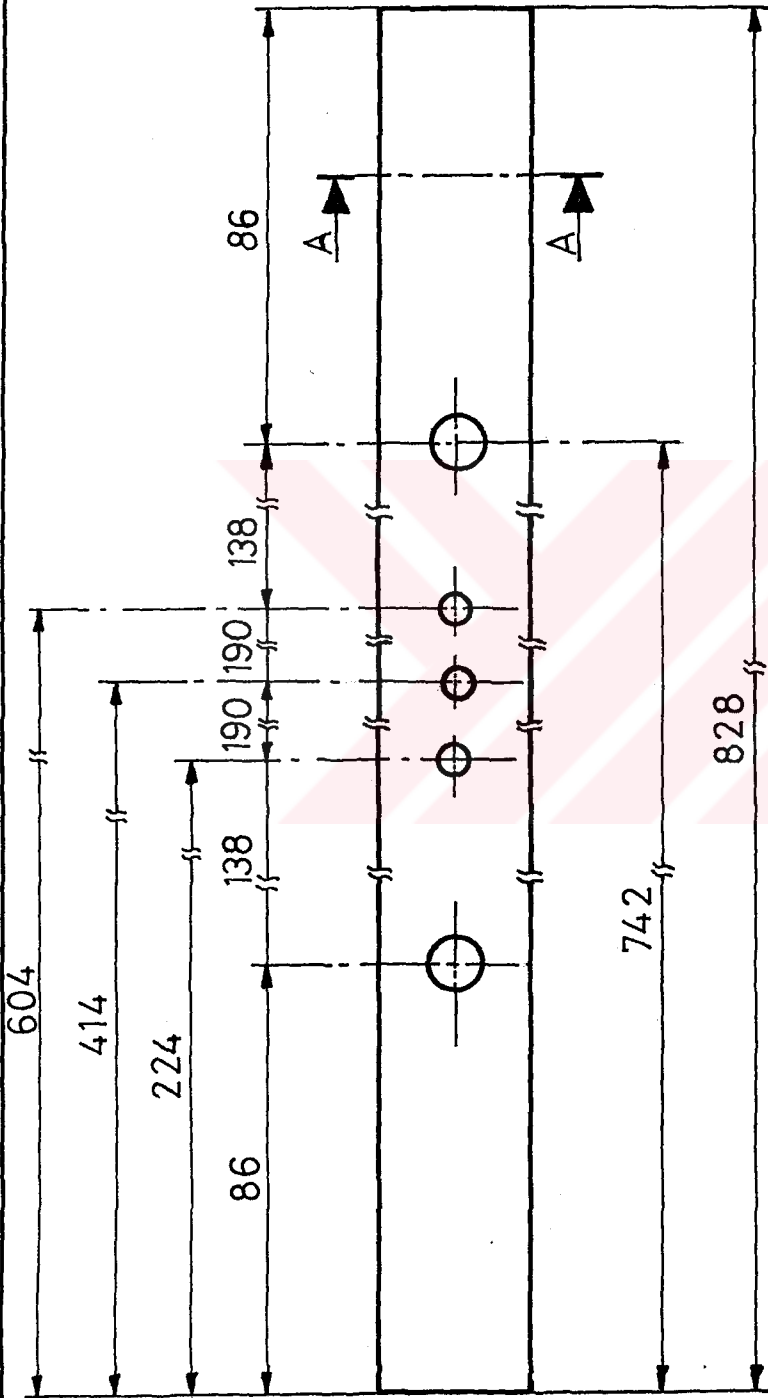
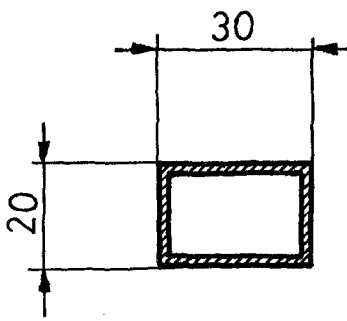
DESIGNED BY	Mehmet TARAKÇI	QUAN 24	Side Flat Matrixs	METU	
DRAWN BY	Mehmet TARAKÇI			Mech. Eng. Dpt.	
SUPERVISOR	Assoc Prof Dr Cemil YAMALI	SCALE 1 / 2		DRAWING NO	21
MATERIAL	0,35mm Galvanized Sheet Iron				



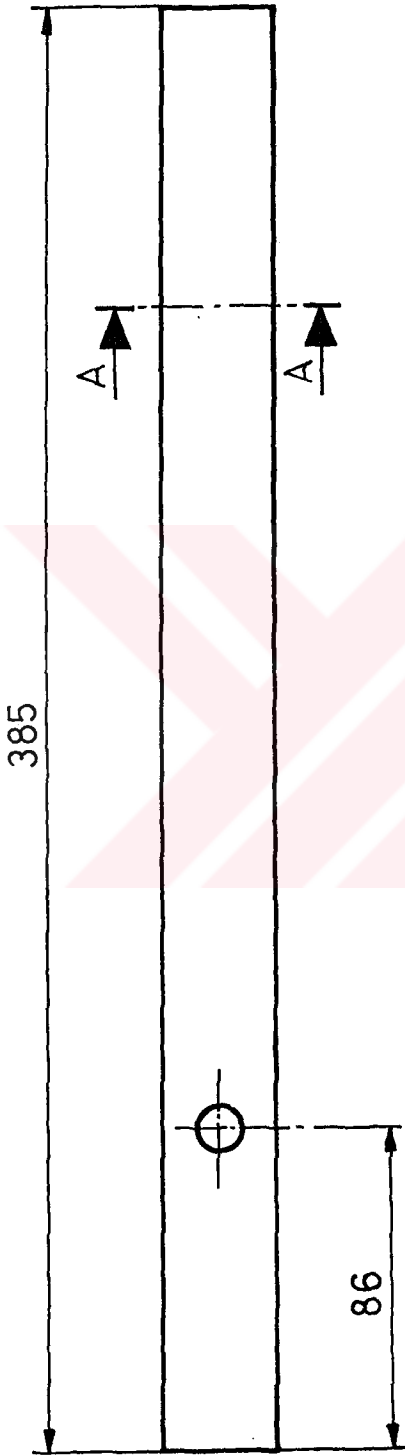
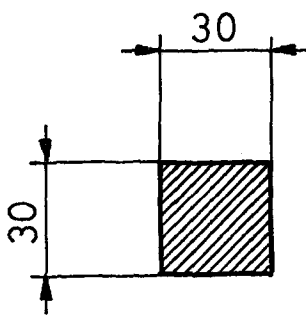
DESIGNED BY	Mehmet TARAKÇI	QUAN.	Part of Housing	METU Mech. Eng. Dpt.	
DRAWN BY	Mehmet TARAKÇI				
SUPERVISOR	Assoc Prof Dr Cemil YAMALI	SCALE		DRAWING NO	22
MATERIAL	40x40x2 Profile	1 / 2			



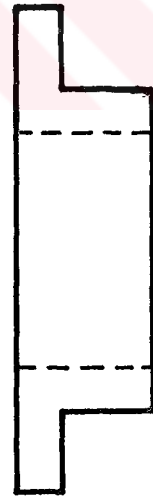
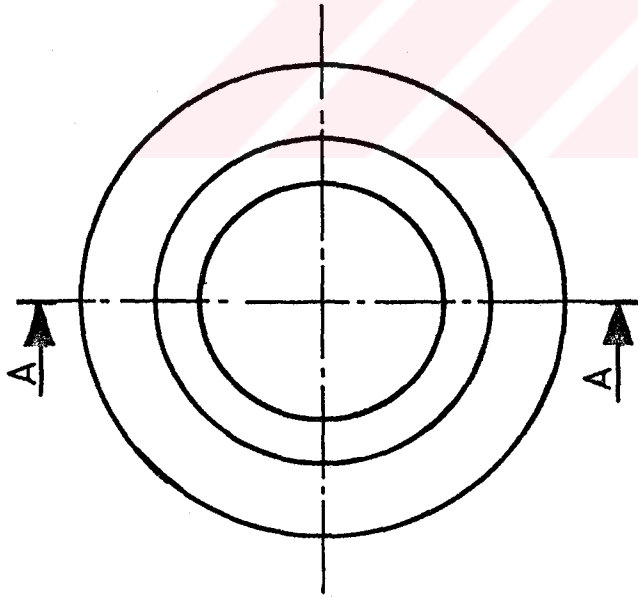
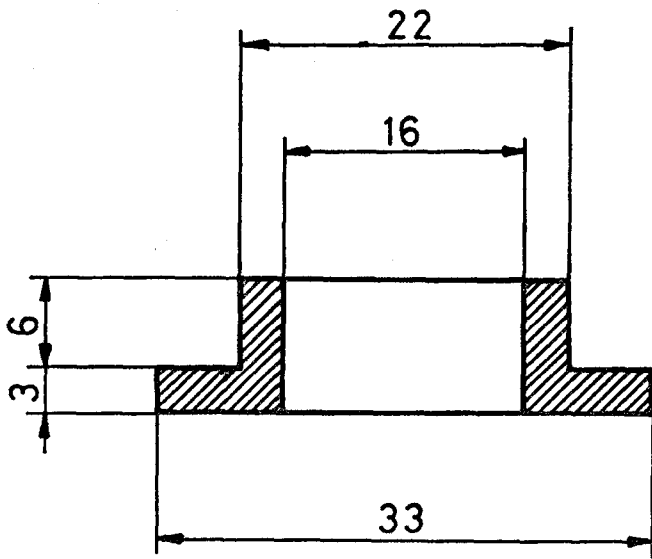
DESIGNED BY	Mehmet TARAKÇI	QUAN.	4	Part of Housing	METU	
DRAWN BY	Mehmet TARAKÇI				Mech. Eng. Dpt.	
SUPERVISOR	Assoc.Prof.Dr.Cemil YAMALI	SCALE	1/1		DRAWING NO	23
MATERIAL	40x40x2 Profile					



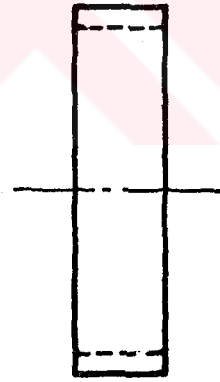
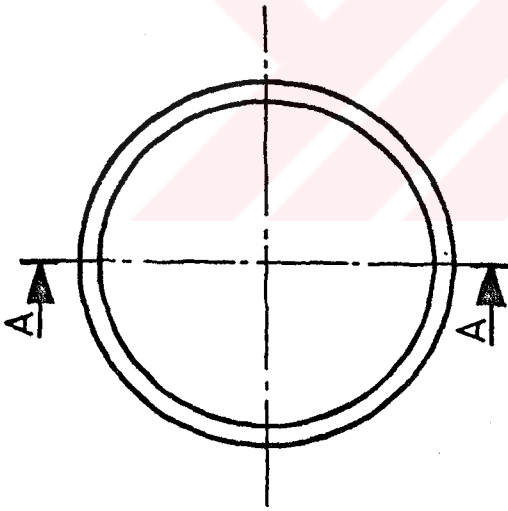
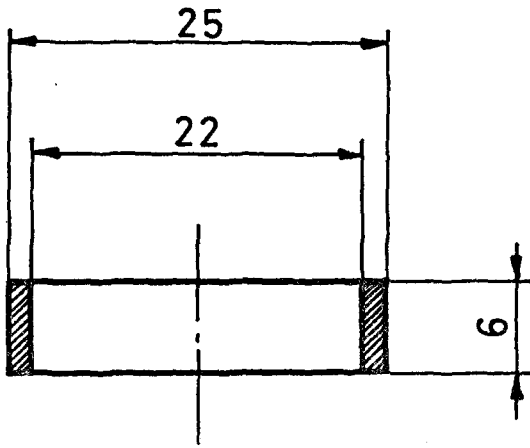
DESIGNED BY	Mehmet TARAKÇI	QUAN.	Part of Housing	MET U Mech. Eng. Dpt.	
DRAWN BY	Mehmet TARAKÇI				
SUPERVISOR	Assoc Prof Dr Cemil YAMALI	SCALE		DRAWING NO	24
MATERIAL	30x20x2 Profile	2 / 3			



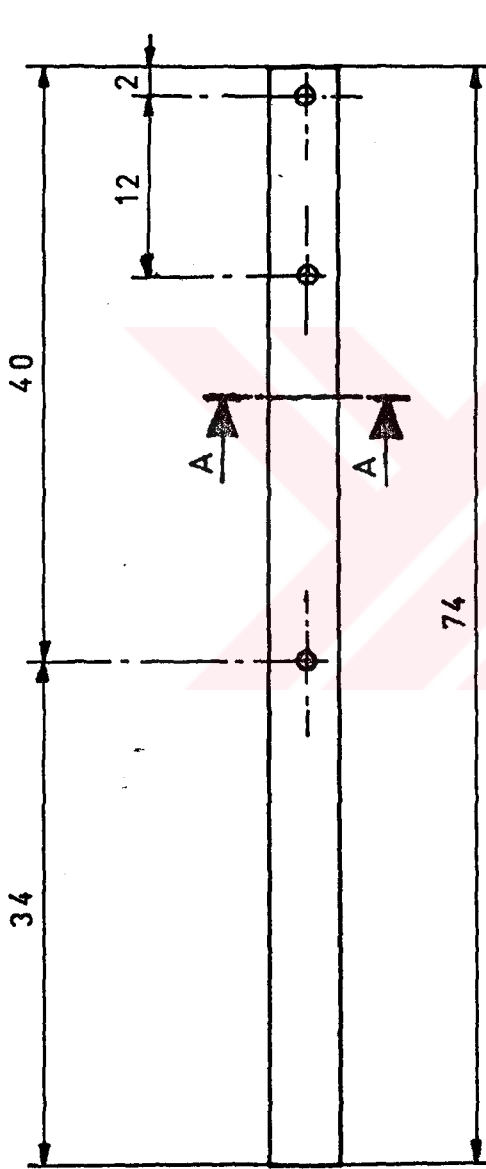
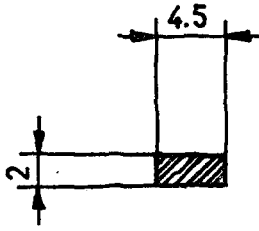
DESIGNED BY	Mehmet TARAKCI	QUAN.	Part of Housing	METU	
DRAWN BY	Mehmet TARAKCI	4		Mech. Eng. Dpt.	
SUPERVISOR	Assoc Prof Dr Cemil YAMALI	SCALE	DRAWING NO	25	
MATERIAL	30x30 Square Iron	1 / 2			



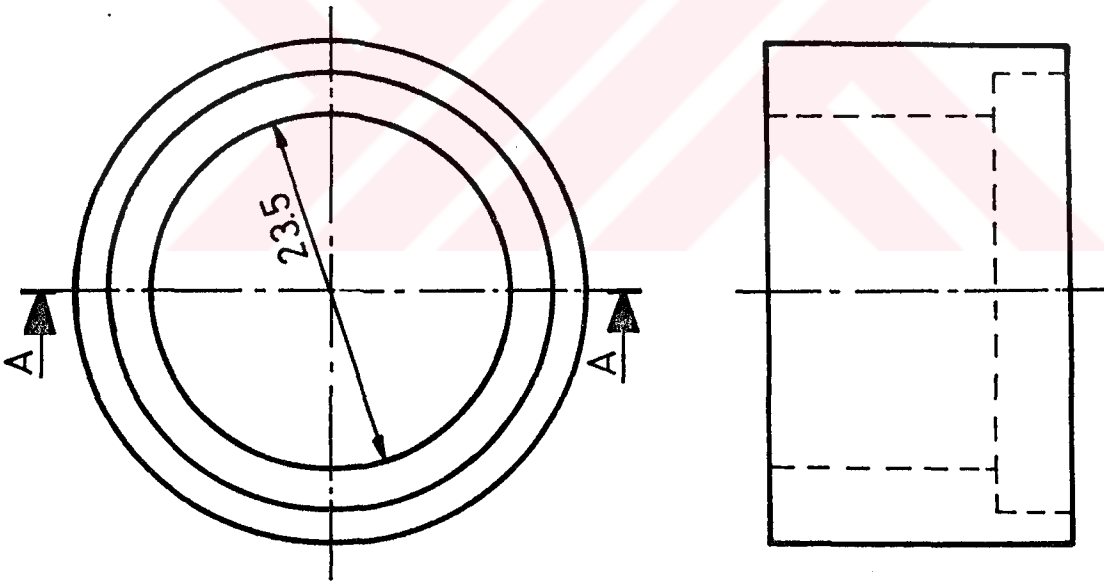
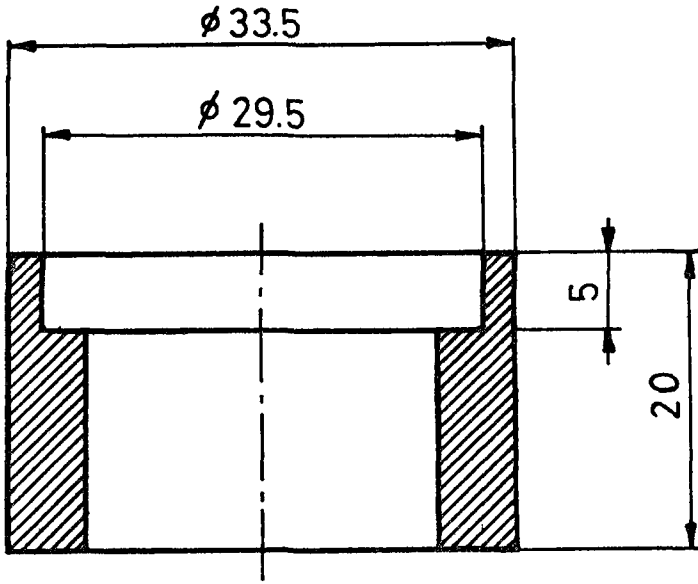
DESIGNED BY	Mehmet TARAKÇI	QUAN. 24	Ring Bearing	METU	
DRAWN BY	Mehmet TARAKÇI			Mech. Eng. Dpt.	
SUPERVISOR	Assoc.Prof.Dr.Cemil YAMALI	SCALE 2 / 1		DRAWING NO	28
MATERIAL	Fiberglass				



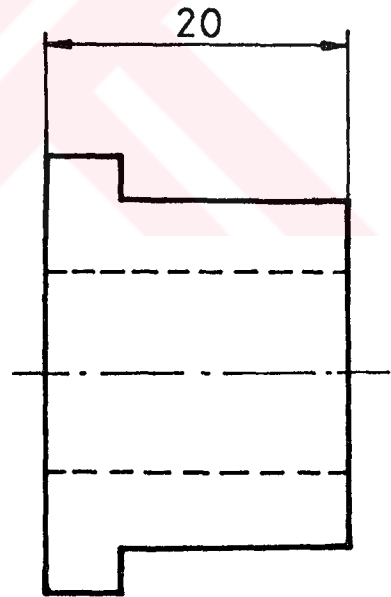
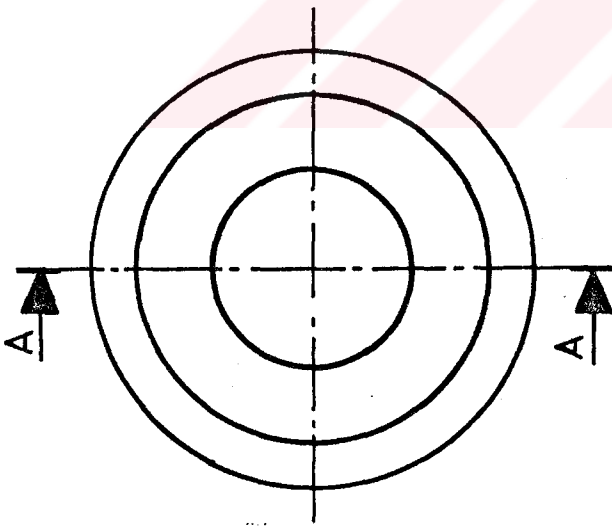
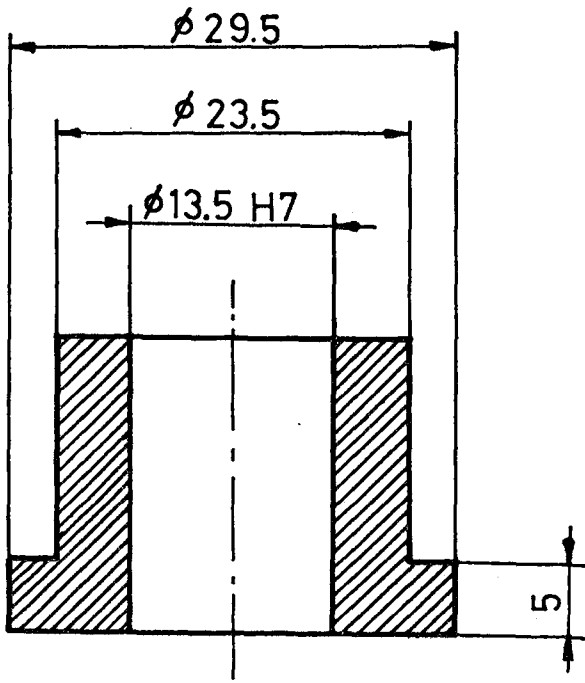
DESIGNED BY	Mehmet TARAKÇI	QUAN. 24	Ring	METU	
DRAWN BY	Mehmet TARAKÇI			Mech. Eng. Dpt.	
SUPERVISOR	Assoc Prof Dr Cemil YAMALI	SCALE 2 / 1		DRAWING NO	29
MATERIAL	Copper				



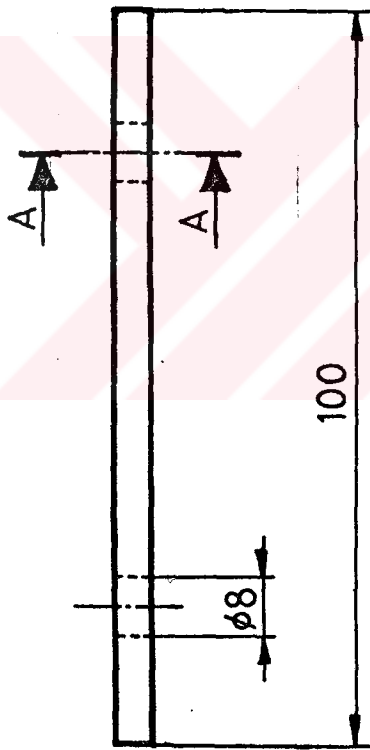
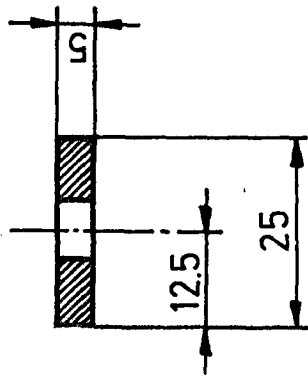
DESIGNED BY	Mehmet TARAKÇI	QUAN.	Copper brush	MET U	
DRAWN BY	Mehmet TARAKCI	24		Mech. Eng. Dpt.	
SUPERVISOR	Assoc Prof Dr Cemil YAMALI	SCALE		DRAWING NO	30
MATERIAL	Copper	2/1			



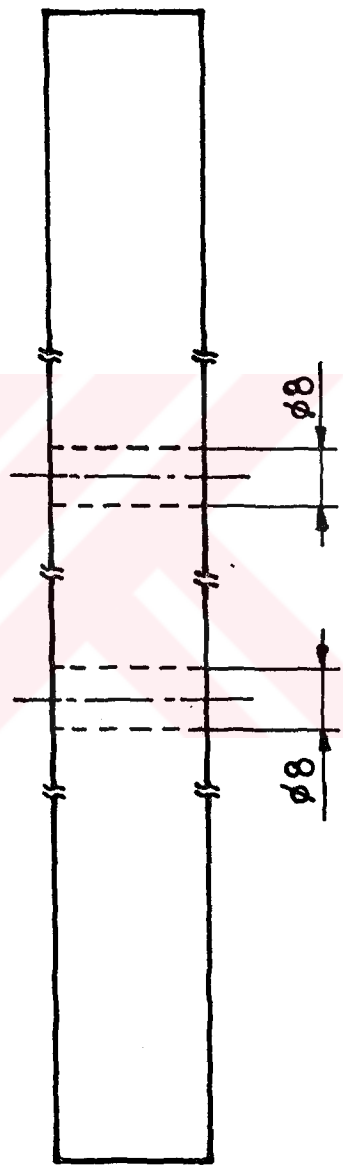
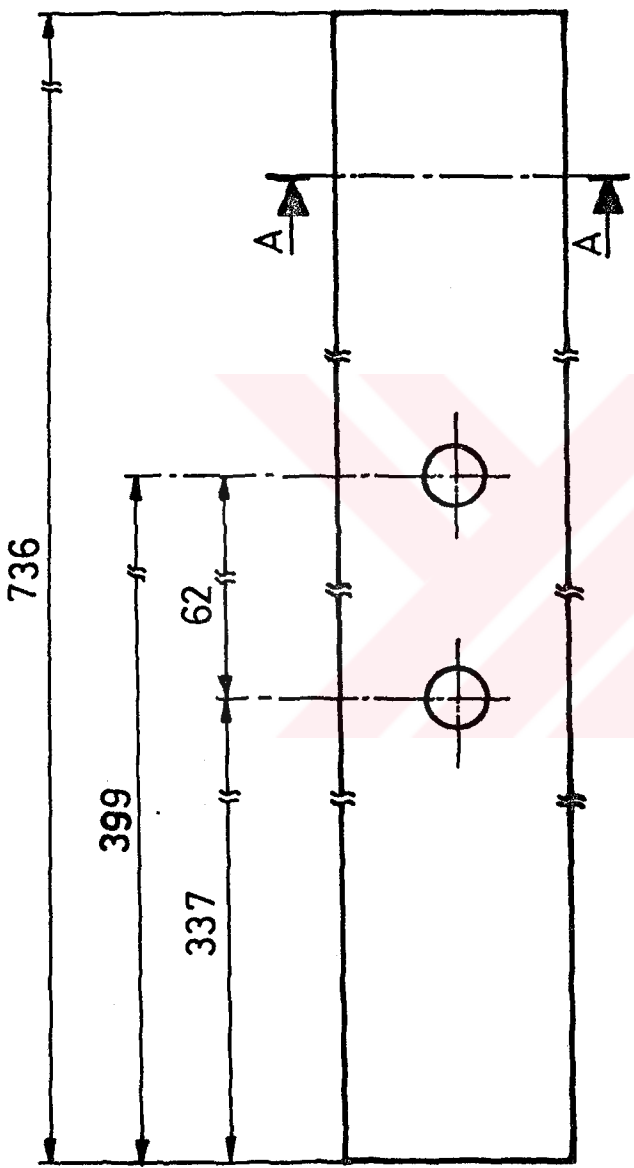
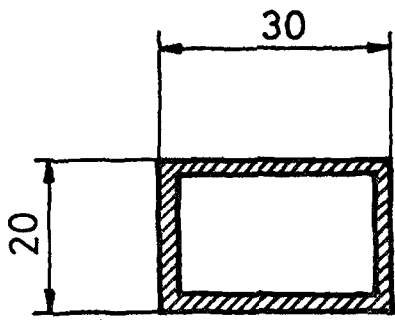
DESIGNED BY	Mehmet TARAKÇI	QUAN.	1	Bearing of Measuring Shaft	METU Mech. Eng. Dpt.	
DRAWN BY	Mehmet TARAKÇI				DRAWING NO	31
SUPERVISOR	AssocProfDr Cemil YAMALI	SCALE	2 / 1			
MATERIAL	ST 60					



DESIGNED BY	Mehmet TARAKÇI	OUAN. 1	Bearing Bronze of Measuring Shaft	MET U Mech. Eng. Dpt.	
DRAWN BY	Mehmet TARAKÇI				
SUPERVISOR	Assoc.Prof.Dr.Cemil YAMALI	SCALE 2 / 1		DRAWING NO	32
MATERIAL	BRONZE				

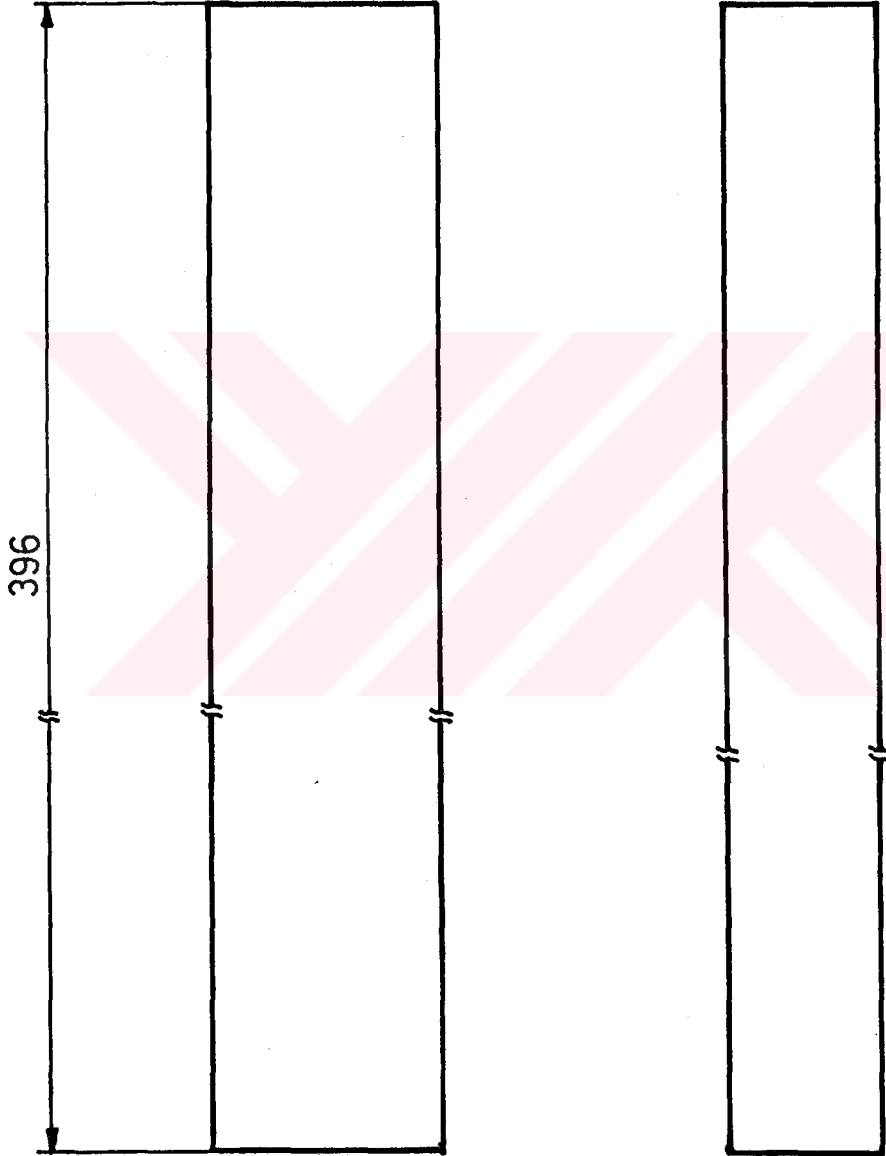
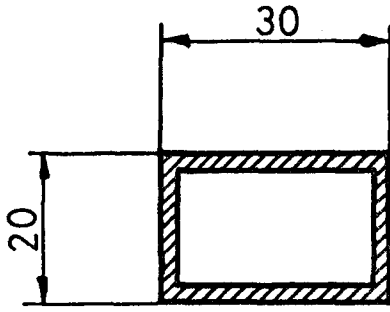


DESIGNED BY	Mehmet TARAKÇI	QUAN. 1	Bearing Flat	METU Mech. Eng. Dpt.	
DRAWN BY	Mehmet TARAKÇI				
SUPERVISOR	AssocProf Dr Cemil YAMALI	SCALE 1/1		DRAWING NO	33
MATERIAL	25x5 Flat Bar				

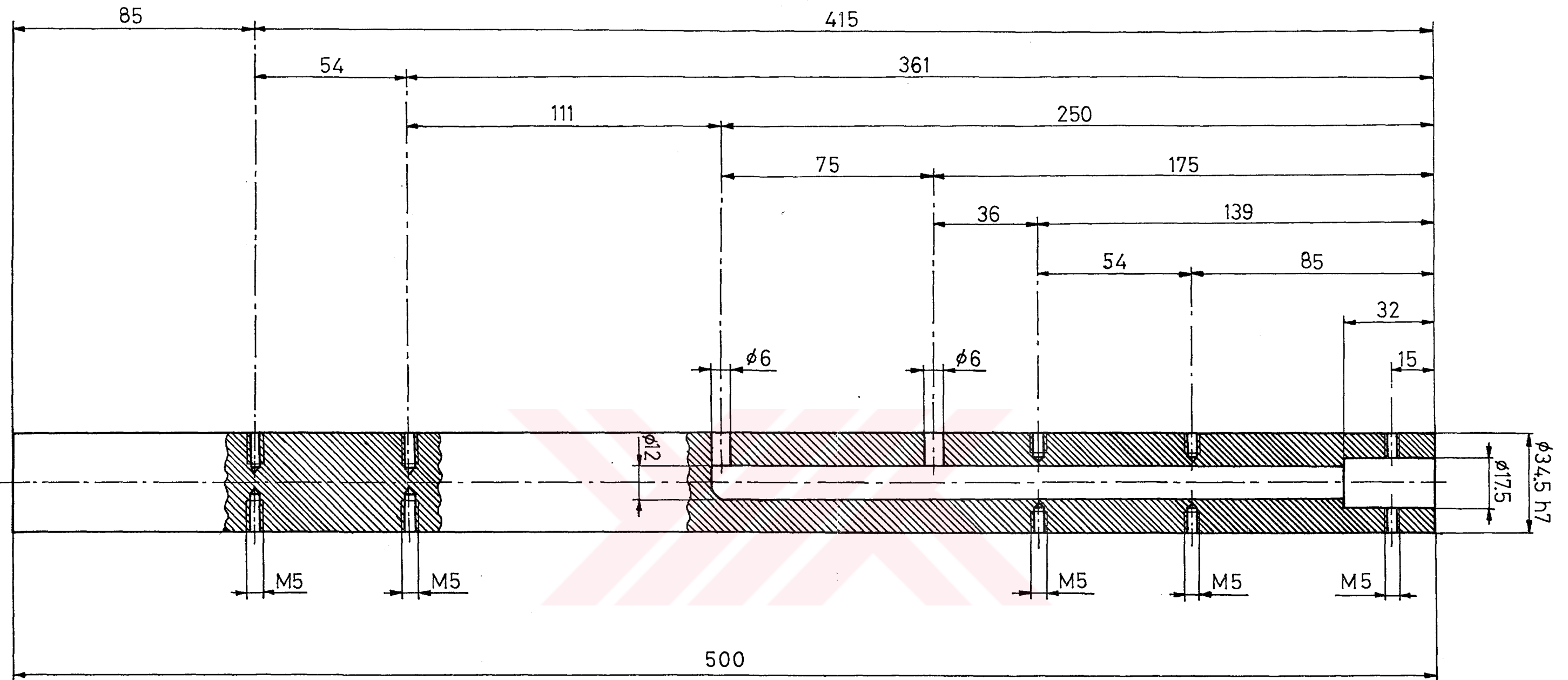


DESIGNED BY	Mehmet TARAKCI	QUAN. 1	Support part of Measuring Shaft	METU	
DRAWN BY	Mehmet TARAKCI			Mech. Eng. Dpt.	
SUPERVISOR	Assoc.Prof. Dr.Cemil YAMALI	SCALE 1/1		DRAWING NO	34
MATERIAL	30x20x2 Profile				

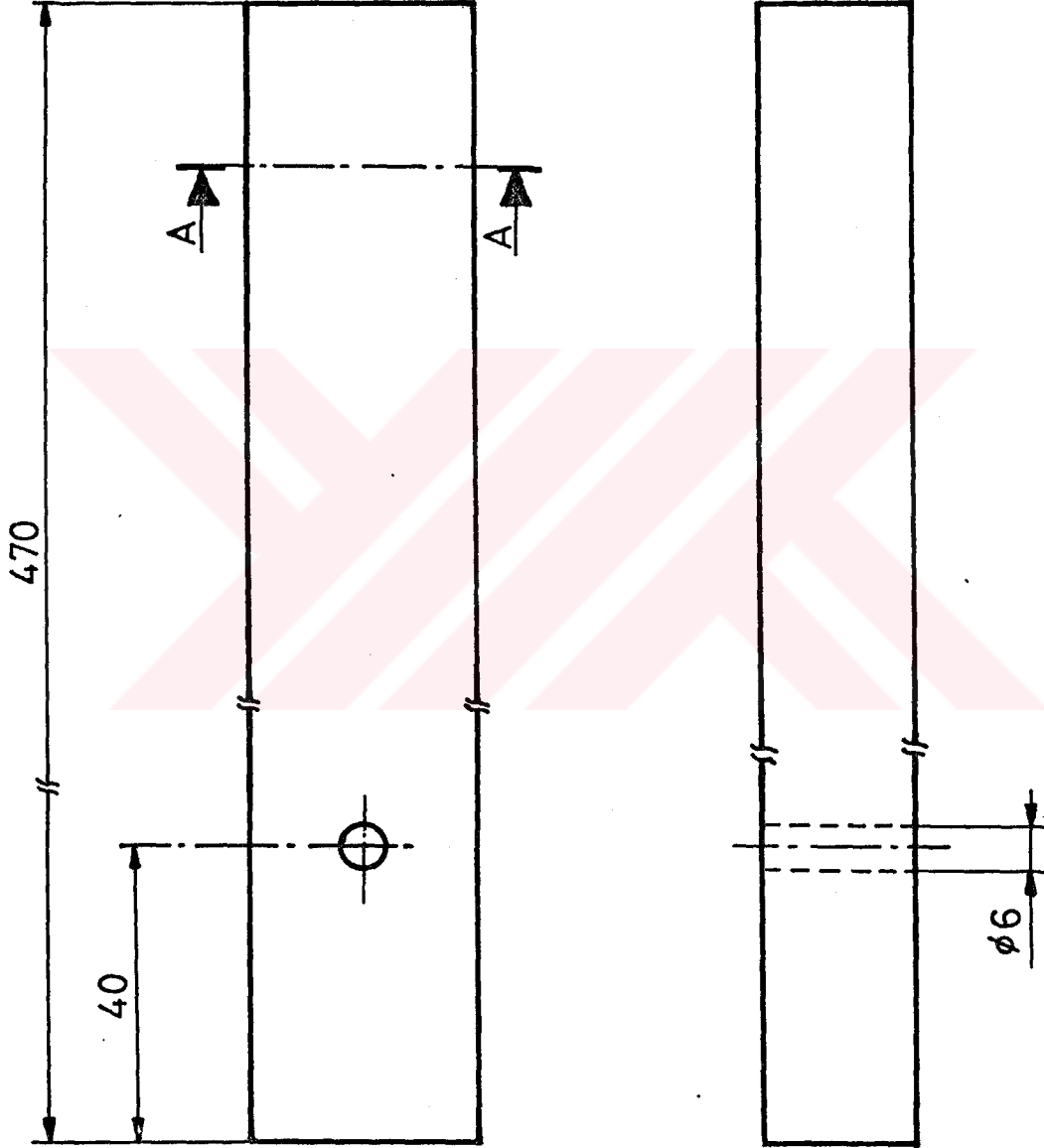
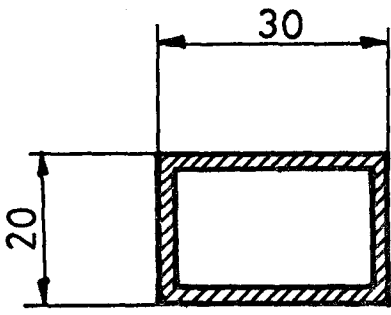
101410124



DESIGNED BY	Mehmet TARAKÇI	QUAN.	Support Part of Measuring Shaft	METU	
DRAWN BY	Mehmet TARAKÇI			2	Mech. Eng. Dpt.
SUPERVISOR	Assoc.Prof.Dr.Cemil YAMALI	SCALE		DRAWING NO	35
MATERIAL	30x20x2 Profile	1/1			



DESIGNED BY	Mehmet TARAKÇI	QUAN.	1	Shaft of R.R.H.E.	METU Mech. Eng. Dpt.
DRAWN BY	Mehmet TARAKÇI	SCALE	7 / 10		
SUPERVISOR	Assoc.Prof.Dr.Cemil YAMALI				
MATERIAL	ST 60				DRAWING NO 7



T. G.
Yükseköğretim Kurulu
Dokümantasyon Merkezi

SIGNED BY	Mehmet TARAKÇI	QUAN.	Support Part of Measuring Shaft	METU	
AWN BY	Mehmet TARAKÇI			4	Mech. Eng. Dpt.
SUPERVISOR	Assoc.Prof.Dr.Cemil YAMALI	SCALE		DRAWING NO	36
MATERIAL	30x20x2 Profile	1/1			